NASA CONTRACTOR REPORT

NASA CR-1054

NASA CR-1054

LUNAR ORBITER IV

Photographic Mission Summary

Prepared by
THE BOEING COMPANY
Seattle, Wash.
for Langley Research Center

NATIONAL AERONAUTICS AND SPACE ADMINISTRATION • WASHINGTON, D. C. • JUNE 1968

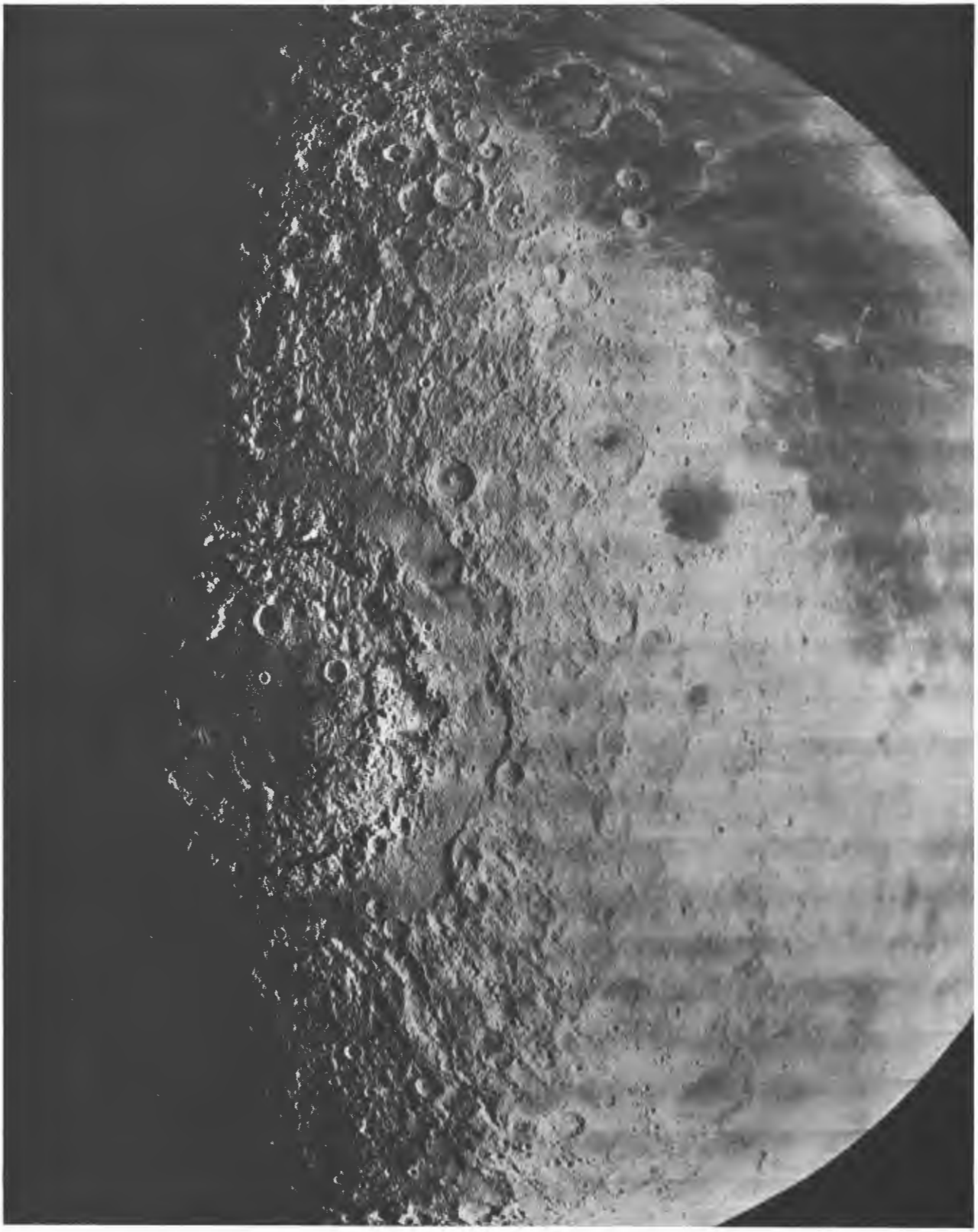

First Detailed View of Orientale Basin
Photo taken by NASA-Boeing Lunar Orbiter IV, May 25, 1967, 05:33:34 GMT, from an altitude of 2,721 kilometers.

NASA CR-1054

LUNAR ORBITER IV

Photographic Mission Summary

Distribution of this report is provided in the interest of information exchange. Responsibility for the contents resides in the author or organization that prepared it.

Issued by Originator as Boeing Document No. D2-100754-1 (Vol. 1)

Prepared under Contract No. NAS 1-3800 by
THE BOEING COMPANY
Seattle, Wash.

for Langley Research Center

NATIONAL AERONAUTICS AND SPACE ADMINISTRATION

For sale by the Clearinghouse for Federal Scientific and Technical Information
Springfield, Virginia 22151 – CFSTI price $3.00

Contents

	Page
1.0 INTRODUCTION	5
1.1 Program Description	5
1.2 Program Management	5
1.3 Program Objectives	6
1.3.1 Mission IV Objectives	7
1.4 Mission Design	8
1.5 Flight Vehicle Description	11
2.0 LAUNCH PREPARATION AND OPERATIONS	19
2.1 Launch Vehicle Preparation	19
2.2 Spacecraft Preparation	21
2.3 Launch Countdown	21
2.4 Launch Phase	22
2.4.1 Launch Vehicle Performance	22
2.4.1.1 Atlas Performance	22
2.4.1.2 Agena Performance	24
2.4.1.3 Spacecraft Performance	24
2.5 Data Acquisition	25
3.0 MISSION OPERATIONS	31
3.1 Mission Profile	31
3.2 Spacecraft Performance	34
3.2.1 Photo Subsystem Performance	35
3.2.2 Power Subsystem Performance	37
3.2.3 Communications Subsystem Performance	40
3.2.4 Attitude Control Subsystem Performance	42
3.2.5 Velocity Control Subsystem Performance	45
3.2.6 Structures, Mechanisms, and Integration Elements Performance	47
3.3 Operational Performance	48
3.3.1 Spacecraft Control	50
3.3.2 Flight Path Control	51
3.4 Ground Systems Performance	55
3.4.1 Space Flight Operations Facility	58
3.4.2 Deep Space Stations	58
3.4.3 Ground Communications System	59
3.4.4 Photo Processing	59
3.4.5 Langley Photo Data Assessment Facility	60
4.0 MISSION DATA	63
4.1 Photographic Data	63
4.1.1 Mission Photography	64
4.1.2 Photo Coverage	67
4.2 Environmental Data	114
4.2.1 Radiation Data	114
4.2.2 Micrometeoroid Data	115
4.3 Tracking Data	116
4.3.1 DSIF Tracking Data System	116
4.3.2 Deep Space Network	116
4.4 Performance Telemetry	117
5.0 MISSION EVALUATION	119

Figures

		Page
1-1	Lunar Orbiter Project Organization	6
1-2	Photo Orbit Sequence of Events	9
1-3	Footprint Orientation	10
1-4	Photo Mission Sequence of Events	12
1-5	Lunar Orbiter Spacecraft	14
1-6	Lunar Orbiter Block Diagram	15
1-7	Photographic Data Acquisition, Reconstruction, and Assembly	16
1-8	Launch Vehicle	17
2-1	Launch Operations Flow Chart	20
2-2	Master Countdown Time Sequence	22
2-3	Earth Track for May 4, 1967	26
3-1	Lunar Orbiter IV Flight Profile	32
3-2	Photo Subsystem	35
3-3	Video Signal Waveform	36
3-4	Power Subsystem	38
3-5	Solar Array Degradation	39
3-6	Communications Subsystem	40
3-7	Attitude Control Subsystem	43
3-8	Velocity and Reaction Control Subsystem	46
3-9	Thermal Paint Coupon Solar Absorptance Coefficients	49
3-10	Pre-Midcourse Encounter Parameters	53
3-11	Perilune Altitude History	56
3-12	Orbit Inclination History	56
3-13	Argument of Perilune History	57
3-14	Ascending Node Longitude History	57
4-1	Pre-Exposed Reseau Mark Characteristics	64
4-2	Field of View for Perilune Photography	66
4-3	Perilune Photography Pointing Orientation	67
4-4	Photo Zones A and B Telephoto Footprints	69
4-5	Photo Zones C and D Telephoto Footprints	71
4-6	Photo Zone S Telephoto Footprints (South Polar)	73
4-7	Photo Zone N Telephoto Footprints (North Polar)	74
4-8	North Latitude Zone Recovery Photo Footprints	75
4-9	South Latitude Zone Recovery Photo Footprints	76
4-10	Geometrical Parameters of Photography	79
4-11	Slant Range vs Framelet Width (Telephoto Lens)	80
4-12 through -41	Selected Lunar Photographs (Wide Angle and Telephoto)	81-113
4-42	Radiation Dosage History	114
4-43	Micrometeoroid Impacts	115

Tables

		Page
1-1	May Launch Window Summary	8
1-2	Exposure Index	13
2-1	Launch Vehicle Preparation Summary	19
2-2	Ascent Trajectory Event Times	23
2-3	AFETR Electronic Tracking Coverage	27
2-4	AFETR Telemetry Coverage	28
3-1	Trajectory Change Summary	34
3-2	Spacecraft Load Currents	39
3-3	Maneuver Summary	44
3-4	Thruster Operations	46
3-5	Velocity Control Engine Performance Summary	47
3-6	Summary of Encounter Parameters	54
3-7	Lunar Orbit Parameter Summary	55
3-8	Transmission Mode Downtime	59
3-9	Measured GRE Film Density	60
4-1	Spacecraft Film Radiation Dosage	64
4-2	Photo Zone Identification	68
4-3	Photo Supporting Data	77
4-4	DSN Telemetry Summary	117

Illustrations

Frontispiece: First Detailed View of Orientale Basin

Wide-Angle Frame 161 – Site IV29B vi

Wide-Angle Frame 152 – Site IV27N 4

Wide-Angle Frame 118 – Site IV22S 18

Wide-Angle Frame 9 – Site IV6A 30

Wide-Angle Frame 109 – Site IV20C 62

Wide-Angle Frame 183 – Site IV32D 118

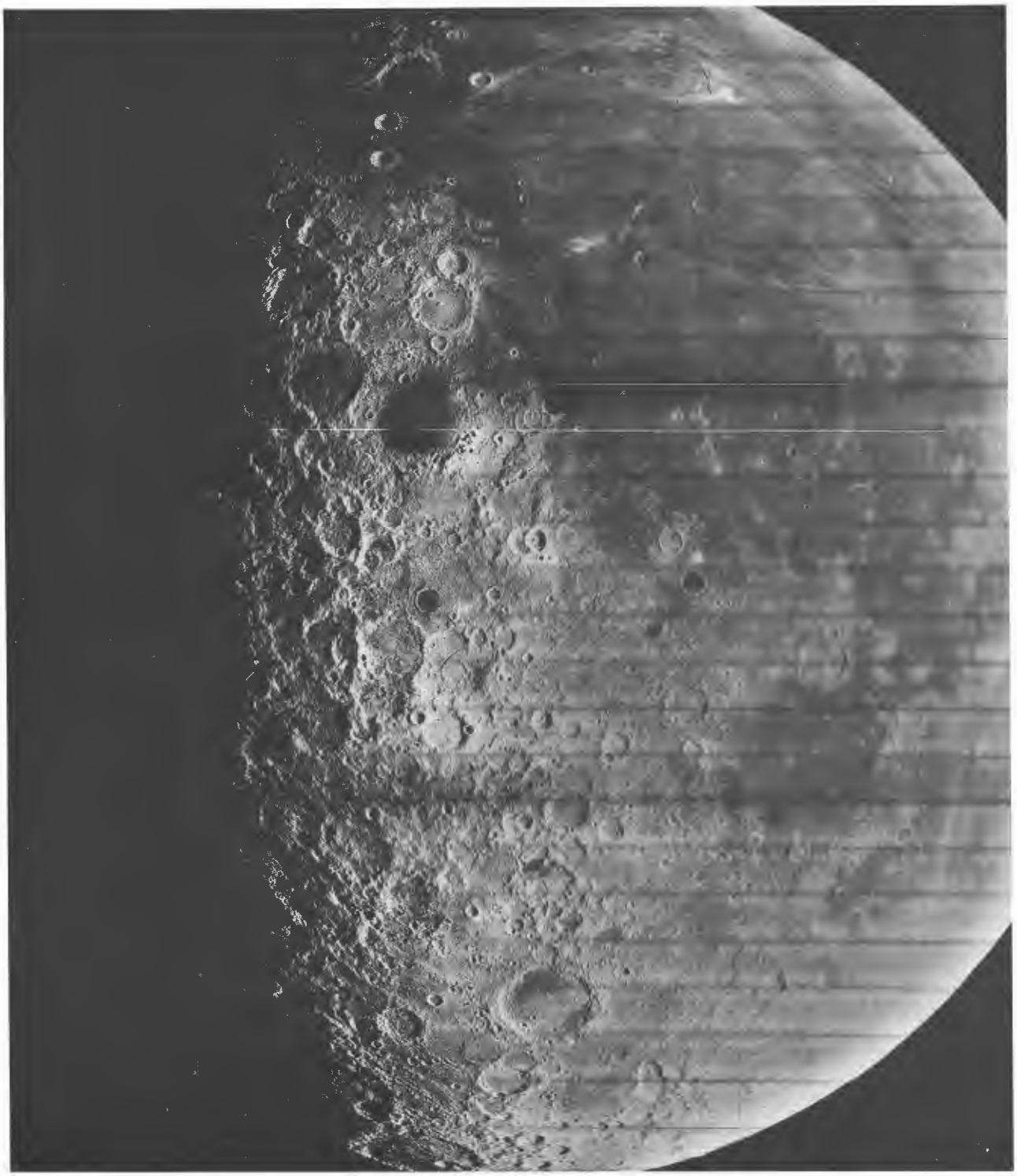

Wide-Angle Frame 161, Site IV29B
Centered at 62.5° W, 14.3° S;
includes Grimaldi, Kepler, Gassendi, and Schickard.

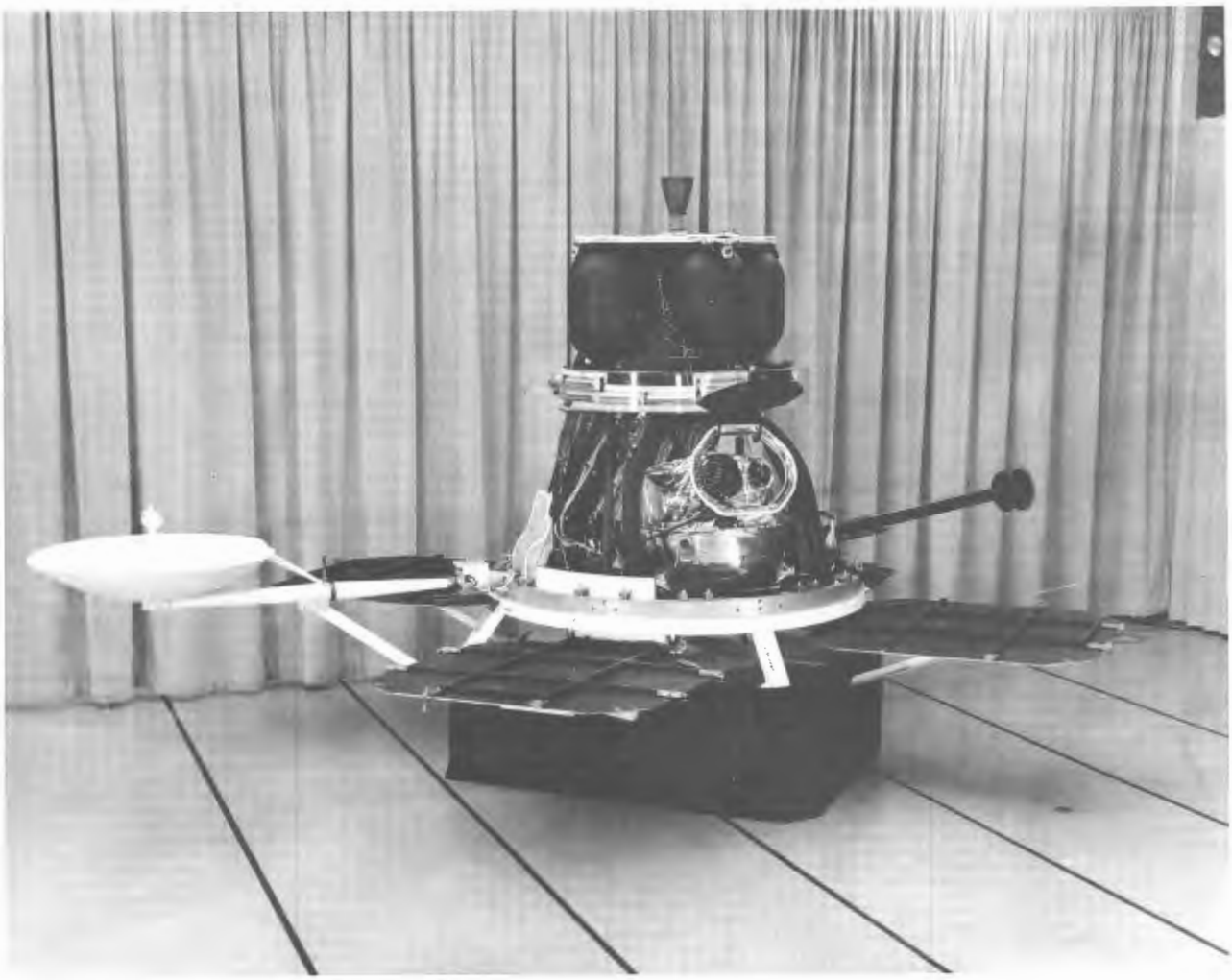

LUNAR ORBITER IV

PHOTOGRAPHIC MISSION SUMMARY

The fourth of five Lunar Orbiter spacecraft was successfully launched from Launch Complex 13 at the Air Force Eastern Test Range by an Atlas-Agena launch vehicle at 22:25 GMT on May 4, 1967. Tracking data from the Cape Kennedy and Grand Bahama tracking stations were used to control and guide the launch vehicle during Atlas powered flight. The Agena-spacecraft combination was boosted to the proper coast ellipse by the Atlas booster prior to separation. Final maneuvering and acceleration to the velocity required to maintain the 100-nautical-mile-altitude Earth orbit was controlled by the preset on-board Agena computer. In addition, the Agena computer determined the maneuver and engine-burn period required to inject the spacecraft on the cislunar trajectory 20 minutes after launch. Tracking data from the downrange stations and the Johannesburg, South Africa station were used to monitor the boost trajectory.

Antenna and solar panel deployment sequences and Sun acquisition were initiated by stored commands shortly after spacecraft separation and before acquisition by the Deep Space Network tracking stations. Events of significance during the cislunar trajectory were the star map and Canopus acquisition sequences completed

about 10 hours after launch, and the single midcourse correction. A relatively large midcourse maneuver (60.85 meters-per-second velocity change) was required because the mission objectives and characteristics were extensively modified after the booster guidance system had been programmed. The booster guidance system was programmed to steer toward a lunar injection point that would result in an orbit inclined at 21 degrees with the equator and having its descending node at about 70-degree AM illumination. The midcourse maneuver shifted the aim point to enable an 85-degree inclined orbit with the ascending node within the AM photographic illumination band. The trajectory change from this maneuver indicated that the second maneuver provided for was not required. Lunar injection occurred 89.7 hours after launch with a velocity change of 659.6 meters per second. Initial parameters of the lunar orbit from which all photography was accomplished were: apolune, 6,114 kilometers; perilune, 2,706 kilometers; period, 721 minutes; and orbit inclination, 85.48 degrees.

Active photography was initiated on Orbit 6 at 15:46 GMT on May 11. During the 30 successive photo orbits (15 days), 199 dual-frame exposures were taken. With minor exceptions, two or three axis maneuvers were made for each photograph. Eighty-six per cent of these exposures were used to provide nearly complete coverage (over 99%) of the nearside of the Moon. Some of the early photos were degraded by light fogging of the film from a combination of condensation on the lens and stray light leakage, which resulted from an operational decision to leave the camera thermal door open after experiencing difficulties with its operation early in the flight. Later in the flight, the apolune photography sequence was modified to rephotograph these areas. The readout advance irregularities that were encountered during the mission were attributed to intermittent signals from the photo subsystem logic control circuitry; however, slight changes in operating procedures were implemented and all but the last seven exposures were processed before the "Bimat cut" command was executed on May 26 during Orbit 36. Priority readout covered all of the significant lunar photos prior to the occurrence of the film advance problem. Final readout was initiated in Orbit 41 on May 29 and completed during Orbit 48 on June 1. Final readout was terminated when all of the desired photos had been read out by either priority or final mode.

Examination of the photos obtained showed that the coverage of the nearside, from the normal perilune and recovery apolune photography, provided visibility of the lunar surface at least 10 times better than that obtainable from current Earth-based observations. Perilune photography, which provided pole-to-pole coverage of the nearside every other orbit, was taken as single-frame exposures from altitudes of approximately 2,600 kilometers near the equator to about 3,600 kilometers for the polar regions. Resolution capability of the telephoto perilune photography varied from about 60 to 90 meters, depending on the slant range to the surface and the location within the frame format. These photos provided the first detailed data on numerous areas of scientific interest in all areas of the visible surface. In addition, the first detailed information on the spectacular Orientale basin at the western limb was obtained. Within the limits of the 6,100-kilometer photographic altitude and acceptable illumination, the apolune photography provided additional information of the farside to be added to the data from the first three missions.

Two micrometeoroid impacts were recorded by the detectors mounted on the periphery of the engine deck but no apparent effect was indicated in the performance data. The spacecraft was also subjected to a large, low-energy plasma cloud from a series of major Sun flares on May 23. There was no apparent film degradation from the radiation encountered.

All mission objectives were accomplished. This mission represents the first attempt to perform an orbital photographic mapping survey from orbit of a celestial body other than Earth. The photo data obtained was used to redefine many of the planned sites for Mission V to optimize and maximize the scientific data requirements.

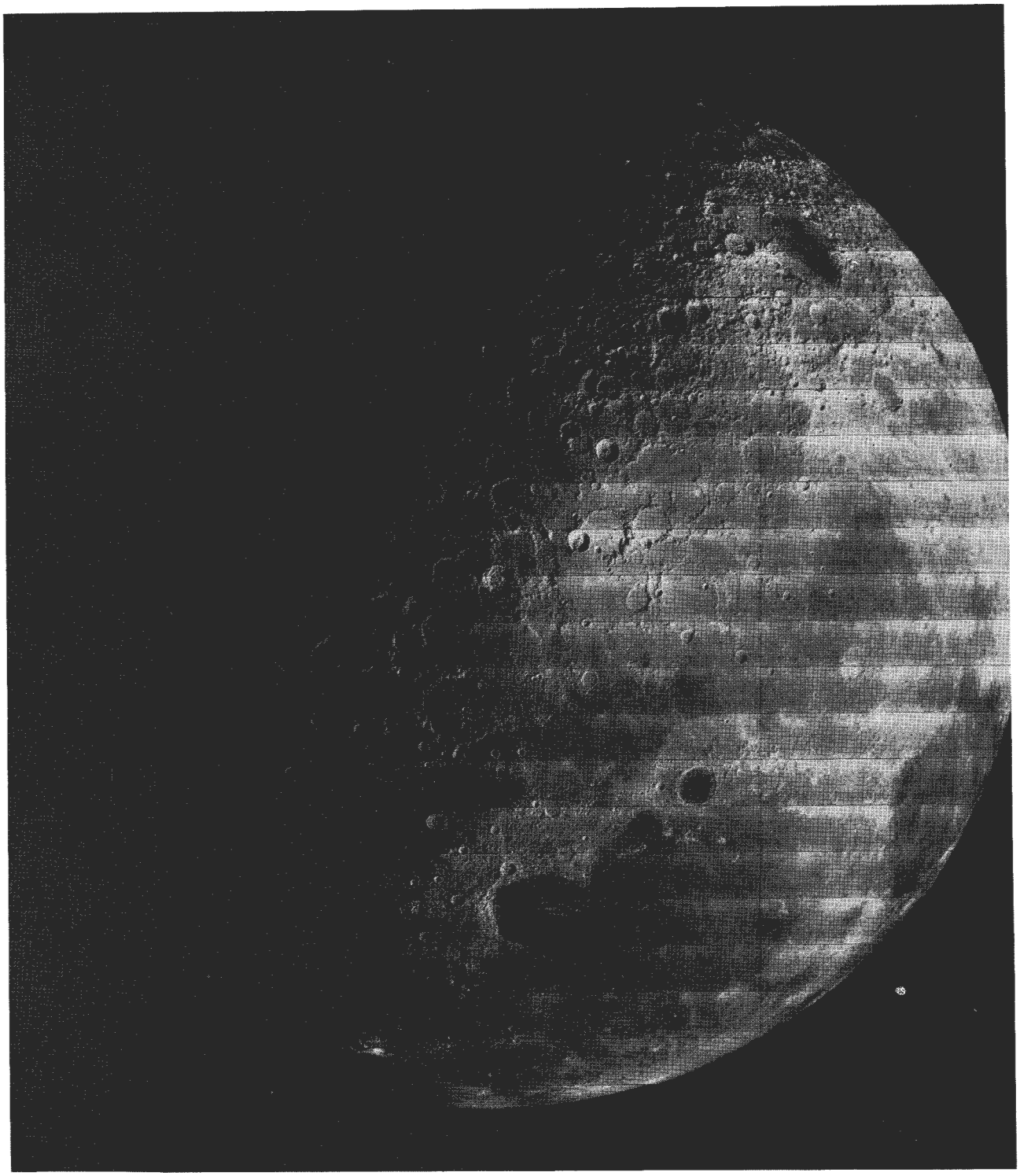

Wide-Angle Frame 152, Site IV27N
Centered at 32.9° W, 71.9° N;
includes Mare Imbrium, Sinus Iridum, Pluto,
north-northwest limb, and farside areas.

1.0 Introduction

The Lunar Orbiter program was formalized by Contract NAS1-3800 on May 7, 1964, as one of the lunar and planetary programs directed by the NASA headquarters Office of Space Sciences and Applications. The program is managed by the Langley Research Center, Hampton, Virginia, with The Boeing Company as the prime contractor. Lunar Orbiter is the third in a succession of unmanned missions to photograph the Moon and to provide lunar environmental data to support the Apollo manned lunar landing mission.

1.1 PROGRAM DESCRIPTION

The primary task of the Lunar Orbiter program was to obtain, from lunar orbit, detailed photographic information of various lunar areas, to assess their suitability as landing sites for Apollo and Surveyor spacecraft, and to improve our knowledge of the Moon. This task was essentially completed during the first three flights. The remaining two spacecraft are now to be used to contribute directly to the solution of the problem of understanding the Moon as an entity.

Site-search missions of potential areas in southern and northern latitude bands within the established Apollo zone of interest ($\pm 5°$ latitude and $\pm 45°$ longitude) were examined by the Lunar Orbiter I and II missions, respectively. Twelve of these sites were rephotographed by a comprehensive integration of vertical, oblique, and forward wide-angle stereo and convergent telephoto stereo photography by the site-confirmation mission of Lunar Orbiter III. Eight candidate sites for early Apollo missions were selected from the data obtained by these three missions. Three sites will be chosen by the Apollo program from this set of eight candidates for the first Apollo landing on the Moon. In addition, secondary-site photography provided extensive coverage of the farside of the Moon and many areas of scientific interest on the nearside of the Moon.

Lunar Orbiter IV's contribution to the scientific knowledge was to perform a broad systematic photographic survey of the lunar surface features at a resolution significantly better than that obtainable from Earth. The coverage pattern included both the near and far sides of the Moon.

It is intended that Lunar Orbiter V's primary mission objective will be orbital photography of selected scientifically interesting areas on the near and far sides of the Moon, and supplemental photography of candidate Apollo sites.

1.2 PROGRAM MANAGEMENT

Successful accomplishment of Lunar Orbiter program objectives requires the integrated and cooperative efforts of government agencies, private contractors, numerous subcontractors, and the worldwide data collection system of the NASA Deep Space Network (DSN). The functional relationship and responsibilities of these organizations are shown in Figure 1-1.

As the prime contractor, Boeing is responsible to the Lunar Orbiter Project Office of the NASA-Langley Research Center for the overall project management and implementation of the complete operating system. Boeing is also responsible for the establishment – with and through the NASA-Langley Research Center – of effective working relationships with all participating government agencies.

The NASA Lewis Research Center supports the Lunar Orbiter program by providing the Atlas-Agena launch vehicle and associated services that are necessary to: (1) ensure compatibility of the spacecraft with the launch vehicle; and (2) launch and boost the spacecraft into the proper cislunar trajectory.

The Air Force Eastern Test Range (AFETR) provides facilities, equipment, and support required to test, check out, assemble, launch, and track the spacecraft and launch vehicle. The AFETR also controls the Atlas launch vehicle trajectory and monitors Agena performance through cislunar injection, separation, and retrofire to ensure orbital separation. Appropriate instrumentation facilities, communications, and data recorders are provided at downrange and instrumentation ships to ensure the availability

of data for boost trajectory control, acquisition by the Deep Space Station tracking radars, and postmission analysis.

The Deep Space Network (DSN) is managed by the Jet Propulsion Laboratory. This network, consisting of the Space Flight Operations Facility (SFOF) and the Deep Space Stations (DSS), provides two-way communications with the spacecraft, data collection, and data processing. Facilities are provided for operational control which interface with Lunar Orbiter mission-peculiar equipment. Support is also provided in terms of personnel, equipment calibration, and housekeeping services.

Goddard Space Flight Center is the agency responsible for the worldwide network of communication lines necessary to ensure prompt distribution of information between the several tracking stations and the Space Flight Operations Facility during the mission and mission training periods.

1.3 PROGRAM OBJECTIVES

The prime project objective of the Lunar Orbiter mission is to secure topographic data regarding the lunar surface for the purpose of extending our scientific knowledge, and selecting and confirming landing sites for Apollo. To accomplish the objective, high-resolution photographic data covering specified areas on the lunar surface and moderate-resolution photographic data coverage of extensive areas are necessary.

Other objectives are to secure information concerning the size and shape of the Moon, the properties of its gravitational field, and lunar environmental data.

Selection of the photo sites for each Lunar Orbiter mission is based on Apollo constraints and preferences as modified to reflect the knowledge gained by preceding missions.

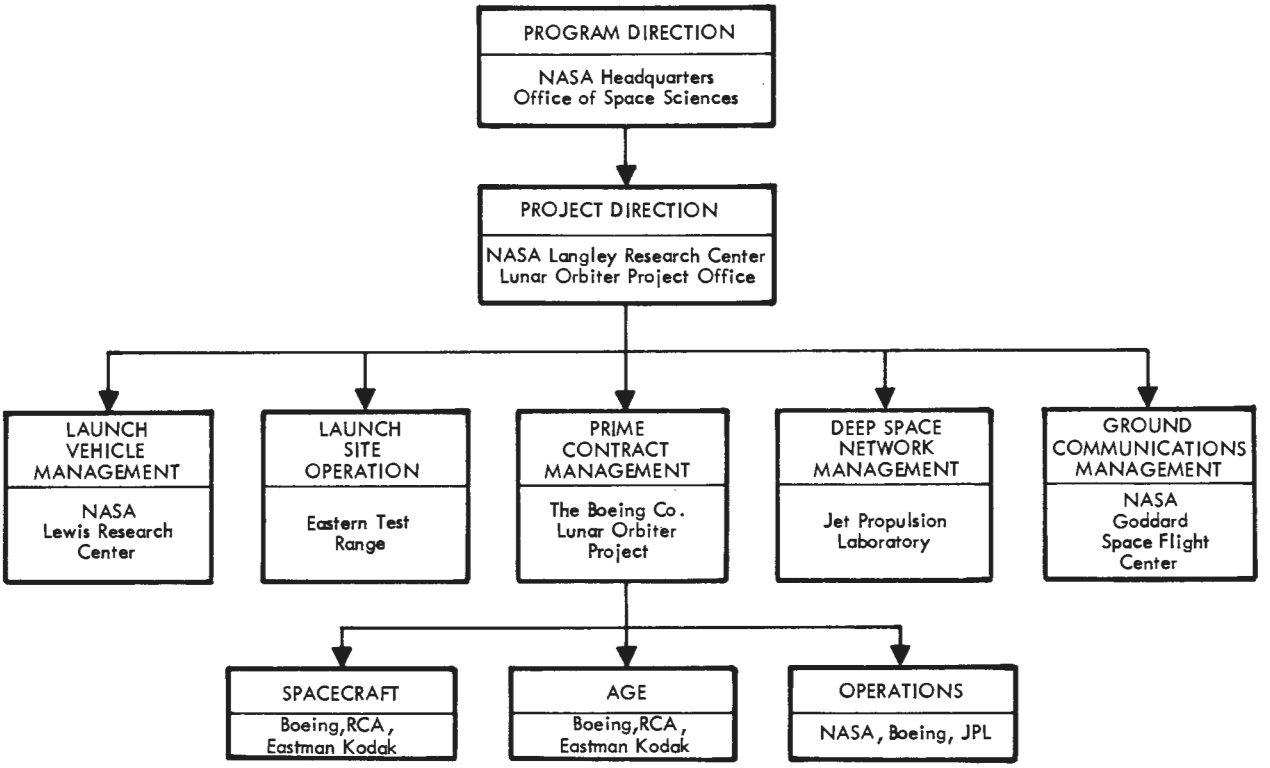

Figure 1-1: Lunar Orbiter Project Organization

Landing sites are desired at a number of locations to fulfill the exploration and scientific objectives of the Apollo program and to provide an adequate launch window. The topography of an Apollo landing module (LM) landing and the approach terrain must be reasonably level to allow satisfactory LM landing radar performance. The surface resolution requirement to enable the selection of suitable sites for Apollo landings is approximately 1 meter.

The selenodetic and environmental mission data objectives require no special instrumentation. Tracking data obtained throughout the mission produce the basic data required to satisfy the selenodetic objectives. Micrometeoroid detectors mounted on the periphery of the spacecraft and radiation detectors mounted internally monitor the lunar environmental data on each flight for transmission to the ground stations.

Completion of the initial primary photographic objectives in the first three missions provided opportunity for expanding program objectives for the remaining two flights. The basic goals of the lunar exploration program, as outlined in the 1963 report of the President's Scientific Advisory Committee, were reviewed to define additional photographic requirements for the Lunar Orbiter program. Additional objectives that were defined to broaden the scientific knowledge required to understand the Moon as an entity are:

- Surveying the entire lunar surface at a resolution significantly better than that obtainable from Earth.
- Examining in detail various surface geological processes identified from this survey.

The photographic results of such a broad survey would be useful not only for identifying interesting targets for the next mission, but would stand for many years as the prime source of data on lunar surface features for planning later exploration of the Moon.

1.3.1 Mission IV Objectives

Specific objectives for Mission IV were defined by NASA as follows:

"Primary:

- To perform a broad systematic photographic survey of lunar surface features in order to increase the scientific knowledge of their nature, origin, and processes, and to serve as a basis for selecting sites for more detailed scientific study by subsequent orbital and landing missions.

Secondary:

- To provide trajectory information which will improve the definition of the lunar gravitational field.
- To provide measurements of the micrometeoroid and radiation flux in the lunar environment for spacecraft performance analysis.
- To provide a spacecraft which can be tracked by the MSFN stations for the purpose of exercising and evaluating the tracking network and Apollo Orbit Determination Program."

The objectives and ground rules for Lunar Orbiter IV stipulated that mission design include the following:

- Contiguous coverage of at least 80% of the lunar nearside at resolutions between 50 and 100 meters.
- Contiguous coverage of as much of the rest of the Moon as possible at the best resolution obtainable.
- Read out all photos in priority readout but have planning available for a final readout if required.
- Conduct the photo mission from the orbit established at lunar injection.
- Satisfy all photo subsystem constraints and capabilities established for prior missions.

Perilune photographic coverage requirements:

- Illumination band from 10 to 30 degrees from the lunar terminator.
- Consecutive series of four exposures parallel to illumination band on each orbit.

- On alternate orbits, photograph the lunar North and South Poles, respectively.
- Extend coverage beyond 90° W longitude if time and attitude control system nitrogen gas are available.

Apolune photographic coverage is restricted by the general illumination of the Moon and because the area directly under the spacecraft is in shadow. Within the limitations imposed by the relative position of the camera axis and the Sun's rays, the camera optical axis will be tilted toward the Sun to place the telephoto footprint in the lighted area. Where this is not possible, the wide-angle coverage will contain the lighted part and the telephoto coverage may be of the shadow area.

1.4 MISSION DESIGN

The Lunar Orbiter spacecraft was designed around its photo subsystem to ensure the maximum probability of success of the photographic mission. Similarly, the mission design maximized the probability of quality photography by placing the spacecraft over the mission target(s) in the proper attitude, altitude, and within the established lighting limitations. Launch vehicle, spacecraft, and photographic considerations were integrated into the design effort to optimize the trajectory and sequence of events to satisfy mission photographic objectives.

Selection of the trajectory was based on conditions that must be satisfied, such as:

- Transit time (Earth to Moon) of approximately 90 hours.
- Midcourse maneuver to alter the injection aiming point from launch vehicle targeting to facilitate injection into near-polar orbit.
- Initial lunar orbit apolune altitude of 6,290 kilometers, perilune altitude of 2,520 kilometers, and orbit period of 12 hours.
- A plane change of approximately 11 degrees at lunar injection to achieve the required near-polar orbit.
- Orbit inclination of approximately 85 degrees at the lunar equator.
- Ascending-node photography on near-side for Canopus acquisition.
- Argument of perilune on lunar equator for equal north-south resolution.
- Posigrade orbit for visibility of injection.

Trajectory and orbit data used for mission design were based on computations using Clarke's model of the Moon with Earth effects. The data used were the output of computer programs covering the following phases:

- Translunar Search Program;
- Translunar Orbit Description Program;
- Lunar Orbit Description Program.

Table 1-1 tabulates launch window characteristics for the May launch periods. The nominal sequence of events presented in the mission event sequence and time line analysis was

Table 1-1: Launch Window Summary

Launch Date (GMT)	Launch Window (GMT)			Launch Azimuth (deg)	
	Start	End	Duration	Start	End
May 4-5, 1967	20:57	00:10	3 hr 13 min	90.0	114.0
5-6 "	20:58	00:22	3" 24"	90.6	114.0
6-7 "	21:03	00:39	3" 36"	91.7	114.0
7-8 "	21:00	01:05	4" 5"	91.5	114.0

based on a launch time approximately 1.6 hours into the first launch window.

The trajectories required to accomplish the photographic objectives during these launch periods were documented in the form of:

- Targeting specifications for the booster agency for a 21-degree orbit inclination mission;
- Tabulated trajectory data;
- Tracking and telemetry coverage plan;
- Mission error analysis;
- Alternate mission studies.

The set of orbit parameters that provided the required coverage of the photo sites determined the sequence and timing of events to obtain the desired photo coverage. Other factors that affected photo subsystem sequences included such operational or spacecraft performance limitations as:

- Start readout no sooner than 18 minutes after earthrise or gap between DSIF view periods to ensure spacecraft acquisition and photo subsystem video adjustments;
- Interval of 18 minutes between end of processing and start of readout to allow TWTA warmup and video adjustments;
- Interval of 5 minutes between end of readout and start of processing to turn off readout and activate processor;
- After initiating photography, process at least two frames every 4.8 hours to reduce Bimat dryout;
- Read out all photos in priority readout.

Optimizing these requirements resulted in a series of photographic sequences that repeated every second orbit. Figure 1-2 shows the sequence of events for every orbit except as indicated for the polar photographs. The circled photograph letters are coded in the same manner as the footprint locations in Figure 1-3.

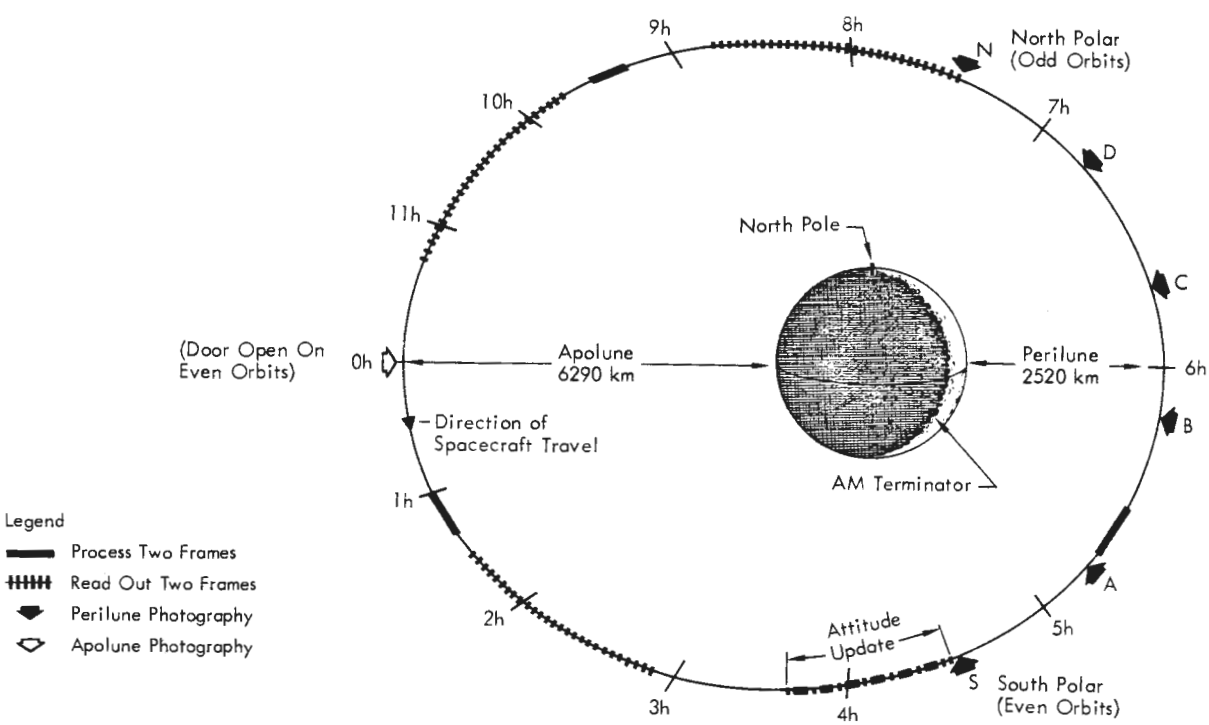

Figure 1-2: Photo Orbit Sequence of Events

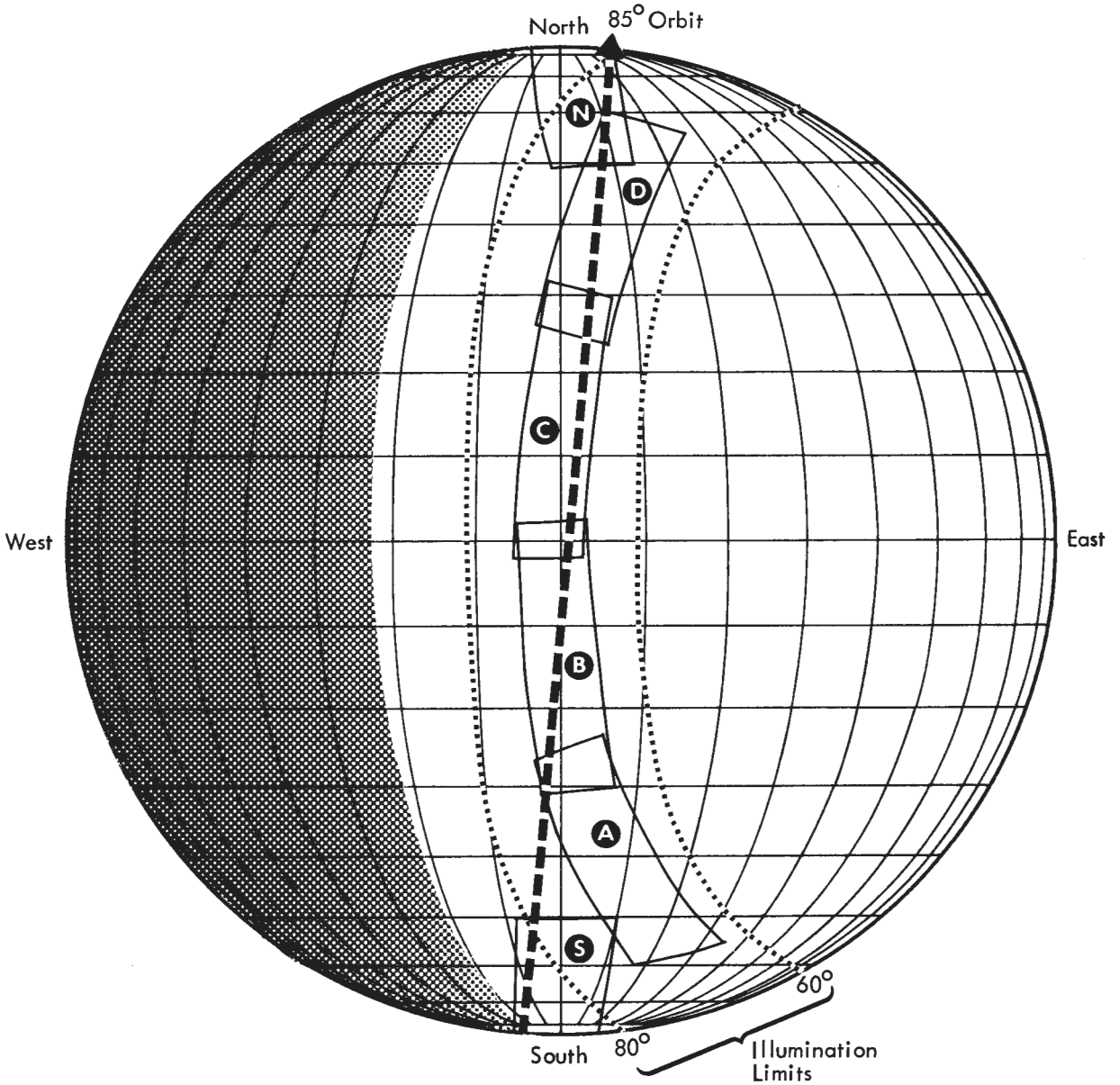

Figure 1-3: Footprint Orientation

Telephoto coverage of perilune photography with respect to the illumination band and orbit track are shown in Figure 1-3. Photos A through D were taken on each orbit while the N photo was taken only on odd orbits and the S photo was taken on even orbits. Successive orbits provided a minimum side overlap of 15% to allow for camera pointing errors and orbit uncertainties. Nearside photography – from 90° E to 90° W longitude – required 29 successive photo orbits (with five single-frame sequences on all orbits except the initial photo pass, which contained five four-frame sequences) to cover 99% of front surface. The static resolution of these photos met or exceeded the mission specification of 100 meters. Provisions were also incorporated in the mission design to extend perilune photography from 90 to 120° W longitude if desired and within the available nitrogen gas supply with no reduction in resolu-

tion, or single photos could be taken at the equator of each orbit providing 460-meter resolution between ±45° latitude by the wide-angle camera. An operational decision was required during the mission to select one of these western limb options or to terminate perilune photography at approximately 90° W longitude.

Apolune photography was based on the coverage obtained by the wide-angle lens system. Nearside illumination requirements placed the terminator at approximately 120° W longitude on the first photo orbit. Therefore, the area between 90 and 120° W longitude was not illuminated for apolune photography. As perilune photography progressed, the apolune coverage proceeded from 120° W to 90° E longitude. Static resolution of farside apolune photography was about 1,200 to 1,600 meters.

The nominal planned sequence of photographic events from injection into lunar orbit to completion of film processing and the "Bimat cut" command (Orbit 38) is shown in Figure 1-4. The ordinate covers the period of one complete orbit (12 hours, 6 seconds) and the abscissa covers successive orbits during the photographic phase of the mission. Time progresses from the bottom to top; the time at the top of any orbit is identical to the bottom of the next orbit. The bar charts at the top represent the approximate viewing periods of the three primary Deep Space Stations. There were two periods(covering three and eight successive orbits, respectively, as shown)when the spacecraft was not visible from Earth. The figure also shows where the photos were taken with respect to time from orbit perilune as well as the time allotted for film processing and priority readout.

Photography of the nearside of the Moon (90° E and 90° W longitude) was to be accomplished between Orbits 6 and 34. Table 1-2 identifies the spacecraft exposures taken on each lunar orbit. The table further identifies the photo areas covered by general area. The nearside sequence contains a four-frame sequence taken on each orbit. Photos are centered on approximate ±14 and ±42° latitudes. The polar photos are centered at approximately ±72° latitude.

1.5 FLIGHT VEHICLE DESCRIPTION

The Lunar Orbiter spacecraft is accelerated to injection velocity and placed on the cislunar trajectory by the Atlas-Agena launch vehicle.

Spacecraft Description – The 380-kilogram (853-pound) Lunar Orbiter spacecraft is 2.08 meters (6.83 feet) high, spans 5.21 meters (17.1 feet) from the tip of the rotatable high-gain dish antenna to the tip of the low-gain antenna, and measures 3.76 meters (12.4 feet) across the solar panels. Figure 1-5 shows the spacecraft in the flight configuration with all elements fully deployed (the mylar thermal barrier is not shown). Major components are attached to the largest of three deck structures which are interconnected by a tubular truss network. Thermal control is maintained by controlling emission of internal energy and absorption of solar energy through the use of a special paint and mirrors covering the bottom side of the deck structure. The entire spacecraft periphery above the large equipment-mounting deck is covered with a highly reflective aluminum-coated mylar shroud, providing an adiabatic thermal barrier. The tank deck is designed to withstand radiant energy from the velocity control engine to minimize heat losses in addition to its structural functions. Three-axis stabilization is provided by using the Sun and Canopus as spatial references, and by a three-axis inertial system when the vehicle is required to operate off celestial references, during maneuvers, or when the Sun and/or Canopus are occulted by the Moon.

The spacecraft subsystems (as shown in the block diagram of Figure 1-6) have been tailored around a highly versatile "photo laboratory" containing two cameras, a film supply, film processor, a processing web supply, an optical electronic readout system, an image motion compensation system (to prevent image smear induced by spacecraft velocity), and the control electronics necessary to program the photographic sequences and other operations within the photo subsystem. Operational flexibility of this photo subsystem includes the capability to adjust key system parameters (e.g., number of frames per sequence, time interval between

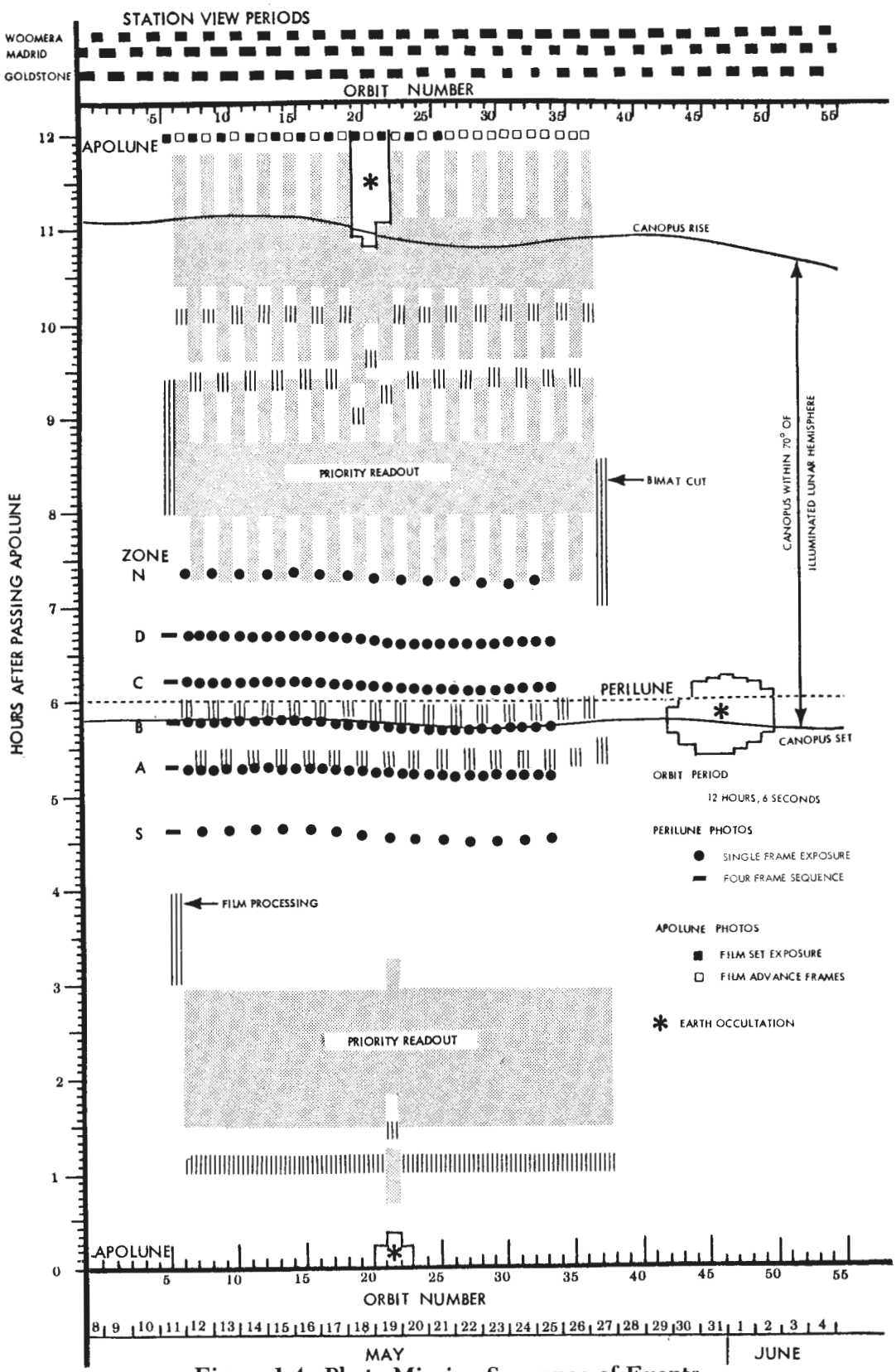

Figure 1-4: Photo Mission Sequence of Events

Table 1-2: Exposure Index

Orbit No.	S/C Exposure No.	Perilune Sequence						Apolune Sequence	
		South			North			Farside	Film Set
		Polar	Temp.	Equat.	Equat.	Temp.	Polar		
6	5 - 25	5 - 8	9-12	13-16•	17-20	21-24		25	
7	26 - 31		26•	27	28	29	30x		31
8	32 - 37	32	33	34	35	36			37
9	38 - 43		38	39	40	41	42		43
10	44 - 51	44	45	46	47	48		50	49,51
11	52 - 57		52	53	54	55	56		57
12	58 - 63	58	59	60	61	62			63
13	64 - 69		64	65	66	67	68		69
14	70 - 75	70	71	72	73	74		75	
15	76 - 81		76	77	78	79	80		81
16	82 - 87	82	83	84	85	86			87
17	88 - 93		88	89	90	91	92		93
18	94 - 99	94	95	96	97	98		99	
19	100 - 105		100	101	102	103	104		105
20	106 - 111	106	107	108	109	110			111
21	112 - 117		112	113	114	115	116		117
22	118 - 123	118	119	120	121	122		123	
23	124 - 129		124	125	126	127	128		129
24	130 - 135	130	131	132	133	134			135
25	136 - 141		136	137	138	139	140		141
26	142 - 147		142	143	144	145		146-147	
27	148 - 153		148	149	150	151	152		153
28	154 - 159	154	155	156	157	158			159
29	160 - 165		160	161	162	163	164	165*	
30	166 - 171	166	167	168	169	170		171+x	
31	172 - 178		172	173	174	175	176	177*,178+	
32	179 - 185	179	180	181	182	183		184+,185+	
33	186 - 192		186	187	188	189	190	191*,192*	
34	193 - 197	193	194	195	196	197			

Recovery photographs:
- * Northern latitudes
- \+ Southern latitudes

- • Door did not open
- x Site not photographed

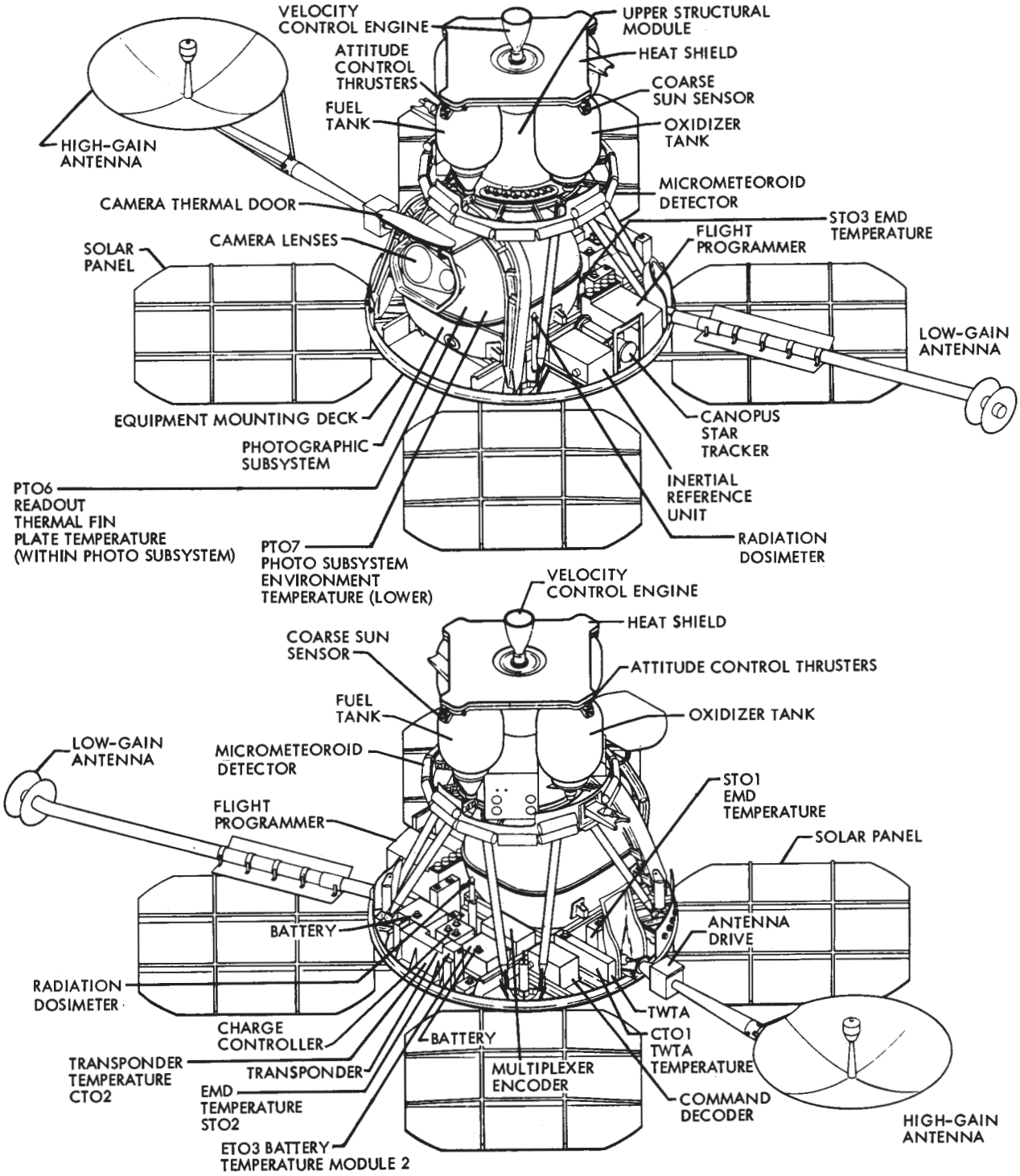

NOTE: SHOWN WITH THERMAL BARRIER REMOVED

Figure 1-5: Lunar Orbiter Spacecraft

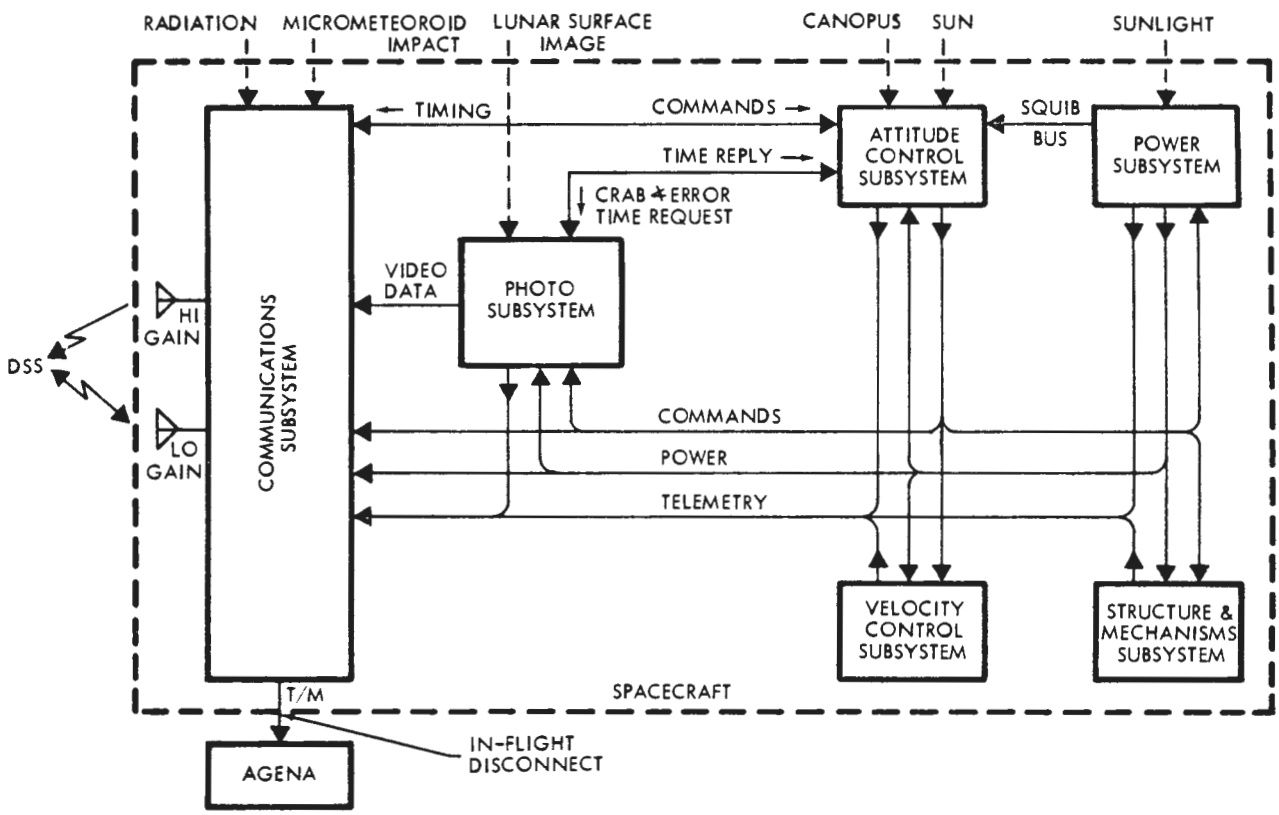

Figure 1-6: Lunar Orbiter Block Diagram

frames, shutter speed, line-scan tube focus) by remote control from the ground.

The influence of constraints and requirements peculiar to successful operation in lunar orbit are apparent in the specific design selected.

- A three-axis stabilized vehicle and control system were selected to accommodate the precise pointing accuracies required for photography and for accurate spacecraft velocity-vector corrections during midcourse, lunar orbit injection, and orbit-transfer maneuvers.

- The spacecraft is occulted by the Moon during each orbit, with predictable loss of communication from Earth. Since spacecraft operations must continue behind the Moon, an on-board command system with a 128-word memory was provided to support up to 16 hours of automatic operation. It can be interrupted at virtually any time during radio communication to vary the stored sequences or introduce real-time commands. The selected programmer design is a digital data processing system containing register, precision clock, and comparators, to permit combining 65 spacecraft control functions into programming sequences best suited to spacecraft operations required during any phase of the mission.

- The communications system high-gain antenna was provided with a ± 360-degree rotation capability about the boom axis to accommodate pointing errors introduced by the Moon's rotation about the Earth.

- Two radiation detectors were provided to indicate the radiation dosage levels in the critical unexposed film storage areas. One detector measured the exposure "seen" by the unexposed film remaining in the shielded supply spool. The second detector measured the integrated radiation exposure seen by

undeveloped film in the camera storage looper. The data from these detectors allow the selection of alternate mission plans in the event of solar flare activity.

The overall operation of taking the lunar pictures, processing the film, and reading out and transmitting the photo video data within the spacecraft is shown in schematic form in Figure 1-7. In addition, the photo reconstruction process at the Deep Space Stations; the 35-mm GRE film copying process at Eastman Kodak, Rochester, New York; and the manual reassembly by NASA and Army Map Service are also shown.

A detailed description of the spacecraft is provided in NASA Report CR 782, *Lunar Orbiter I Photographic Mission Summary – Final Report.* Changes incorporated on Lunar Orbiters II and III are defined in NASA Reports CR 883 and CR (*) – *Lunar Orbiters II and III Photographic Mission Summary – Final Reports,* respectively. Certain other changes peculiar to Mission IV to accommodate spacecraft objectives are listed below.

- Power subsystem charge controller maximum charging current was changed from 2.85 to 1.05 amperes because of continuous polar orbit illumination and to reduce thermal problems.
- Maximum allowable nitrogen storage tank pressure was increased from 3,850 to 4,100 psi to provide the increased maneuver capability necessary for the photo mapping mission maneuver requirements.
- Installed optical solar reflectors on 20% of the equipment mounting deck as an aid to spacecraft thermal control.
- Installed different thermal coating coupons and monitoring telemetry sensors to continue the thermal paint degradation studies.

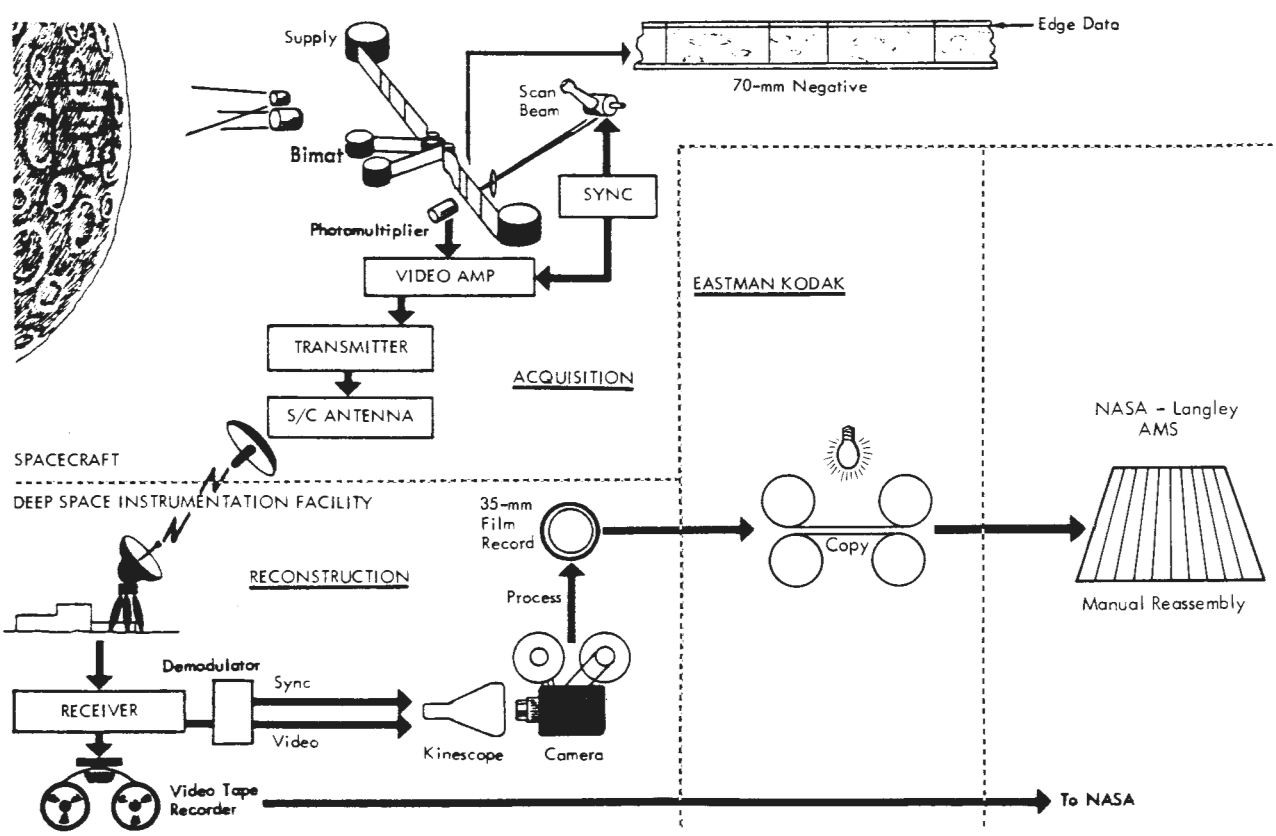

Figure 1-7: Photographic Data Acquisition, Reconstruction, and Assembly

* To be published.

Launch Vehicle – The Atlas-Agena combination is a two-and-a-half-stage vehicle as illustrated in Figure 1-8.

Two interconnected subsystems are used for Atlas guidance and control – the flight control (autopilot) and radio guidance subsystems. Basic units of the flight control subsystem are the flight programmer, gyro package, servo control electronics, and hydraulic controller. The main ground elements of the radio guidance subsystem are the monopulse X-band position radar, continuous-wave X-band doppler radar (used to measure velocity), and a Burroughs computer. The airborne unit is a General Electric Mod III-G guidance package which includes a rate beacon, pulse command beacon, and decoder. The radio guidance subsystem interfaces with the flight control (autopilot) subsystem to complete the entire guidance and control loop. All engines of the SLV-3 Atlas are ignited and stabilized prior to launch commitment.

The upper stage, an Agena space booster, includes the spacecraft adapter and is adapted for use in the Lunar Orbiter mission by inclusion of optional and "program-peculiar" equipment. Trajectory and guidance control is maintained by a preset on-board computer. The Agena engine is ignited twice: first to accelerate the Agena-Lunar Orbiter combination to the velocity required to achieve a circular Earth orbit, and second to accelerate the spacecraft to the required injection velocity for the cislunar trajectory.

The Agena Type V telemetry system includes an E-slot VHF antenna, a 10-watt transmitter, and individual voltage-controlled oscillators for IRIG standard channels 5 through 18 and channel F. Channels 12 and 13 are used to transmit spacecraft vibrational data during the launch phase. Channel F contains the complete spacecraft telemetry bit stream during the launch phase.

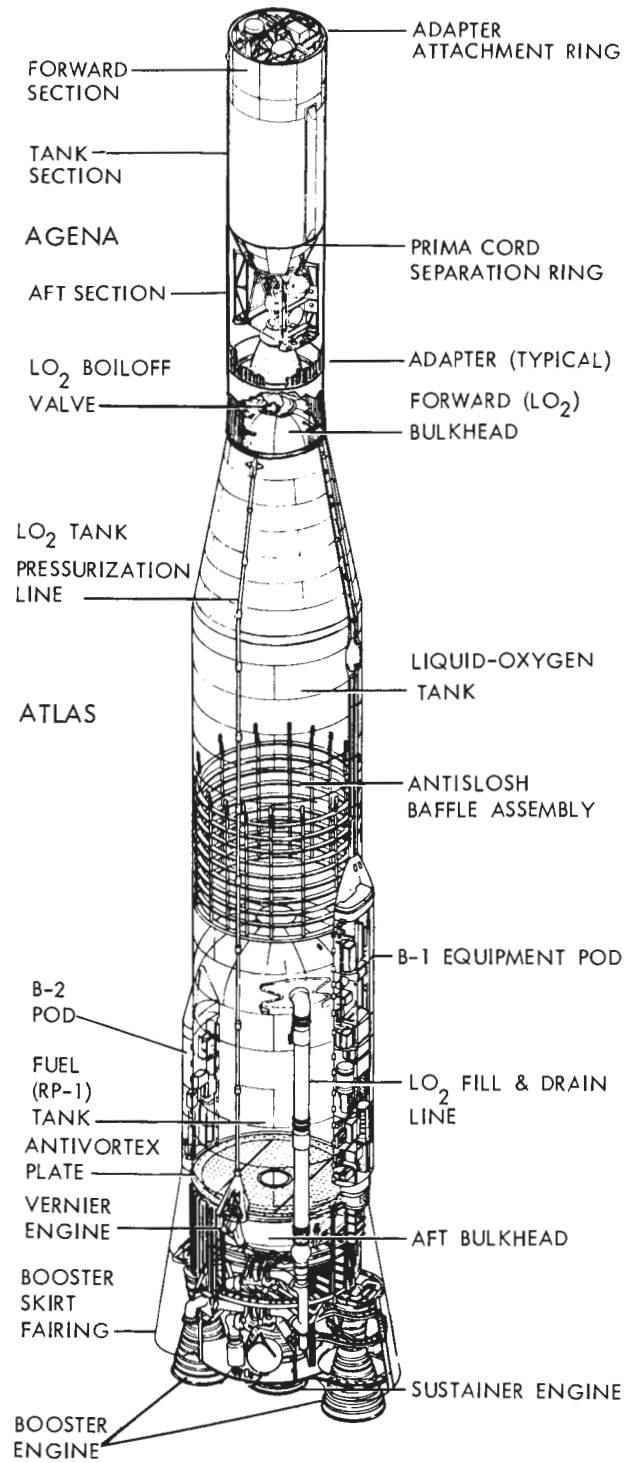

Figure 1-8: Launch Vehicle

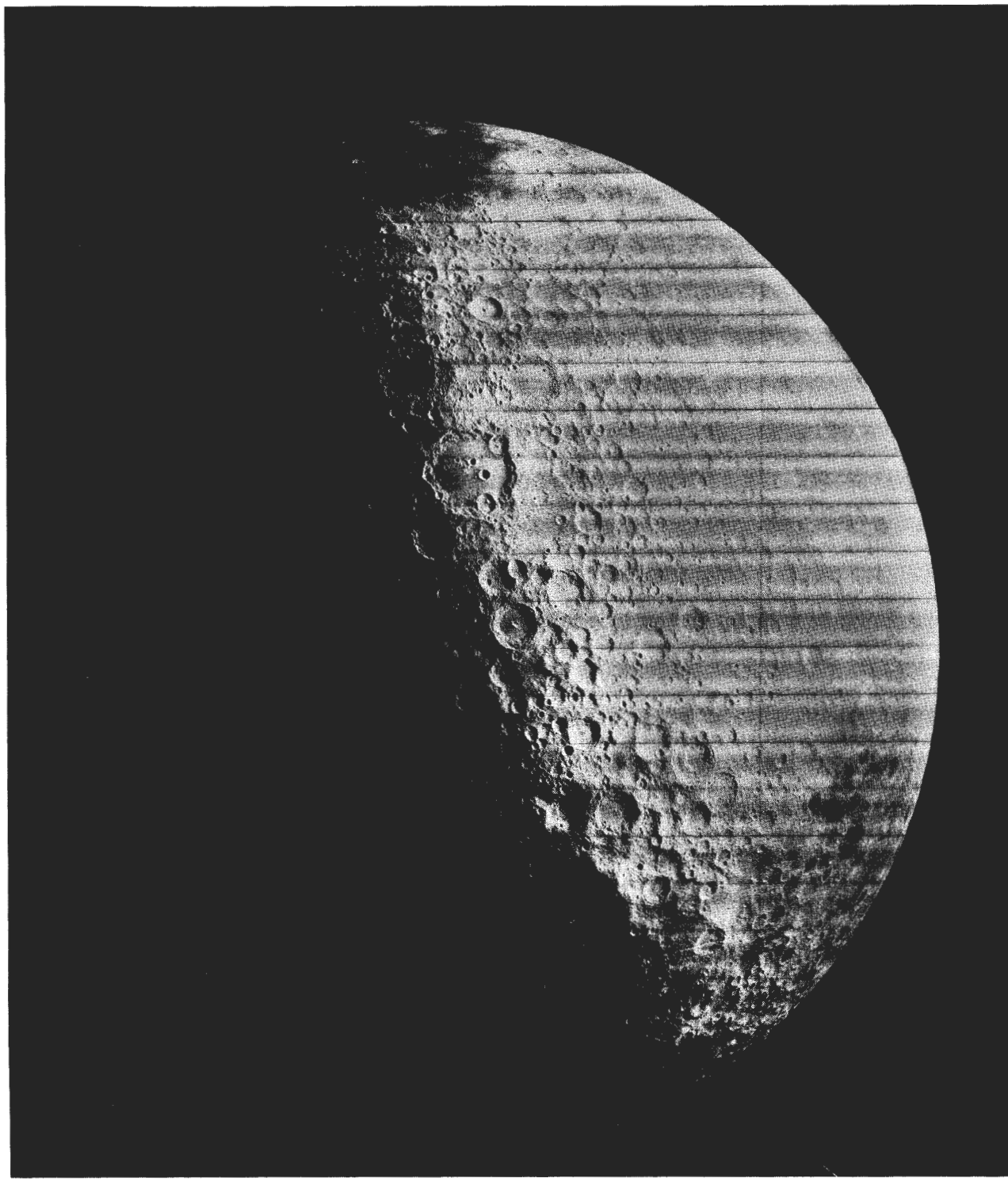

Wide-Angle Frame 118, Site IV22S
Centered at 5.4°W, 72.0°S;
includes Clarius, Moretus, southern limb, and farside areas.

2.0 Launch Preparation and Operations

Lunar Orbiter IV mission preparation started with arrival of the spacecraft at ETR, where it was assembled, tested, and readied for launch. The Atlas-Agena boost vehicle and the Lunar Orbiter spacecraft each received quality acceptance tests at the individual contractor's plants prior to delivery to the AFETR. Early planning included dissemination of information to the launch agency for proper programming of the Atlas-Agena system for the projected launch days. Activities at AFETR of the Atlas, Agena, and Lunar Orbiter spacecraft were integrated so that all systems were properly checked out to support the scheduled launch date. Lunar illumination requirements, Earth-Moon geometry, and Sun-Moon relationships required that these plans be geared to use the available launch windows.

Control of the launch was delegated to the Lewis Research Center, supported by the downrange stations and appropriate instrumentation ships located in the Atlantic and Indian Oceans. Upon acquisition of the spacecraft by the Deep Space Network tracking stations, control of the Lunar Orbiter mission was passed from the AFETR to the Space Flight Operations Facility at Pasadena, California.

The following sections summarize the activities and performance prior to acquisition by the Deep Space Network.

2.1 LAUNCH VEHICLE PREPARATION

The Lunar Orbiter IV launch vehicle consisted of the Atlas SLV-3, Serial Number 5804, and the Agena-D, Serial Number 6633, boosters. Significant prelaunch events in launch vehicle preparation are shown in Table 2-1.

Upon arrival at AFETR, each vehicle was prepared for launch as summarized in Figure 2-1, which shows the test and checkout functions performed in buildup of the integrated flight vehicle.

During normal test and checkout procedures, the following problems were encountered and corrected as indicated.

A brief discussion of the out-of-the-ordinary tasks performed and problems encountered during testing follows.

Table 2-1: Launch Vehicle Preparation Summary

Date	Event
3-1-67	Agena arrived at AFETR
3-2-67	Atlas arrived at AFETR
3-13-67	Atlas erected on Pad 13
3-30-67	Booster flight acceptance composite test (B-FACT) conducted
4-6-67	Fuel and LOX tanking test
4-19-67	Booster adapter mated to Atlas
4-25-67	Second B-FACT conducted
4-28-67	Atlas-Agena mated

2.1.1 Atlas SLV-3

- During the booster final acceptance composite test (B-FACT) on April 25, 1967, prior to opening the main fuel valve at zero time, the sustainer's fuel duct pressure was noted to be at approximately the same pressure as the fuel tank; hence, the sustainer fuel prevalve was replaced. Further testing disclosed that the fuel start tank vent check valve was leaking at a rate of 2080 standard cubic inches per minute. The check valve was also replaced.
- During propellant utilization (PU) calibration tests, the PU valve travelled full open. Subsequent tests disclosed that the current to the PU servo valve was erratic and high. The Rocketdyne hydraulic control package was replaced.
- The following were replaced because of erratic output during system tests: separation bottle pressure transducer, the booster control pneumatic regulator, and the sustainer pneumatic regulator.
- On March 27, 1967, the sustainer pitch feedback voltage indicated an engine hard-over condition. The engine would not respond to command. Investigation resulted in replacement of the sustainer pitch actuator.
- When the staging discrete was inserted at T +130 during testing on April 10, the B programmer failed to initiate BECO and was replaced.

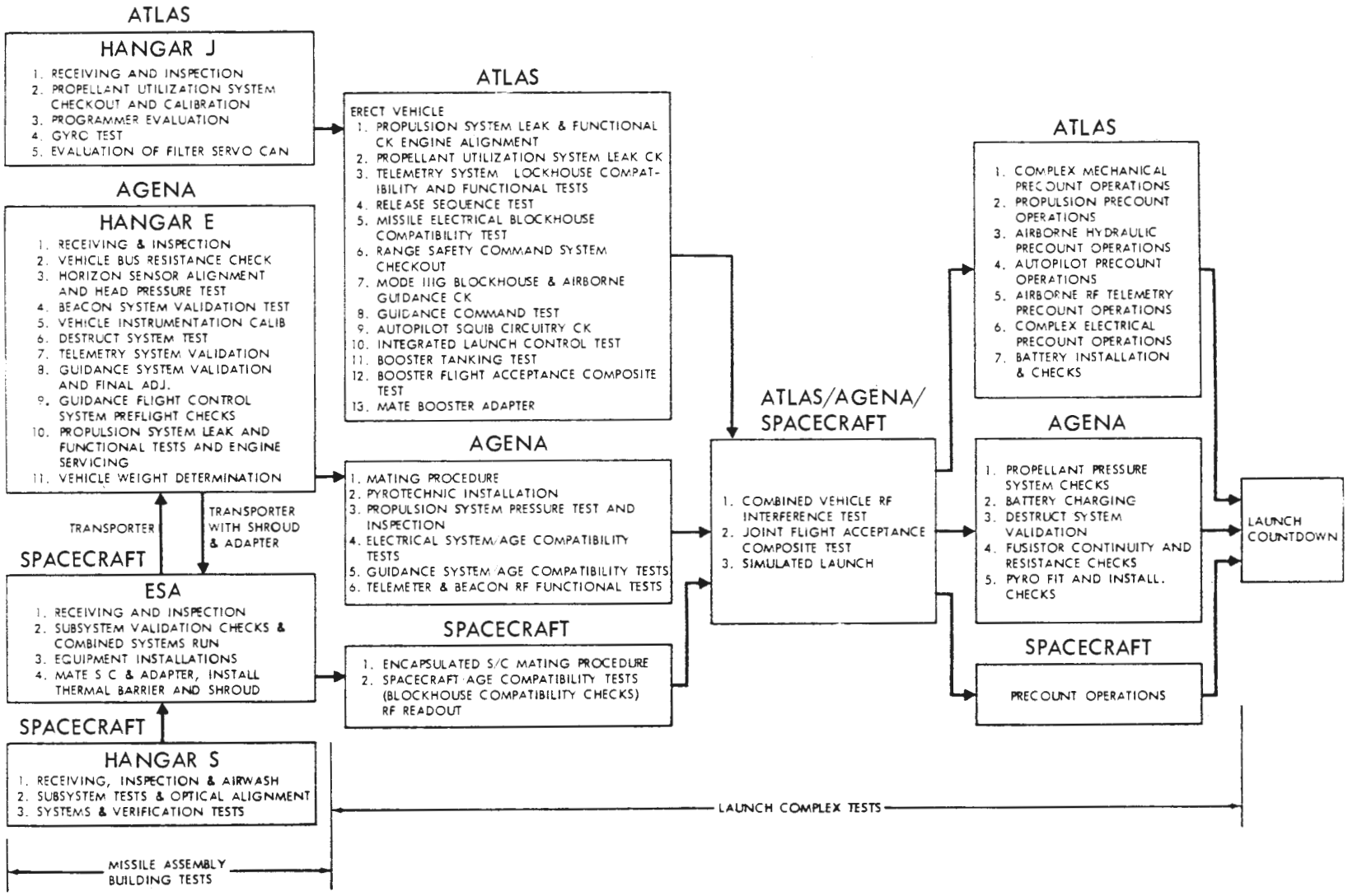

Figure 2-1: Launch Operations Flow Chart

- The telemetry transmitting set was replaced due to a noisy composite signal.

2.1.2 Agena

The Agena-D, Serial Number 6633, arrived at ETR on March 1, 1967 (this later-than-usual arrival was caused by late replacement of the modified propellant isolation valves). The following problems were encountered and corrected during prelaunch testing.

- During receiving inspection, a damaged fuel vent quick-disconnect was discovered and replaced.
- The Agena telemetry transmitter was replaced after tests proved the transmitter frequency was low.
- The velocity meter and counter were replaced just before launch countdown due to a short velocity meter countdown and the inability to load the counter with consistency. Confidence testing was accomplished early in the count.
- As a confidence measure, the turbine pump ball bearings (fuel and oxidizer only) were replaced with bearings having radial clearance on the high side of specifications. Also, the pump oil was changed to MIL D oil.

The several flight acceptance tests performed were conducted with no flight vehicle problems.

2.2 SPACECRAFT PREPARATION

Lunar Orbiter Spacecraft 7 arrived at Cape Kennedy on November 21, 1966, to serve as backup for Mission III. The spacecraft was tested at Hangar "S" and at the explosive safe area. After the February launch of Mission III, Spacecraft 7 was placed in storage until needed for Mission IV.

Spacecraft 3 arrived at Cape Kennedy on March 10, 1967, for use as a backup unit for Mission IV.

On March 23, 1967, Spacecraft 7 was removed from storage and retested in accordance with preflight test requirements documentation. Modifications were made to the spacecraft due to the substantially different type of mission which was to be flown on Mission IV. No significant discrepancies were disclosed by the retests.

On April 13, the spacecraft was moved to the explosive safe area for final testing, installation of ordnance, loading of the photo subsystem, fueling, and final weight and balance checks. Due to a fuel overflow during fuel loading, it was necessary to offload the fuel and refuel the spacecraft. Final weight and balance checks confirmed that the proper amount of fuel was aboard.

On April 25, the encapsulated spacecraft was moved to a Merritt Island launch area storage facility to await arrival of the Agena on the pad. At this time, Spacecraft 3 was brought to the ESA for final testing and fueling. A leaking fill and test valve was discovered and changed on on this backup spacecraft. Encapsulation of this spacecraft provided the capability, if necessary, of exchanging spacecraft and supporting a launch date of May 5, 1967.

2.3 LAUNCH COUNTDOWN

Following matchmate of Spacecraft 7 to the Agena on April 29, tests were conducted to verify impedance and interface compatibility. The joint flight acceptance composite test (J-FACT) took place on May 1, 1967 without spacecraft participation. No launch vehicle problems occurred during J-FACT.

On May 2, 1967, the spacecraft simulated launch was conducted in accordance with the planned time sequences, without launch vehicle participation. All spacecraft systems functioned normally.

On May 4, 1967, the launch countdown started at T-530 minutes. No deviations occurred to the planned countdown. During the planned hold at T-60, the time between Agena spacecraft separation and solar panel deployment was increased from 1 minute 20 seconds to 2 minutes to ensure there would be no contact between the Agena and the deploying solar panels. A simplified countdown sequence for the spacecraft and supporting functions is shown in Figure 2-2.

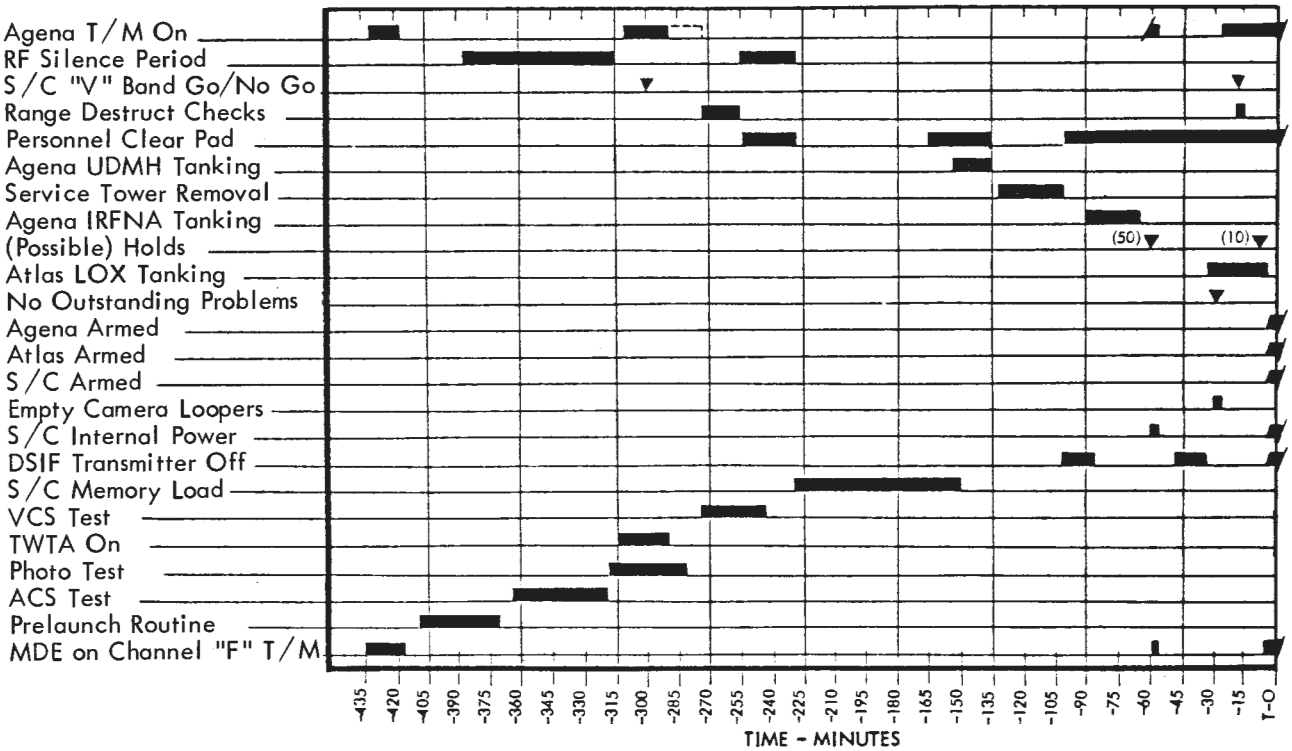

Figure 2-2: Master Countdown Time Sequence

Liftoff occurred on schedule at 22:25:00.571 GMT under favorable weather conditions.

2.4 LAUNCH PHASE

The launch phase covers performance of the Lunar Orbiter D flight vehicle from liftoff through spacecraft separation from the Agena and subsequent acquisition of the spacecraft by the Deep Space Network.

2.4.1 Launch Vehicle Performance

Analysis of vehicle performance, trajectory, and guidance data indicated that all launch vehicle objectives were satisfactorily accomplished.

Atlas objectives were to:

- Place the upper stage in the proper coast ellipse as defined by the trajectory and guidance equations;
- Initiate upper-stage separation;
- Start the Agena primary timer;
- Relay the jettison spacecraft shroud command;
- Start the secondary timer commands of the launch vehicle.

Agena objectives were to:

- Inject the spacecraft into a lunar-coincident transfer trajectory within prescribed orbit dispersions;
- Perform Agena attitude and retro maneuvers after separation to ensure noninterference with spacecraft performance.

All of these objectives were accomplished and the launch vehicle performance was well within the prescribed parameters.

Table 2-2 provides a summary of planned and actual significant events during the ascent trajectory. All times are referenced to the liftoff time of 22:25:00.571 GMT, May 4, 1967.

2.4.1.1 Atlas Performance

All Atlas SLV-3 (Serial Number 5804) systems performed satisfactorily and a satisfactory ascent trajectory was attained. Ambient temperatures, monitored in the thrust section, indicated cool-

Table 2-2: Ascent Trajectory Event Times

Event	Programmed Time (+Sec)	Measured Time (TIM) (+Sec)
Liftoff 2-in. Motion	0.0	22:25:00.571 GMT
Booster engine cutoff	128.9	128.2
Sustainer engine cutoff	288.2	289.4
Start primary sequence timer	292.2	292.1
VECO - uncage gyros, jettison H/S fairings	308.3	310.1
Nose shroud ejection	310.5	312.5
SLV-3 - Agena separation	312.5	315.0
Separation backup (sequence timer)	338.2	338.1
Initiate - 120 deg/min pitch rate	345.2	345.0
Transfer to -3.21 deg/min pitch rate; Pitch H/S to IRP	350.2	350.2
Arm engine control	365.2	365.0
First-burn ignition (90% P_c)	366.4	366.3
First-burn cutoff (V/M cutoff switch)	518.7	518.2
Transfer to -4.20 deg/min pitch rate	542.2	542.2
Horizon sensors to 0.21-degree bias position	545.2	544.8
Second-burn ignition (90% P_c)		1761.24
Second-burn cutoff		1848.66
Agena-spacecraft separation		2013.03

ing trends indicative of cryogenic leakage after 73 seconds of booster operation. This leakage did not affect the thrust output of the booster. Vehicle acceleration reached peak values of 6.2g and 3.1g at booster and sustainer engine cutoff, respectively. Telemetered data and performance calculations indicated that 1,157 pounds of liquid oxygen and 776 pounds of fuel remained at sustainer engine cutoff. This was equivalent to 6.1 seconds of additional engine burn time.

Launch vehicle stability was maintained throughout all phases of Atlas powered flight by the Atlas flight control system. All staging and separation operations and response to guidance steering and discrete commands were satisfactory. The transients and oscillations associated with the staging sequence were normal. Residual angular rates and displacements were essentially zero at vernier engine cutoff (VECO). Postflight evaluation of ground and telemetered vehicleborne data indicated that both the Mod III-A ground station and the Mod III-G airborne-guidance equipment performed satisfactorily. The launch vehicle was acquired as planned and good track was maintained in both the track and rate subsystems until launch plus 374.1 seconds (well beyond Atlas-Agena separation) when the received signal strength was at the noise level. Range rate noise during the sustainer-vernier phase of flight was less than 0.7 foot per second (peak to peak) while the lateral rate noise averaged 0.014 foot per second.

The following coast ellipse and insertion parameters at VECO + 2 seconds were obtained from the guidance-system data.

Semi-major axis	14,512,065 feet
Semi-minor axis	12,707,853 feet
Velocity magnitude	18,518 feet per second
Velocity to be gained	+0.45 foot per second
Filtered yaw velocity	+0.83 foot per second
Filtered altitude rate minus desired altitude rate	+2.39 feet per second

2.4.1.2 Agena Performance

Agena D (Serial Number 6633) performed satisfactorily subsequent to separation from the Atlas and placed the spacecraft on the desired cislunar trajectory.

The primary sequence timer was started 0.1 second earlier than nominal; therefore, all timer-controlled functions were proportionately early. Engine performance calculations, based on telemetered data, showed the average combustion chamber pressure was 517.5 psig and that 16,357 pounds of thrust were developed during the first-burn period. The average turbine speed was measured at 25,273 rpm. Based on a computed total flow rate of 55.82 pounds per second, the specific impulse was calculated to be 293.0 lb-sec/lb. First-burn duration (from 90% chamber pressure to velocity-meter-initiated engine shutdown) was 151.9 seconds, 0.4 second shorter than predicted. Engine performance evaluation during the second burn was based on limited data retransmitted from a range instrumentation ship. This data indicated that the burn period was 87.3 seconds, 0.1 second longer than predicted.

Velocity meter performance during the first burn was satisfactory and the telemetry remained in the accelerometer output mode through loss of signal at Antigua. The last observed tailoff pulse occurred 543.3 seconds after launch.

Programmed pitch and roll maneuvers during the Atlas booster operation were sensed by the caged Agena gyros. Small disturbances were also noted at BECO and booster staging. Minor roll and yaw oscillations were recorded during the Atlas sustainer engine operation. Normal vehicle disturbances were recorded at engine ignition and were negligible at engine shutdown.

Performance of the Agena computer was satisfactory in controlling vehicle attitude during both the Earth orbit period and the cislunar trajectory injection maneuver.

2.4.1.3 Spacecraft Performance

Spacecraft performance during the period from liftoff to acquisition by the Deep Space Network was satisfactory. Operational data indicated

that antenna deployment occurred 1 minute, 57.5 seconds after spacecraft separation. Solar panels were deployed by stored program command and functioning properly 25.8 seconds later.

2.5 DATA ACQUISITION

The Earth track of the Lunar Orbiter IV mission is shown in Figure 2-3. Significant events and planned coverage of the AFETR facilities are shown on this trajectory plot.

The AFETR preliminary test report showed the data coverage presented in the following tables. A list of electronic tracking coverage from all stations is contained in Table 2-3, together with the type of tracking operation employed for each period. Telemetry data recording is summarized in Table 2-4 by recording station and telemetry frequency.

Lunar Orbiter telemetry data were recorded via Channel F of the Agena link and also via the spacecraft telemetry system. Prior to spacecraft separation, spacecraft transmissions (2298.3 MHz) were made with the antenna in the stowed position.

Weather conditions during the launch operation were favorable. The upper wind shears were within acceptable limits. At liftoff, the following surface conditions were recorded.

Temperature	77°F
Relative humidity	71%
Visibility	10 miles
Dew point	66°F
Surface winds	15 knots at 130°, gusting to 21 knots
Clouds	Clear
Pressure (sea level)	30.070 inches of mercury

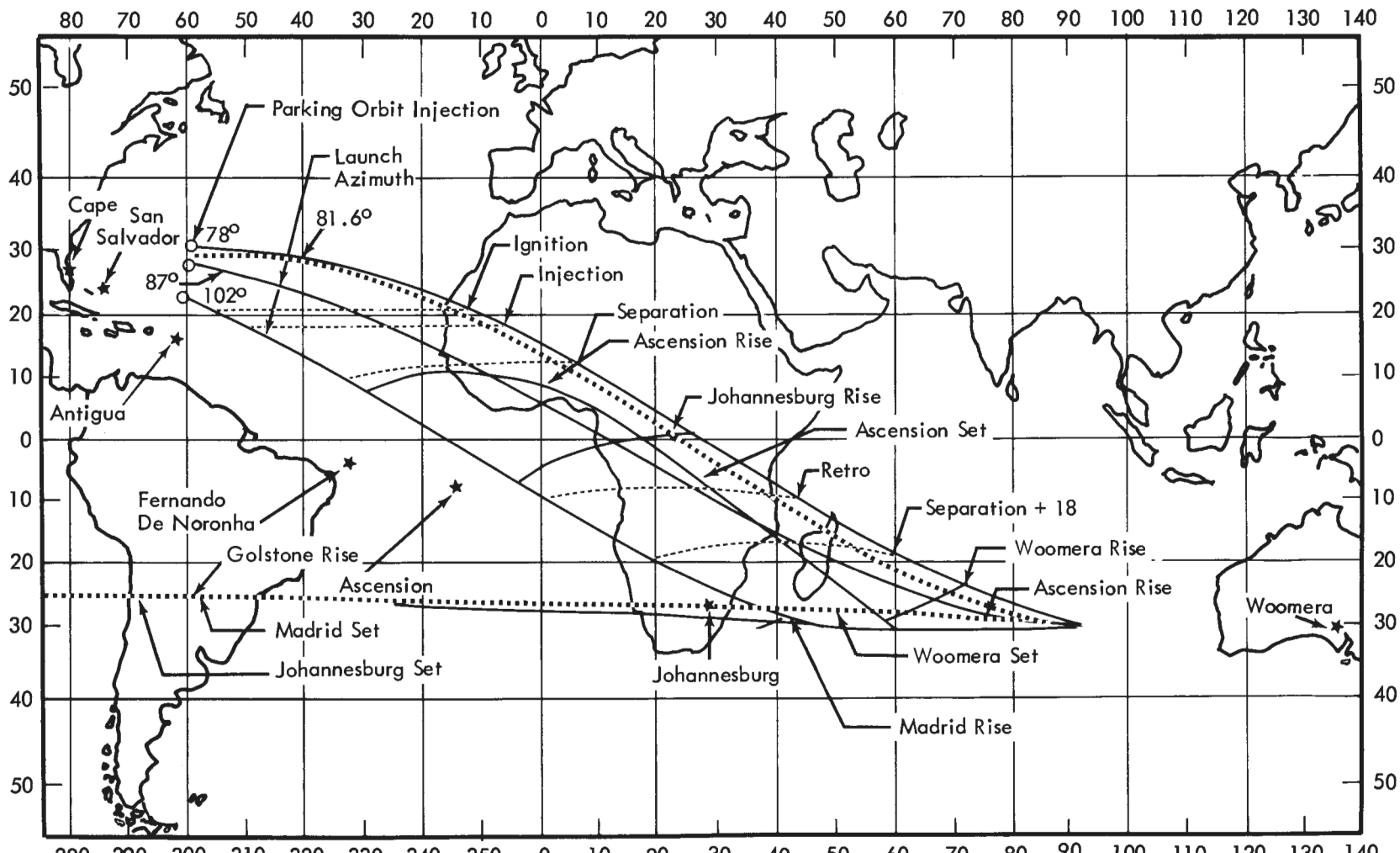

Figure 2-3: Earth Track for May 4, 1967

Table 2-3: AFETR Electronic Tracking Coverage

Location	Radar No.	Period of Coverage (sec)		Mode of Operation*
		From	To	
Radar				
Station 0 Patrick AFB	0.18	14	308	AB
		308	351	AS
		351	473	AB
Station 1 Cape Kennedy	1.1	0	114	IR
		114	126	AS
	1.2	0	2	TV
		2	116	IR
		116	126	AS
	1.16	8	62	AS
		62	265	AB
Station 19 Kennedy Space Center	19.18	13	78	AS
		78	300	AB
		300	370	AS
		370	380	AB
Station 3 Grand Bahama	3.16	80	465	AB
	3.18	92	438	AB
Station 7 Grand Turk	7.18	200	626	AB
Station 91 Antigua	91.18	380	760	AB
Station 12 Ascension	12.18	1,197	1,560	AB
Station 13 Pretoria, Africa	13.16	1,861	2,593	AB
RIS Uniform	T-11-C	2,065	2,630	AB
		2,842	2,854	AB
		4,190	4,583	AB
Special Instrumentation				
Station 1	Tel ELSSE	12	110	F
		4	449	
		13	110	F
		4	459	
		14	110	P
		4	433	

* Modes of Operation:

AB = Automatic Beacon Track
AS = Automatic Skin Track
F = Flight Line
IR = Infrared Track
TV = Television
P = Program

Table 2-4: AFETR Telemetry Coverage

Location		Link (MHz)	Period of Coverage (sec)	
			From	To
Station 1 Tel II	Cape Kennedy	244.3 Agena	-420	481
		249.9 Atlas	-420	476
		2,298.3 Lunar Orbiter	-420	270
Station 1 Tel IV	Cape Kennedy	244.3	-420	491
		249.9	-420	491
		2,298.3	-420	231
		2,298.3	312	467
Station 3	Grand Bahama	244.3	40	522
		249.9	40	522
		2,298.3	105	532
Station 4	Eleuthera	249.9	90	535
Station 91	Antigua	244.3	324	787
		2,298.3	365	760
Station 12	Ascension	244.3	1,173	1,660
		2,298.3	1,178	1,470
Station 13	Pretoria, Africa	244.3	1,780	2,800
		2,298.3	1,856	2,035
		2,298.3	2,074	2,645
Mobile Range Instrumentation Facilities				
RIS Lima		244.3	696	1,141
RIS Whiskey		2,298.3	1,482	1,889
		244.3	1,476	2,003
RIS Uniform		244.3	1,985	4,100
		2,298.3	–	No Lock
RIS Yankee		244.3	2,065	5,330
		2,298.3	2,077	3,407
		2,298.3	3,440	5,330

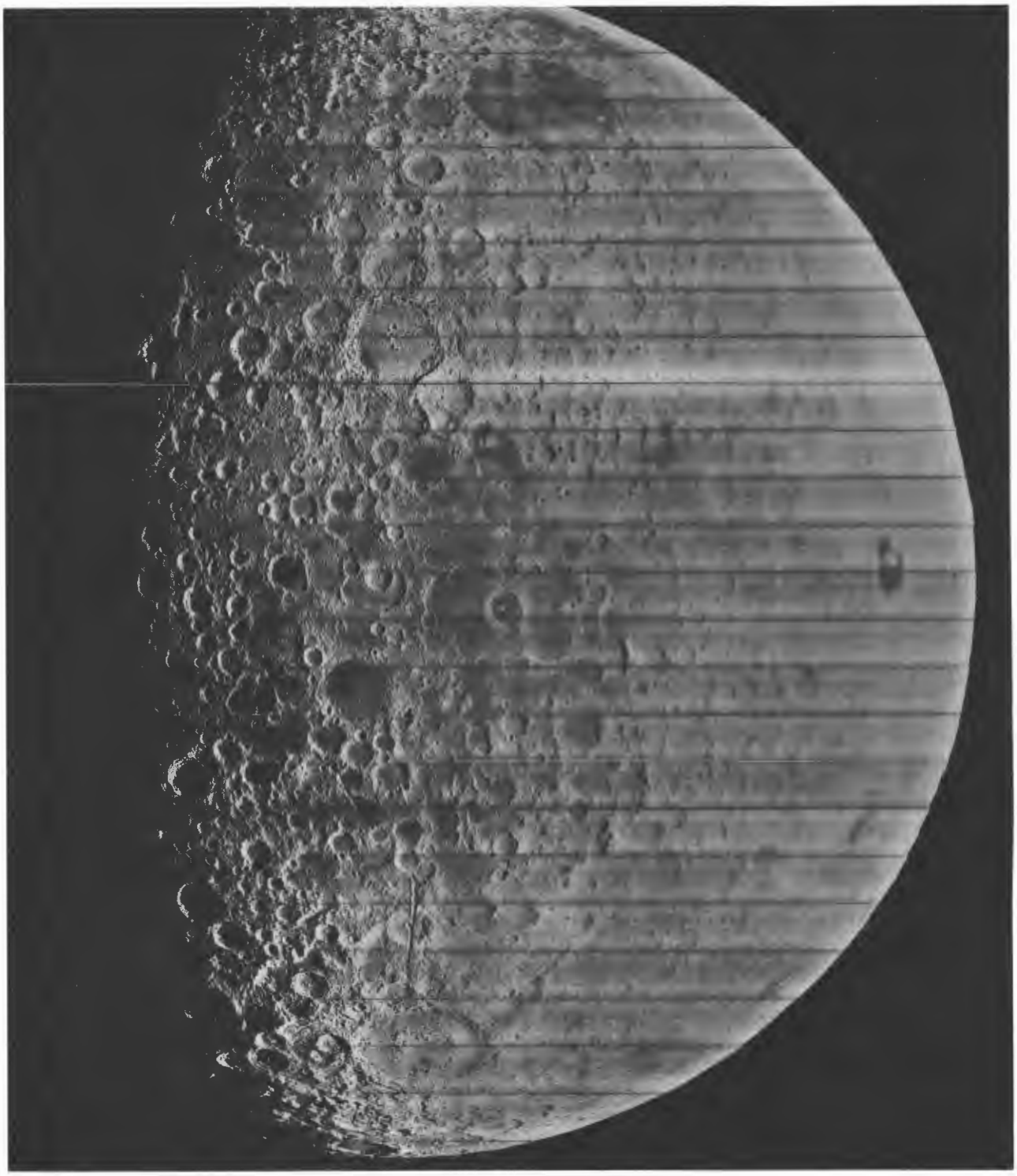

Wide-Angle Frame 9, Site IV6A
Centered at 97.2°E, 42.4°S;
includes Mare Smythii, southeastern limb, and farside areas.

3.0 Mission Operations

Operation and control of Lunar Orbiter IV required the integrated services of a large number of specialists stationed at the Space Flight Operations Facility (SFOF) in Pasadena, California, as well as at the worldwide Deep Space Stations. The Langley Research Center exercised management control of the mission through the mission director. Two primary deputies were employed: the first, the launch operations director located at Cape Kennedy; the second, the space flight operations director located at the SFOF in Pasadena.

Launch vehicle and spacecraft performance after liftoff was monitored in the launch mission control center at ETR by the mission director. Telemetry data was used by the launch team and was relayed in real time to the SFOF through the Cape Kennedy Deep Space Station. This dissemination of spacecraft performance data to the launch and operations teams enabled efficient and orderly transfer of control from Cape Kennedy to the SFOF.

Flight control of the mission was centralized at the SFOF for the remainder of the mission. All commands to the spacecraft were coordinated by the spacecraft performance analysis and command (SPAC) and flight path analysis and command (FPAC) team of subsystem specialists and submitted to the space flight operations director for approval prior to being transmitted to the DSIF site for retransmission to the spacecraft.

Operational performance of the spacecraft and the worldwide command, control, and data recovery systems is presented in the following sections.

3.1 MISSION PROFILE

The Lunar Orbiter IV space vehicle (as previously defined) was successfully launched at 22:25:00.571 GMT on May 4, 1967 from Launch Complex 13 at AFETR. Liftoff occurred at the scheduled time midway in the launch window for May 4, at the flight azimuth of 100.8 degrees identified with Launch Plan 4H.

Figure 3-1 provides a pictorial summary of the 28-day photographic lunar mapping mission of Lunar Orbiter IV. The timing of events from countdown initiation through spacecraft acquisition by the Woomera Deep Space Station are given with respect to the liftoff time. The remaining mission functions are referenced to Greenwich Mean Time. A small inset diagram illustrates the sequence of photographic and attitude control functions repeated on each of the 29 photo orbits. With the exception of rephotographing specific nearside areas from apolune and cutting the Bimat before all of the photos taken were processed, the lunar surface mapping mission was conducted as planned.

Also shown in Figure 3-1 are the major events during the powered portion of the flight necessary to inject the spacecraft on the cislunar trajectory. The major spacecraft functions required to make it fully operational and oriented to the celestial references to achieve and maintain the desired lunar orbit are shown.

The Lunar Orbiter IV spacecraft was acquired by the Woomera, Australia Deep Space Station 49 minutes after launch. Initial performance telemetry data verified that the spacecraft antenna and solar panel deployment sequences had been accomplished. The Sun acquisition sequence was completed 58 minutes after launch. A first attempt to produce a star map and acquire Canopus 6 hours, 50 minutes after launch was unsuccessful due to the presence of light reflections. Approximately 2 hours later a successful star map was produced and Canopus was acquired at 8:26 GMT on May 5.

A relatively large midcourse maneuver (ΔV of 60.85 meters per second) was required, even though the Agena injection was well within design tolerances. This was required because the launch vehicle programming was completed for a mission similar to Lunar Orbiter III (21-degree inclination) prior to definition of the Lunar Orbiter IV photographic mapping mission (85-degree inclination). The maneuver

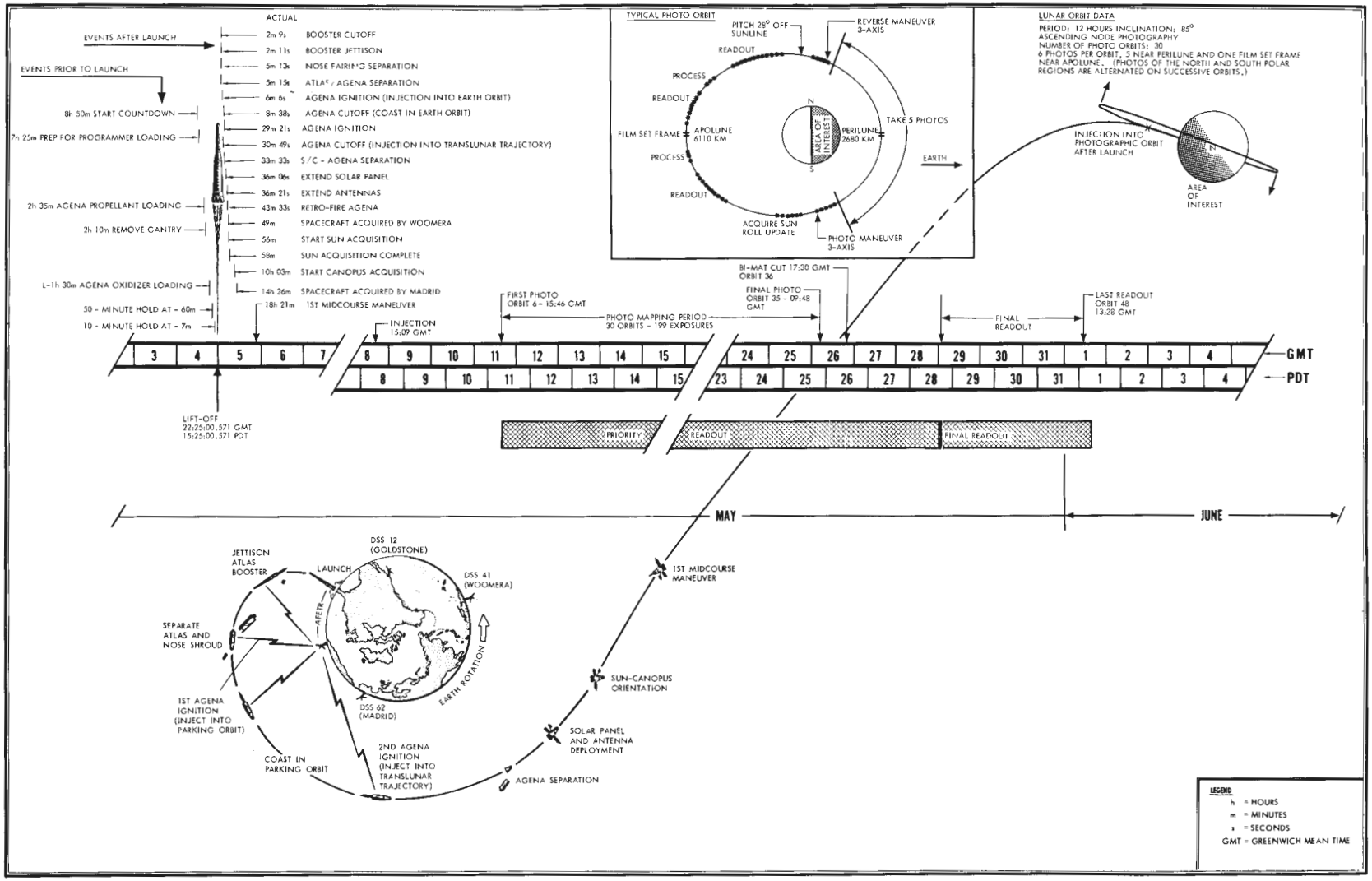

Figure 3-1: Lunar Orbiter IV Flight Profile

was initiated at 16:45 GMT (18 hours, 20 minutes after launch) and successfully completed with 52.3 seconds of engine operation. This maneuver rotated the injection point, in the plane of the Moon, from a 21-degree descending-node orbit to an 85-degree ascending-node orbit. Even though a large midcourse maneuver was necessary, the results were well within design tolerances and the second maneuver was not required.

Injection into the near-polar orbit was initiated 88 hours, 44 minutes after launch and required a velocity reduction of 659.6 meters per second during the 501.7 seconds of engine operation. Initial orbit parameters were: apolune, 6,114 kilometers; perilune, 2,706 kilometers; period, 721 minutes; and orbit inclination, 85.48 degrees. This orbit was used to conduct the photographic mapping mission.

During Orbits 3 and 5, the Goldstone test film in the spacecraft was read out and recorded during two-station visibility periods to verify photo subsystem operation. The first photos were taken on Orbit 6 and consisted of five four-frame sequences in slow mode (nominal 8 seconds between exposures) covering the south polar, mid-latitudes, and equatorial areas. The multiple exposures were required to move the film-leader splice through the photo subsystem in a reasonable period of time. All remaining nearside (perilune) photos were exposed as five single-frame exposures on each orbit, including alternate orbit photos of the north and south polar regions.

Failure of the spacecraft camera thermal door to open for the third photo sequence during Orbit 6 and the first photo during Orbit 7 necessitated changes in operational photo command sequences to ensure continued photography. To compensate for camera lens cooling and prevent moisture condensation on the camera windows and lenses, the spacecraft was oriented so that the oblique sun rays could warm the windows. This maneuver also resulted in light leakage past the baffles producing light fogging of the exposed but unprocessed film, and local degradation in the lunar photographs, which was not detected until the photos were read out. As the mission progressed it was possible by real-time commands to partially close the camera thermal door and maintain reliable opening for camera operations. This procedure eliminated the light leakage and, by reducing the cold-sink source, allowed the window temperature to rise, thereby gradually reducing the window fogging that had occurred.

A plan was developed and implemented during Orbit 29 to rephotograph specific areas where nearside perilune photography was degraded by the above problems. Apolune photos were taken of northern or southern latitude bands as the specific longitudes rotated into the illumination band. During 30 successive orbits, a total of 199 dual frame (wide-angle and telephoto) exposures were taken.

Priority readout was initiated on Orbit 7. Film positioning and readout duration were controlled so that the blank film-set exposures were not read out. Readout was normal for 55 sequences. Beginning in Orbit 24, a spurious and intermittent "readout looper-full" signal occurred that terminated the readout sequence. Alternate procedures were developed and implemented to reset the photo subsystem electronics memory by an automatic restart sequence, thereby enabling readout to continue. During Orbit 35, a spurious "readout looper empty" signal occurred, preventing the readout looper from emptying. When this film could not be advanced through the readout looper to the takeup reel, a decision was made to cut the Bimat before the readout looper was filled, initiate final readout, and recover those photos not read out in priority readout. Film had been processed to Telephoto Frame 196 prior to Bimat cut. The spacecraft film was advanced through a series of short readout and film advance sequences so that the final readout would include the last frame processed.

Final readout was initiated on Orbit 41 and completed on Orbit 48 on June 1. During this period, readout proceeded from Telephoto Frame 196 to Frame 107 as determined by operations directives, since this was the last frame not read out during priority readout. Readout was continuous except for stops at station handover and

occasional spurious "readout looper full" and "empty" signals. Final readout was terminated when all desired photos had been recovered. The exposures read out during Mission IV priority and final readout provided coverage of approximately 99% of the nearside. The high-latitude photographs included some circumpolar farside areas not previously photographed, as shown in Figures 4-23 and 4-24.

Micrometeoroid hits were recorded on May 12 and 18 with no detectable effect or damage to other systems. During the early cislunar trajectory, the spacecraft passed through the equatorial plane of the inner Van Allen belt, where the highest radiation intensity exists. In addition, it passed through a magnetic storm in the outer electron belt. The cassette detector recorded a total of 5.50 rads exposure during this period. Solar flares were reported on May 23 and 25. As a result, the camera looper radiation detector increased from 3 to 66 rads. The maximum rate of change was 6 rads per hour. These radiation levels produced no fogging on the exposed and unprocessed film and no degradation in the photo data was detected.

3.2 SPACECRAFT PERFORMANCE

Lunar Orbiter IV performance has been evaluated with respect to program and specific mission objectives and also as influenced by unusual operational modes induced by flight problems and methods adapted to continue the mission. Accordingly, the performance of each subsystem is discussed in the following paragraphs and contains a brief functional description.

To place the photo subsystem in the proper location and attitude at the right time to obtain the desired photographs, the Lunar Orbiter was required to:

- Change the injection point, in the plane of the Moon, from a 21-degree descending-node orbit to an 85-degree ascending-node orbit by the midcourse maneuver.
- Be injected into a selected orbit about the Moon, whose size, shape, and center of gravity and mass are not precisely known.
- Conduct the photographic mission from a near-polar initial orbit.
- Continue to operate in an unknown radiation environment and in an unknown density of micrometeoroids over an extended period.
- Accomplish a precise two- or three- axis attitude maneuver prior to photographing each specified location and actuate the camera at precisely the commanded time.
- Provide the tracking and doppler signals required to determine the orbit parameters and compute the photographic mission maneuvers.

Failure to satisfy any of these conditions could jeopardize successful accomplishment of the Lunar Orbiter mission. How well Lunar Orbiter IV accomplished these critical tasks is shown in Table 3-1 and is indicative of the control accuracy accomplished by the attitude and velocity control subsystems.

Table 3-1: Trajectory Change Summary

Function	Desired Trajectory	Velocity Change (meters per sec)		Actual Trajectory
		Desired	Actual	
Cislunar Midcourse	Aim $\overline{B}\cdot\overline{T}$ 710 km Point $\overline{B}\cdot\overline{R}$ 9754 km	60.85	60.84	Aim $\overline{B}\cdot\overline{T}$ 726 km Point $\overline{B}\cdot\overline{R}$ 9808 km
Lunar Orbit Injection	Perilune 2700.8 km Apolune 6110.9 km Inclination 85.47 deg Period 720 min	659.62	659.62	Perilune 2706.3 km Apolune 6110.9 km Inclination 85.48 deg Period 721 min

3.2.1 Photo Subsystem Performance

Photo subsystem performance was satisfactory for two thirds of the active photo-taking portion of the mission. Early in the mission, faulty door operation caused the cameras to be exposed to abnormal temperature and lighting conditions which produced local degradation on the spacecraft film. Late in the mission, intermittent internal signals interrupted the normal readout periods and improperly initiated film processing. Alternate operational and control sequences were developed and appropriate commands transmitted to offset these effects and continue the photography readout. The film handling irregularity required the execution of "Bimat cut" shortly before the planned time. The photo mission was concluded when all of the exposed and processed spacecraft film had been read out and recorded. There was no detectable fogging of the spacecraft film from the solar flare activity encountered near the end of the mission.

The Lunar Orbiter photo subsystem simultaneously exposes two pictures at a time, processes film, and converts the information contained on the film to an electrical signal for transmission to Earth. The complete system, shown schematically in Figure 3-2, is contained in a pressurized temperature-controlled container.

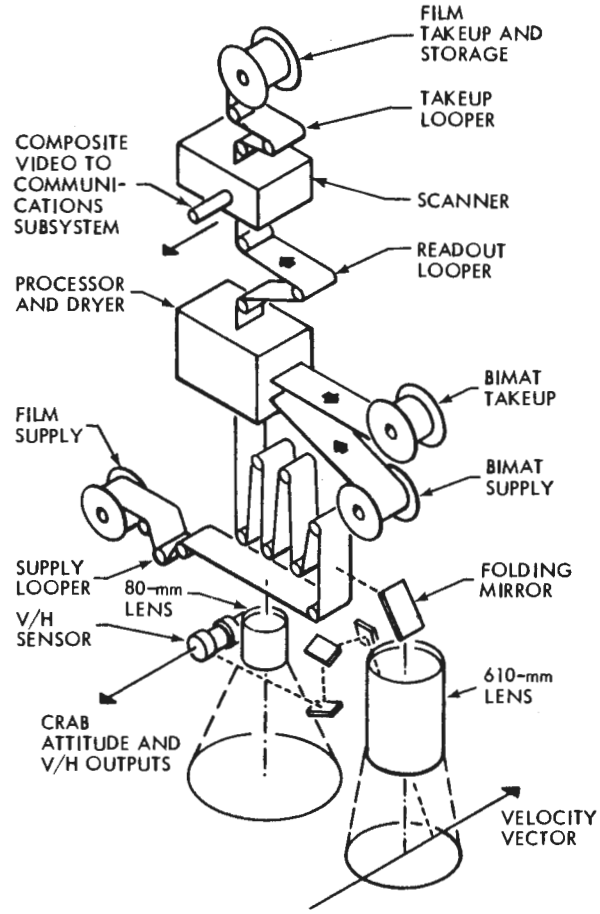

Figure 3-2: Photo Subsystem

The camera system features a dual-lens (telephoto and wide-angle) optical system that simultaneously produces two images on the 70-mm SO-243 film. Both lenses operate at a fixed aperture of f/5.6 with controllable shutter speeds of 0.04, 0.02, and 0.01 second. A 0.21 neutral-density filter is added to the 80-mm (wide angle) lens to nearly equalize light transmission characteristics of the two lens systems.

A double-curtained focal-plane shutter is used with the telephoto lens and a between-the-lens shutter is used with the wide-angle lens. Volume limitations within the photo system container necessitated the use of a mirror in the optical path of the 610-mm lens. This mirror caused reversal of all telephoto images on the spacecraft film (along the long axis of the 610-mm lens format) with respect to the wide-angle system.

An auxiliary sensing system, which operates through the telephoto lens, samples the lunar-terrain image and determines a velocity-to-height (V/H) ratio. This output controls the linear movement of each camera platen to compensate for image motion at the film plane (IMC). The V/H ratio also controls the spacing of shutter operations to provide the commanded overlap. Camera exposure time for each frame is exposed on the film in binary code by 20 timing lights. V/H was not used on Mission IV.

The latent-image (exposed) film is developed, fixed, and dried by the processor-dryer. Processing is accomplished by temporarily laminating the emulsion side of the Bimat film against the SO-243 film emulsion as the film travels around the processor drum.

Photographic data are converted by the readout system into an electrical form that can be transmitted to the ground receiving station. Scanning the film with a 6.5-micron-diameter high-intensity beam of light produces variations in transmitted light intensity proportional to the changes in film density. A photo-multiplier tube converts these variations to an analog electrical voltage, and the readout system electronics adds timing and synchronization pulses, forming the composite video signal shown in Figure 3-3. Thus, it is possible to transmit continuous variations in film tone or density rather than the discrete steps associated with a digital system. The electrical signals are fed to a video amplifier and passed to the modulation selector; transmission is via a traveling-wave-tube amplifier (TWTA) and high-gain antenna.

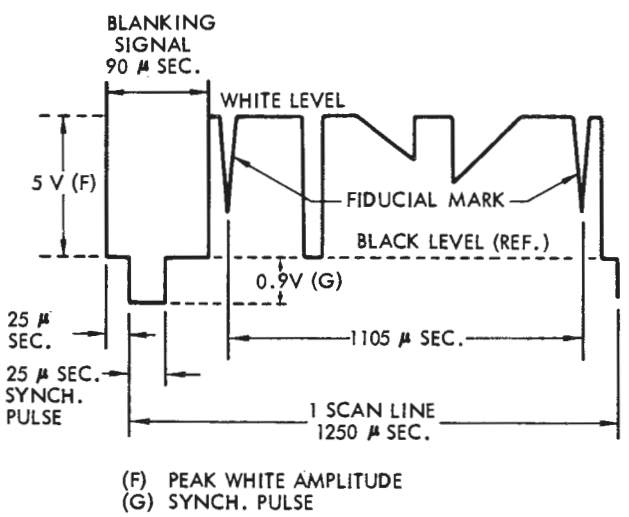

Figure 3-3: Video Signal Waveform

Evaluation of the mission photos showed that performance of the camera and processor was normal for the environmental conditions imposed during the photo mission. Completion of the broad systematic photographic survey of the lunar surface required employment of the photo subsystem in two modes, which exceeded the design or planned operational employment. These were the photography of all sites, subsequent to the first photo orbit sequence, as single-frame sequences with the long axis of the telephoto frame parallel to the direction of motion, and the requirement to read out all photos in the priority readout mode. The single-frame exposures were all satisfactorily performed except for one wide-angle photo. Except where the planned priority readout sequences were interrupted by operational problems, the priority readout requirement was accomplished.

Unlike previous missions, the photo subsystem was exposed to environmental conditions early in the mission which exceeded the design and operational limits and caused some local degradation of the photos. Operational control procedures, developed to counteract the effects of leaving the camera thermal door open, produced adverse effects on the exposed spacecraft film. To offset the cooling effect of the open camera thermal door, the spacecraft was oriented to direct sufficient heat into the photo subsystem to maintain the lens and window temperatures above the dew point. This control concept allowed light to penetrate the light baffle system, between the camera lenses and the photo subsystem shell, and fog the exposed but unprocessed film in the camera looper. Upon review of the first readout of film at Goldstone (concurrently at SFOF), the film fogging problem was recognized; by changing the spacecraft pitch attitude, the light through the baffle system was eliminated. However, condensation was formed on the camera window due to reduced temperature. The camera thermal door was partially closed and the condensation was completely evaporated by Orbit 13. Excellent photographs were obtained for the remainder of the mission.

The "readout looper full" signal terminates readout and initiates film processing as a safety feature under normal circumstances. After successive premature uncommanded readout terminations and processing periods, the processing-readout sequence was reduced from two-frame increments to a single-frame duration. In addition, the readout electronics memory was configured during readout to re-initiate the readout command just prior to the completion of each optical-mechanical scanner cycle during readout. This procedure allowed readout to continue until Orbit 30, May 23. During evaluation of this problem and subsequent

implementation of satisfactory control procedures, two wide-angle and the intervening telephoto exposure were not scanned in priority readout.

Beginning in Orbit 26, intermittent problems related to the spurious "readout looper full" signal were encountered. These were uncommanded initiation of film processing, failure to stop processing with the normal stop command, abnormal operation of film takeup through the readout looper, and failure of the readout electronics to come on when commanded. These abnormal processing operations were initially controlled by commanding "solar eclipse on," which placed the photo subsystem in a complete standby mode and prohibited any processing. By processing all exposed film in the camera storage looper, the processor can also be inhibited while at the same time permitting photo readout to continue. This latter procedure was implemented during Orbit 31 until Bimat was cut. The photo-taking portion of the mission was terminated shortly before the planned time, when the film takeup motor which was inhibited by the faulty signals failed to empty the readout looper. "Bimat cut" was initiated so that the "Bimat clear" indication would occur before the readout looper was full. (This was required so final readout could be performed.) During the next 2.5 days, several especially developed procedures were used to gradually advance the 12 frames of the processed film through the readout system in preparation for initiating final readout.

Final readout, beginning with Telephoto Exposure 196, was initiated on May 29. The readout continued in an essentially normal manner and was considered complete after reading out Wide-Angle Frame 107 because the remaining exposures were obtained during priority readout. During the mission, there were a total of 153 readout periods, of which two were the Goldstone test film and 123 occurred during priority readout.

Analysis of the photo subsystem performance data during the readout and processing abnormalities indicated that the operation was consistent with a faulty indication from the readout looper encoder, resulting in a spurious "full," "empty," or "partial full" signal. Further evaluation showed that one segment of a four-segment shaft position encoder is the common return for each of the above signals. Circuit and logic analysis further showed that these indicated conditions would occur with an intermittent open in this return circuit. Since this segment is conductive, by brush contact, throughout the 360-degree shaft rotation, an intermittent separation of brush contact with the common return segment is the most probable cause of the abnormality. Thus, a simultaneous indication of the three conditions of the looper could exist and the performance of the photo system would be dependent on the actual mode of operation. Additional ground testing of similar encoders failed to produce the failure modes evidenced in flight. In addition, the contact resistance measurements obtained were within established design tolerances.

Although problems were encountered during the mission, changes in operational procedures enabled the recovery of all significant photos taken and processed.

3.2.2 Power Subsystem Performance

Unlike previous missions, the power subsystem solar panels were exposed to the Sun during the entire mission. Battery power was required only prior to solar panel deployment and during the midcourse and injection maneuvers. At all other periods, electrical power was supplied directly from the solar array. Performance of the subsystem was satisfactory in all respects during the entire mission.

All electrical power required and used by the spacecraft is generated by the solar cells mounted on the four solar panels. Solar energy is converted into electrical energy to supply spacecraft loads, power subsystem losses, and charge the hermetically sealed nickel-cadmium battery. The subsystem is shown schematically

in Figure 3-4. Excess electrical energy is dissipated through heat dissipation elements. The shunt regulator also limits the output of the solar array to a maximum of 31 volts. Auxiliary regulators provide closely regulated 20-volt d.c. outputs for the temperature sensors and the telemetry converter. Charge controller electronics protect the battery from overvoltage and overtemperature conditions by regulating the charging current. The 12-ampere-hour battery (packaged in two 10-cell modules) provides electrical power at all times when there is insufficient output from the solar array.

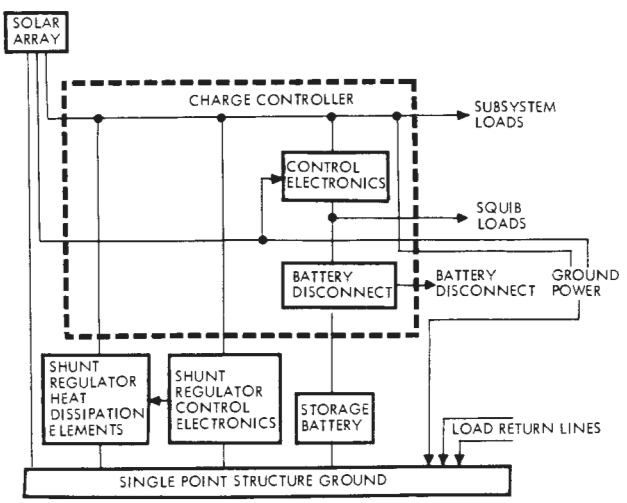

Figure 3-4: Power Subsystem

Each of the four solar panels has 2,714 individual solar cells mounted in a 12.25-square-foot area. The N-on-P silicon solar cells on each solar panel are connected into five diode-isolated circuits. Individual circuits are connected in series-parallel combinations.

The spacecraft battery provided all electrical demands from 6 minutes prior to launch until Sun acquisition approximately 36 minutes after launch. Solar panel deployment and Sun acquisition occurred during a period when performance telemetry was not recorded; it was estimated, however, that the battery was discharged approximately 3.2 ampere-hours for a 24.6% depth of discharge. At 50 minutes after launch, when spacecraft telemetry data was acquired, the solar array was deployed and supplying 12.91 amps at 30.72 volts. The array temperature at this time was approximately 80°F, and the battery was charging at 1.025 amps.

During the midcourse maneuver, initiated 18 hours, 8 minutes after launch, the spacecraft was pitched 67.6 degrees off the sunline. This spacecraft orientation required the use of battery power to meet the electrical load demands for a period of 13 minutes. For the remainder of the cislunar phase, the solar panels were normal to the Sun with an output of 12.85 amps at 30.56 volts. Of this power, 107 watts were required by the spacecraft and about 250 watts were dissipated by the shunt regulator.

The lunar injection maneuver was initiated about 88.7 hours after launch and required a 96.1-degree pitch maneuver. Thirty-one minutes later the Sun was reacquired. Battery power was required to meet the electrical demands for 22 minutes during this period. The total discharge capacity was estimated as 1.93 ampere-hours for a 14.9% battery depth of discharge. For the remainder of the mission, the spacecraft electrical loads were supplied directly from the solar array.

The charge controller circuitry was modified for Lunar Orbiter IV to limit the charging current to 1.05 amps rather than the 2.85 amps used for previous missions. This reduction was based on the mission and trajectory design containing no Sun occultation periods. As a result, the permissible off-Sun angle was increased because the spacecraft load demands were decreased and reduced the heat input to the equipment mounting deck. Representative loads for various spacecraft operating modes are shown in Table 3-2.

Solar array degradation parameters during the photo mission are shown in Figure 3-5. The decrease in the solar intensity is a predictable function based on the Sun-Moon spatial geometry. The change in degradation prior to the solar event was comparable with the results of previous missions. Of interest is the apparent recovery and improvement in the array output beginning about 2 days after the solar event. The

Table 3-2: Spacecraft Load Currents

Operational Mode	Photo Heaters			Spacecraft Loads (Amps)		
	Inhibited	Solar Eclipse On	Solar Eclipse Off	MIN	NOM	MAX
Cislunar	X			3.43	3.62	3.75
Cislunar		X		3.75	4.25	4.55
TWTA On	X			5.23	5.29	5.41
Engine Burn		X		7.64	8.53	8.71
Photo Standby + TWTA			X	5.11	5.90	6.86
Processing + TWTA			X	5.17	6.80	7.52
Readout	X			6.38	6.74	6.80

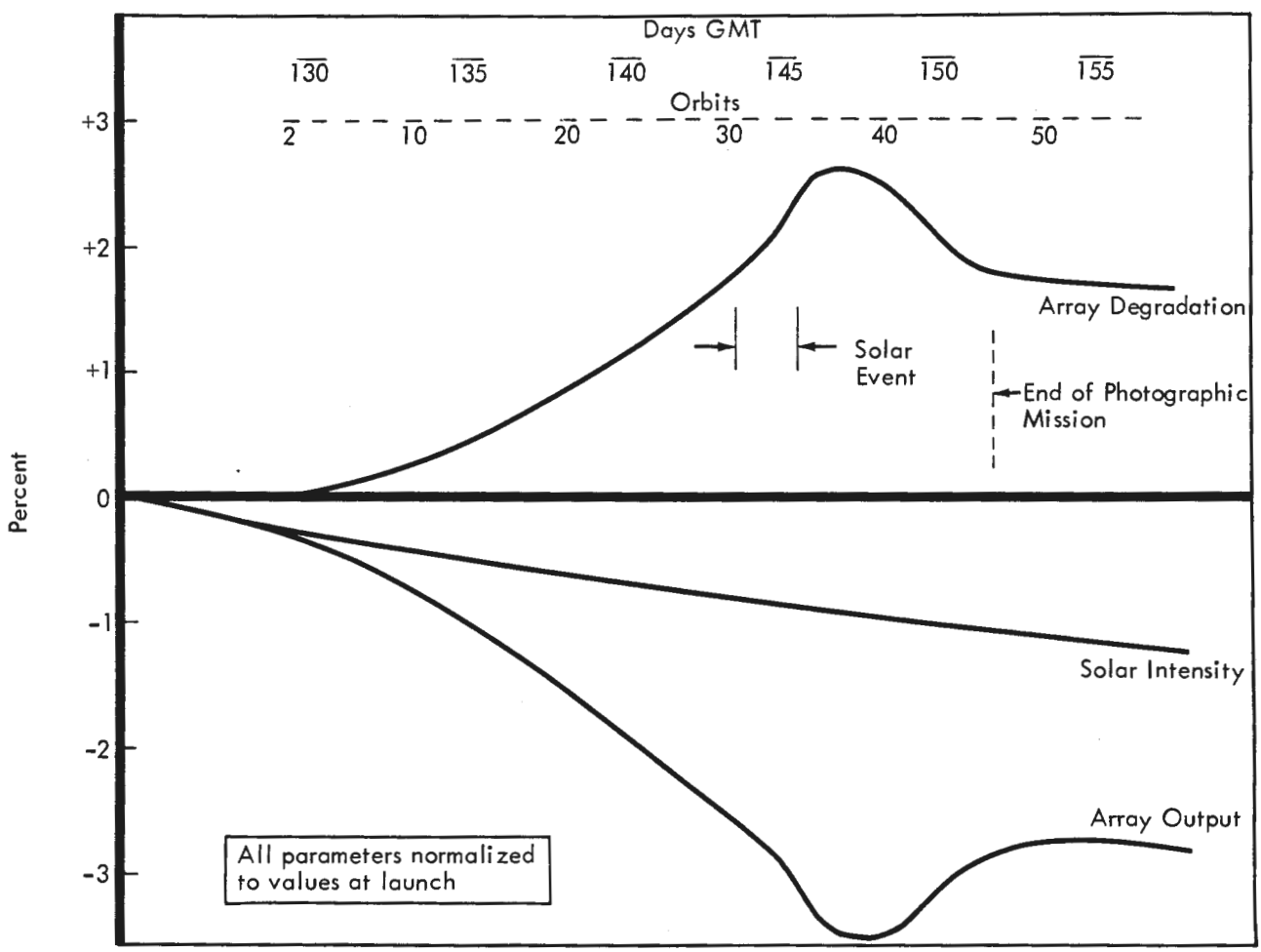

Figure 3-5: Solar Array Degradation

cause of this phenomenon is not understood, but does represent an area where further investigation is indicated.

3.2.3 Communications Subsystem Performance

Although the communications subsystem was operated differently during Mission IV, the performance was satisfactory in all phases. The traveling-wave-tube amplifier was turned on for 90% of the time in lunar orbit and was left on to support Manned Space Flight Network tests during the extended mission. The ground transmission frequency was offset (about 330 Hz) to produce minimum interference with Lunar Orbiters II and III.

The Lunar Orbiter communications system is an S-band system capable of transmitting telemetry and video data, doppler and ranging information, and receiving and decoding command messages and interrogations. Major components of the communication subsystem, shown in Figure 3-6, are the transponder, command decoder, multiplexer encoder, modulation selector, telemetry sensors, traveling-wave-tube amplifier, and two antennas.

The transponder consists of an automatic phase tracking receiver with a nominal receiving frequency of 2116.38 MHz, narrow- and wide-band phase detectors, a phase modulator, and a 0.5-watt transmitter with a nominal frequency of 2298.33 MHz. In the two-way phase-lock mode the transmitted frequency is coherently locked to the received frequency in the ratio of 240 to 221.

The command decoder is the command data interface between the transponder receiver and the flight programmer. To verify that the digital commands have been properly decoded, the decoded command is temporarily stored in a shift register, and retransmitted to the DSIF by the telemetry system. After validating proper com-

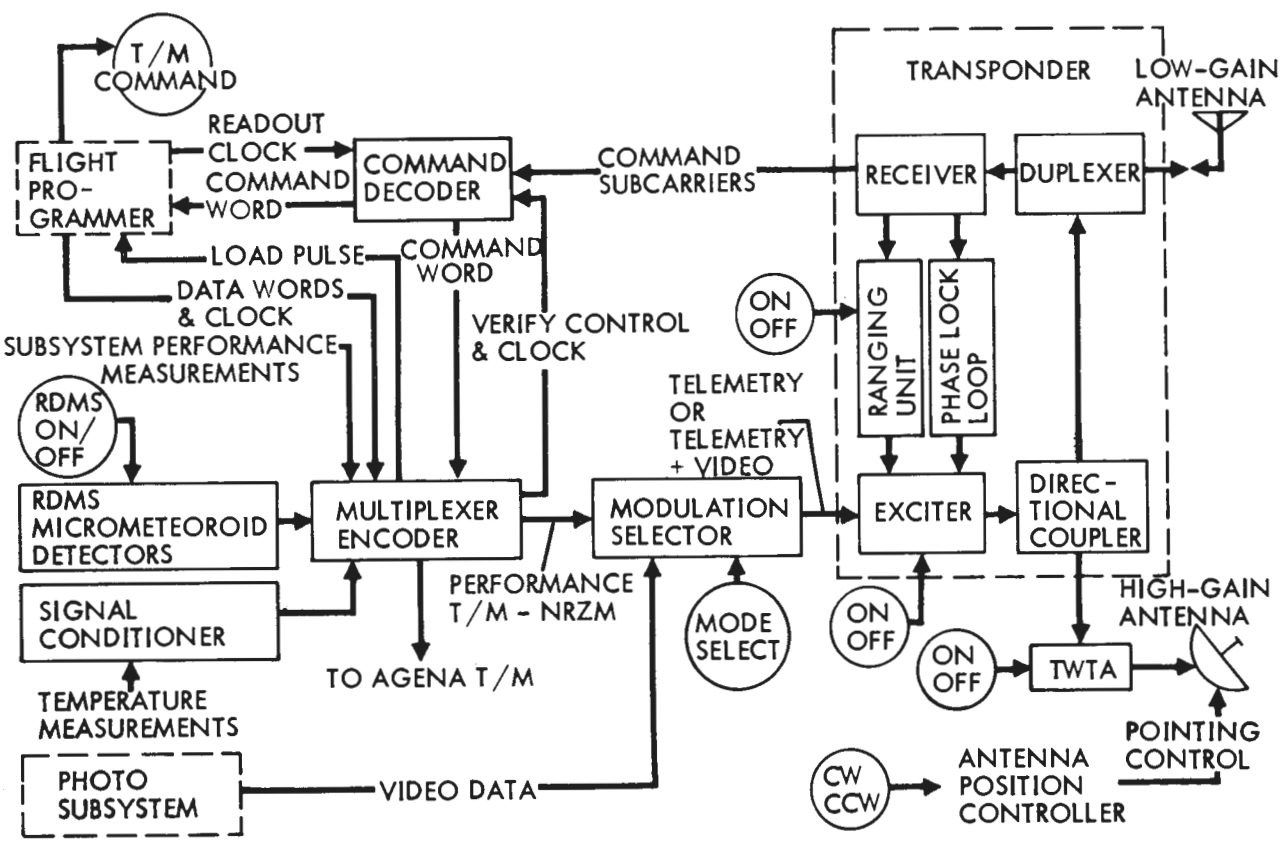

Figure 3-6: Communications Subsystem

mand decoding, appropriate signals are transmitted to the spacecraft to shift the stored command into the flight programmer for execution at the proper time. The command decoder also contains the unique binary address of the spacecraft.

The PCM multiplexer encoder is the central device that puts performance telemetry data into the desired format for transmission. Seventy-seven inputs are sequentially sampled at one sample per frame, and one channel is sampled at eight times per frame in the analog section. The output of these 85 data samples is converted from analog to digital form. The multiplexer also combines the 20-bit flight programmer words, the 133 one-bit discretes, and the four-bit spacecraft identification code into nine-bit parallel output words.

The modulation selector mixes the photo video information and the 50-bit-per-second performance telemetry information for input to the transponder for transmission. The selector receives control signals from the flight programmer to operate in one of the following modes.

Mode	Data Type	Antenna Employed
1	Ranging and performance telemetry	Low Gain
2	Photo video and performance telemetry	High Gain
3	Performance telemetry	Low Gain

(A Mode 4 exists which is implemented by selecting the normal Mode 2 modulation but exercising the Mode 3 transmission method when no video input data are available. The selection of this particular mode increases the available power in the downlink carrier.)

The telemetry system samples the output of sensors within the various spacecraft subsystems. Normal telemetry data channels include such information as temperatures, pressures, voltages, currents, and error signals. Special instrumentation includes 20 micrometeoroid detectors located on the tank deck periphery. Radiation dosage measurement, in the form of two scintillation counter dosimeters and the associated logic, are mounted in the photo subsystem area.

The traveling-wave-tube amplifier (TWTA) consists of a traveling-wave tube, a bandpass filter, and the required power supplies. This equipment, used only to transmit the wide-band video data and telemetry (Mode 2) during photo readout, has a minimum power output of 10 watts. All of the necessary controls and sequencing for warmup of the traveling-wave tube are self-contained.

The spacecraft employs two antennas, a high-gain antenna that provides a strongly directional pattern and a low-gain antenna that is omnidirectional. The low-gain antenna is a biconical-discone slot-fed antenna mounted at the end of an 82-inch boom. The high-gain antenna is a 36-inch parabolic reflector that provides at least 20.5 db of gain within ± 5 degrees of the antenna axis. The radiated output is right-hand circularly polarized. The antenna dish is mounted on a boom and is rotatable in 1-degree increments about the boom axis to permit adjustments for varying relative positions of the Sun, Moon, and Earth.

The Deep Space Station at Johannesburg, Africa (DSS-51) first acquired the spacecraft transmissions 32 minutes after launch at a signal strength of -130.0 dbm, using the acquisition aid antenna. (This was 4.6 minutes before the spacecraft antenna deployment.) Two-way lock was not established due to tracking slew rate constraints imposed on the ground antenna drive system, and track was lost after 8.5 minutes. The Woomera Deep Space Station (DSS-41) acquired the spacecraft approximately 45 minutes after launch with a signal strength of -135 dbm. Two-way lock was established 3.5 minutes later and solid track was maintained for about 7.5 hours. Communications Mode 4 was commanded off 77 minutes after launch.

Overall performance of the communications subsystem in the high-power, low-power, command, and ranging and/or tracking modes was satisfactory. The high-power mode was turned on 15 times and used for 516 hours during the 28-day mission. During the cislunar

phase, the ground transmitter frequency was varied to determine the best lock frequency so that the static phase error was effectively 0 degree. This information was used during the mission to reacquire two-way lock. Otherwise, a predetermined offset (330 to 400 Hz) ground transmitting frequency was used to provide a minimum of interference between Lunar Orbiter IV and the other orbiting spacecraft. This technique worked satisfactorily throughout the mission.

At the completion of the photographic mission, the TWTA was left in the "on" condition. This decision was based on the secondary mission objective to support the manned space flight network stations and evaluation of the Apollo orbit determination program, and to provide the maximum life of this strong signal by reducing the on-off switching cycles, thereby reducing the thermal stresses in the component elements.

3.2.4 Attitude Control Subsystem Performance

Significant differences in orbit parameters (including continuous solar illumination) and mission photo requirements with respect to previous missions resulted in major changes in spacecraft operational employment, maneuver requirements, and environmental control. The 586 maneuvers performed, as compared to the previous mission range of 284 to 383, are indicative of the increased complexity and activity associated with the mapping mission. Although some difficulties occurred during the photo mission, their effect on overall mission performance was minimized by appropriate changes in real-time operational procedures. Subsystem performance was generally satisfactory in supporting all mission objectives.

Execution of all spacecraft events and maneuvers is controlled by or through the attitude control subsystem, Figure 3-7, to precisely position the spacecraft for picture taking, velocity changes, or orbit transfers.

The basic operating modes are:

Celestial Hold – The basic references in this mode are the Sun and Canopus; the gyro systems operate as rate sensors. This mode was planned for use during normal cruise operations and as the initial conditions for all commanded attitude changes. (In practice, Canopus was used as a reference only and the roll axis was maintained in inertial hold.)

Inertial Hold – The basic references in this mode are the three gyros operating as attitude-angle sensors. This mode was used during all attitude and velocity change maneuvers.

Maneuver Mode – In this mode the spacecraft acquires the commanded angular rate about a single axis. The remaining two gyros are held in the "inertial hold" mode.

Engine On, Inertial Hold – This mode is similar to the previously defined "inertial hold" mode except that the pitch and yaw error signals during the velocity change are also used to control the engine actuators.

Limit Cycling – The spacecraft is commanded to maintain a position within ± 0.2 degree for all photographic and velocity control maneuvers or whenever commanded. (The normal deadband is ± 2 degrees.)

Control Assembly – The onboard digital programmer directs the spacecraft activities by either stored-program command or real-time command. The unit provides spacecraft time, performs computations and comparisons, and controls 120 spacecraft functions through real-time, stored, and automatic program modes. The information stored in the 128-word memory is completely accessible at all times through appropriate programming instructions.

The inertial reference unit maintains the spacecraft attitude. Three gyros provide appropriate rate or angular deviation information to maintain proper attitude and position control. A linear accelerometer provides velocity change information in increments of 0.1 foot per second to the flight programmer during any firing of the velocity control engine.

Sun sensors are located in five positions about the spacecraft to provide spherical coverage and ensure Sun acquisition and lock-on and the

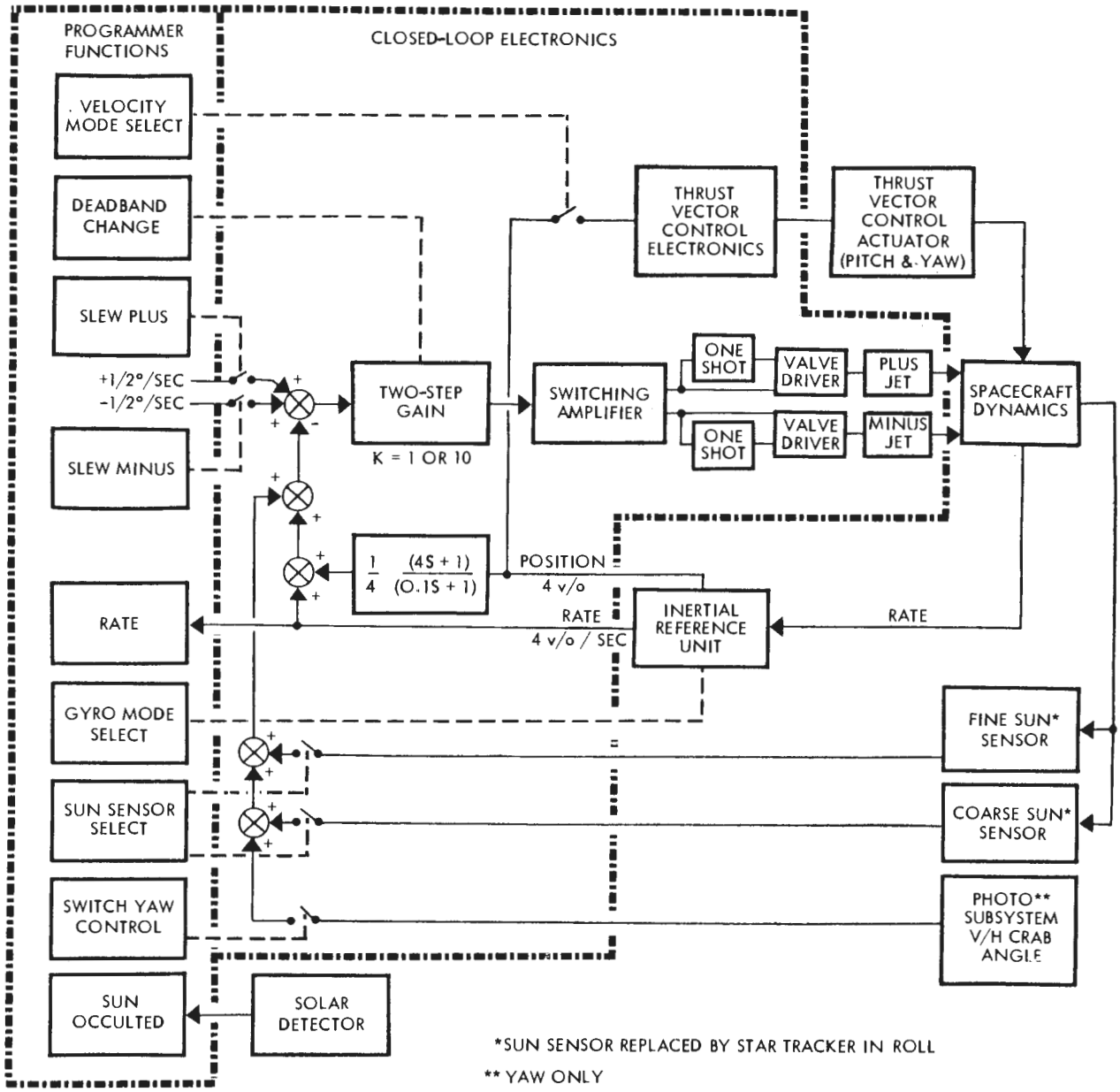

Figure 3-7: Attitude Control Subsystem

resulting alignment of the solar panels. Error signals are generated whenever angular deviation from the spacecraft-sunline exists. A celestial reference line for the spacecraft roll axis is established by identifying the celestial body that the star tracker acquires, locks on, and tracks. Under normal conditions the star, Canopus, is used for this purpose; however, any known celestial body of suitable brightness and within the tracker's field of view as the spacecraft is rotated about the roll axis can be used to satisfy this function.

The closed-loop electronics provides the switching and electronic controls for the reaction control thrusters and positioning of the velocity control engine actuators. Attitude maneuver and control are maintained by the controlled ejection of nitrogen gas through the cold-gas thrusters mounted on the periphery of the

engine deck. During a velocity control maneuver, gimbaling of the velocity control engine is used to maintain stable orientation of the spacecraft.

Multi-axis spacecraft maneuvers were required to perform the two velocity maneuvers and orient the spacecraft for the photo sequences. Three-axis maneuvers were executed prior to the first and after the last exposure of each orbit. All other perilune and apolune lunar photos were taken after two-axis maneuvers. During the perilune photo sequence, the initial three-axis maneuver was performed from a celestial reference attitude. Each subsequent maneuver was made as a change from the previous position of the celestial references. During the 27-day mission, 586 single-axis maneuvers were executed to support all operational functions. The 85-degree (near polar) orbit employed for Mission IV resulted in the spacecraft being illuminated by the Sun for the entire mission. Therefore, it was necessary to dissipate more heat from the spacecraft by thermal pitch-off maneuvers. Table 3-3 identifies the maneuvers performed for each function. During the mission there were a total of 83 Sun acquisitions, of which 81 were accomplished in the narrow deadband attitude control mode.

Continuous solar illumination also significantly reduced the use of the Canopus tracker, which operated in the open-loop mode to determine the roll attitude. Once or twice during each 12-hour orbit, the tracker was turned on and the spacecraft positioned so that the star Canopus was within the field of view. The error signal obtained from this sequence was used by the subsystem analyst to accurately establish the roll position. Between update maneuvers the roll attitude was determined by applying the measured spacecraft drift rates. During some operating periods the tracker locked on glint. (Postmission tests showed some wires and mounting screws on the power dissipation resistor panel on the low-gain antenna boom and

Table 3-3: Maneuver Summary

Function	Planned	Actual			
	Total	Roll	Pitch	Yaw	Total
Velocity Change	8	4	4	0	8
Photography	466	202	209	93	504
Attitude Update	30	13	0	1	14
Thermal Pitch-Off	27	0	41		41
Star Map and Other	3	7	10	2	19
Total	534	226	264	96	586
Narrow Deadband		225	261	96	582
Wide Deadband		1	3	0	4
Total		226	264	96	586

the solar panel stowing brackets were reflecting light into the star tracker light baffle system field of view, causing the sensors to lock on the glint light.) The tracker was operated for a total of 28 hours and 46 minutes during the photo mission, including 113 on-off cycles, of which 22 were the result of locking on glint. Although the tracker was not used in the closed-loop mode to control the roll position of the spacecraft, the error signal data obtained provided this equivalent information via telemetry to the control center subsystem analyst to the same degree of accuracy. There was no difficulty in commanding accurate orientation of the spacecraft to support photography. For a period of nearly 60 hours, beginning on May 27, the bright-object sensor was closed when the spacecraft was pitched off the Sun -40 degrees.

All commands received from the command decoder were properly acted upon by the flight programmer. These included 3,666 real-time commands and 3,445 stored program commands. The repetitive execution of stored-program routines increased this total by approximately 20,000 individual commands. The total clock error during the mission was +0.96 second, which reflects a drift rate of 1.505 milliseconds per hour.

The low and stable gyro drift rates of the inertial reference unit contributed to the lower than expected gas usage rate, even though long periods were spent in the $\pm$0.2-degree limit cycle control mode. Gyro drift rates measured on May 8 were found to be:

- Roll -0.045 degree per hour
- Pitch -0.11 degree per hour
- Yaw +0.02 degree per hour

Calculated roll positions, based on extrapolation of the measured drift rates over periods up to 72 hours, were within 1 degree of the position established by the star tracker error signals.

Performance of the closed-loop electronics was satisfactory during flight. Proper switching functions to support the flight programmer output commands to the inertial reference unit, Sun sensors, Canopus star tracker, sensor outputs, and vehicle dynamics were accomplished. There were several instances where the telemetry performance data indicated the plus-pitch thruster was on, but the pitch error signal did not decrease from the -0.2-degree limit. At all other times, thruster operation and pitch error signals were normal. Investigation of the abnormality, which did not effect overall performance of the mission, indicates that an intermittent failure of the one-shot-multivibrator circuitry output pulse (11 $\pm$1 milliseconds) occurred.

The thruster driver is triggered by an "OR" gate signal from either the output of an 11-millisecond one-shot multivibrator through the threshold detector or directly from the threshold detector when the output signal exceeds 2 volts for a period greater than 11 milliseconds. It was concluded that the thruster driver was being triggered by an error signal of less than 3-millisecond duration (minimum time to energize thruster solenoid to allow nitrogen gas flow). Additional tests were conducted on subsequent flight spacecraft to verify proper operation of the circuits. Over 19,000 individual thruster operations were performed during the photographic mission. The estimated breakdown is shown in Table 3-4.

Sun sensor operation was satisfactory throughout the mission. Initial acquisition was completed when telemetry data from Woomera tracking was obtained. The capability of switching between fine and coarse sensing modes significantly added to spacecraft attitude control capability and minimized nitrogen gas usage during off-Sun operations. Additional data was obtained on the shift in Sun sensor error output signals by the presence of moonlight.

3.2.5 Velocity Control Subsystem Performance

A larger midcourse maneuver velocity change was required on this mission because the lunar injection point and type of orbit required was changed after premission targeting of the launch vehicle. Velocity control subsystem performance and operation was excellent during the two propulsion maneuvers (midcourse and orbit injection) performed.

Table 3-4: Thruster Operations

Mode	Thruster Operations			
	Roll	Pitch	Yaw	Total
Limit Cycle	4,980	6,225	6,640	17,845
Maneuvers (Commanded and internally programmed)	452	611	275	1,338
Total	5,432	6,836	6,915	19,183

The velocity control subsystem provides the velocity change capability required for mid-course correction, lunar orbit injection, and orbit adjustment as required. The spacecraft includes a 100-pound-thrust, gimbaled, liquid-fuel rocket engine. The propulsion system uses a radiation-cooled bipropellant liquid rocket engine that employs nitrogen tetroxide (N_2O_4) as the oxidizer and Aerozine-50 (a 50-50 mixture by weight of hydrazine and unsymmetrical dimethylhydrazine, UDMH) as the fuel. The propellants are expelled from the tanks by pressurized nitrogen acting against teflon expulsion bladders. The propellants are hypergolic and no ignition system is required.

The engine is mounted on two-axis gimbals with electrical-mechanical actuators providing thrust directional control during engine operations. A central nitrogen storage tank provides (through separate regulators) the gas required to expel: (1) the propellants in the velocity control system and (2) the gas for the attitude control thrusters. The nominal gas pressure for Mission IV was increased from 3,500 to 4,000 psi to provide for the additional maneuvers of the photo mission. Figure 3-8 identifies subsystem components and shows how they are connected. The specified propellant load provides a nominal velocity change capability of 1,017 meters per second at an oxidizer-to-fuel ratio of 2.0 and a propellant expulsion efficiency of 98%.

Flight performance data obtained during the two engine-burn periods were evaluated and the velocity control engine performance results are summarized in Table 3-5.

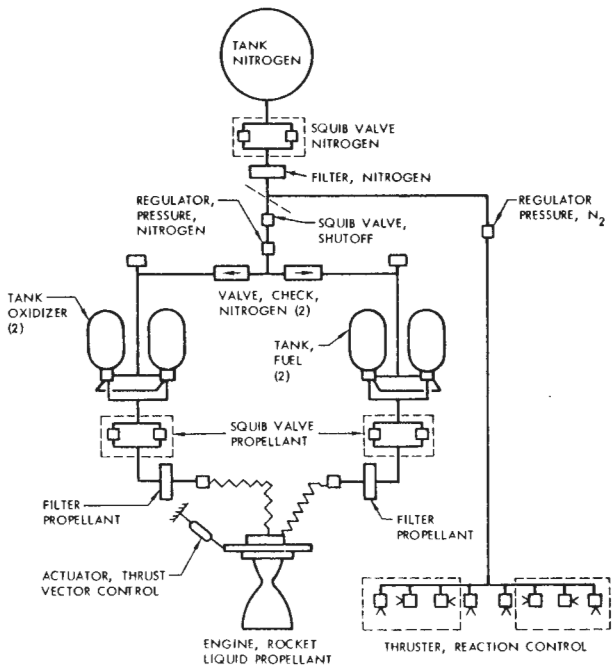

Figure 3-8: Velocity and Reaction Control Subsystem

The two engine burn periods imparted a total spacecraft velocity change of 720.46 of the calculated 1,008.4 ± 43 meters-per-second total capability. Engine valve temperatures were between 69 and 73°F during the injection burn period. Approximately 54 minutes after the maneuver, the temperature reached a maximum of 104.8 degrees.

Table 3-5: Velocity Control Engine Performance Summary				
	Velocity Change (meters per second)	Burn Time (seconds)	Thrust (pounds)	Specific Impulse (seconds)
Midcourse				
Predicted	60.85	53.8±1.6	98	276
Actual	60.84	52.7	100	276
Injection				
Predicted	659.62	501.4±8.5	100	276
Actual	659.62	501.7	100	276

Gimbal actuator position changes during the two engine burn periods varied between −0.20 and +0.07 degree in pitch and −0.03 to +0.20 degree in yaw. These changes reflect the motion of the spacecraft center of gravity as the propellants were consumed. Propellant heaters were activated four times for a total operating time of 244 minutes.

3.2.6 Structures, Mechanisms, and Integration Elements Performance

All components comprising the structure, thermal control, wiring, and mechanisms – except for the camera thermal door – operated properly during the mission. The mirrors mounted on the equipment mounting deck for this mission produced the desired reduction in spacecraft temperatures.

The Lunar Orbiter spacecraft structure includes three decks and their supporting structure. The equipment mounting deck includes a structural ring around the perimeter of a stiffened plate. Mounted on this deck are the photo subsystem and the majority of the spacecraft electrical components.

The tank deck is a machined ring, v-shaped in cross section, closed out with a flat sheet. Fuel, oxidizer, and nitrogen tanks are mounted on this deck. The 20 micrometeoroid detectors are located on the periphery of the ring. The engine deck is a beam-stiffened plate that supports the velocity control engine, its control actuators, the reaction control thrusters, and the heat shield that protects the propellant tanks during engine operation.

Prior to the deployment, the low- and high-gain antennas are positioned and locked along the edges of these three decks. The four solar panels are mounted directly under the equipment mounting deck and in the stowed position are compactly folded into the space below it. Electrically fired squibs unlock the antennas and the solar panels at the appropriate time to permit them to be deployed into the flight attitude.

Spacecraft thermal control was passively maintained. An isolating thermal barrier, highly reflective on both the interior and exterior surfaces, encloses the spacecraft structure, except for the Sun-oriented equipment mounting deck and the insulated heat shield on the engine deck. The objective was to maintain the average spacecraft temperature within the thermal barrier within the range of 35 to 85°F. The equipment mounting deck exterior surface was painted with a zinc-oxide-pigment, silicone-based paint selected to achieve the desired heat balance. This paint has the properties of high emissivity in the infrared region and low absorption at the wavelengths that contain most of the Sun's emitted heat. Twenty percent of the equipment mounting deck surface was covered with mirrors in a geometric pattern (to reflect solar energy and thereby reduce the thermal heat dissipation problem); the remaining surface was exposed to the Sun.

A camera thermal door protects the photo subsystem lenses from heat loss and direct sunlight except during photographic periods. Immediately prior to each photographic sequence, the door is opened to permit photography.

Antenna deployment, solar panel deployment, and actuation of the nitrogen isolation squib valve sequences were initiated after spacecraft separation by stored program commands. These sequences were verified as completed by the first telemetry frame of data received from the Woomera tracking station.

Except for the period of the midcourse maneuver, the spacecraft was aligned with the Sun during the entire cislunar trajectory. Spacecraft temperatures remained within design limits, thus confirming the effectiveness of the mirrors mounted on the equipment mounting deck. Data from the remainder of the mission showed that the solar absorptivity of the painted areas was similar to previous missions. The combination of 20% mirrors and 80% painted surface resulted in a one-third improvement in the effective absorptivity of the mounting deck surface. Beginning in Orbit 3 (33 hours after lunar orbit injection) the spacecraft was pitched off the sunline orientation for spacecraft temperature control. Pitch-off (up to 44 degrees) maneuvers were periodically required for the remainder of the mission because of the lack of any spacecraft cooling periods during Sun occultation. These pitch-off maneuvers maintained the spacecraft temperatures within the operating limits in this more severe thermal environment.

Four types of thermal paint coupons were mounted on Lunar Orbiter IV to obtain absorptivity data. The paint samples were:

1) S-13G coating over a base coating of B-1056;
2) S-13G white paint only;
3) Hughes Surveyor inorganic white;
4) B-1060 white paint.

The solar absorptance coefficient of each paint sample was calculated from spacecraft telemetry data and is shown in Figure 3-9 plotted against mission elapsed time and also converted to equivalent full Sun exposure hours.

On one photo sequence in Orbit 6 and in Orbit 7, the camera thermal door failed to open when commanded, resulting in the failure to photograph two sites. A series of real-time commands and procedures were developed during the mission to control the door opening operation, which were successful in support of mission photography and photo subsystem thermal balance.

Postmission analysis of the failure indicated that the most probable cause was the motor, with the inner pawls (stepping pawls) hanging up on the inner pawl retainer ring. A review of drawings for manufacture and assembly of the motor shows a possible tolerance buildup that could permit 0.01 inch interference between the inner pawl and the inner pawl retaining ring. The investigation further indicated that such motors having a small number of operating cycles were susceptible to this failure mode. After a relatively few additional cycles, this type of failure did not recur. Tests were also run to determine whether the adverse thermal environment could have warped the door, thus producing the intermittent failure. There was no indication of any such effect over the temperature ranges tested.

3.3 OPERATIONAL PERFORMANCE

Operation and control of the Lunar Orbiter IV spacecraft required the integrated services of a large number of specialists stationed at the Space Flight Operations Facility (SFOF) in Pasadena, California, as well as at the worldwide Deep Space Stations (DSS). Mission advisors and other specialists were assigned from the Lunar Orbiter Project Office, supporting government agencies, Jet Propulsion Laboratory, the Deep Space Stations, and The Boeing Company.

The Langley Research Center exercised management control of the mission through the mission director. Two primary deputies were employed: the first, the launch operations director located at Cape Kennedy; the second, the space flight operations director located at the SFOF. Once the countdown started, the

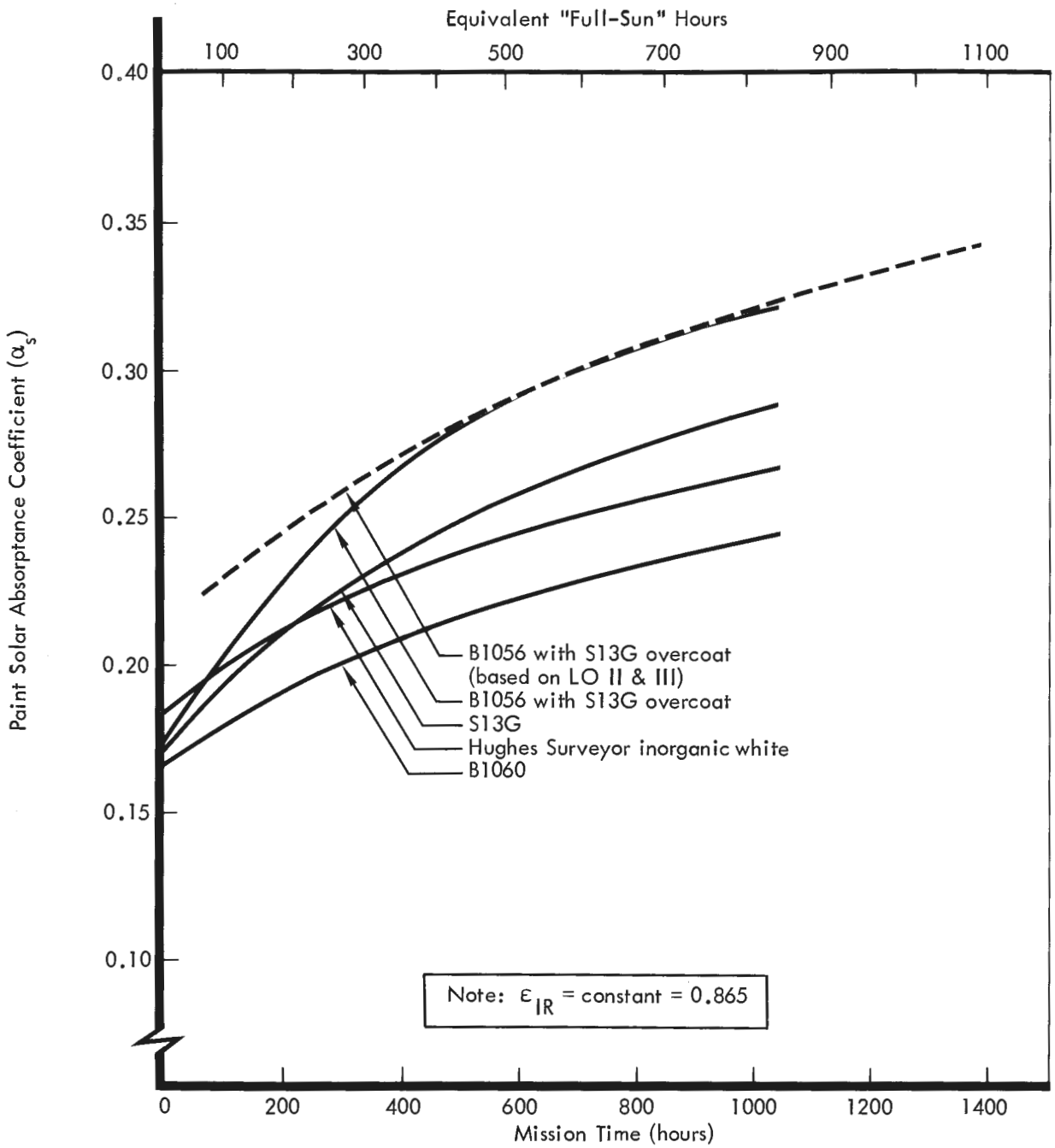

Figure 3-9: Thermal Paint Coupon Solar Absorptance Coefficients

launch operations director directed the progress of the countdown on the launch pad, while the space flight operations director directed the countdown of the Deep Space Network. From the time that these countdowns were synchronized, all decisions (other than Eastern Test Range safety factors) regarding the countdown were made by the mission director, based on recommendations from the launch operations director and/or the space flight operations director.

After liftoff, launch vehicle and spacecraft performance was monitored in the launch mis-

sion control center at ETR by the mission director. Telemetry data were used by the launch team and were relayed in real time to the SFOF through the Cape Kennedy DSS. Dissemination of spacecraft performance and tracking data to the launch team and the operations team enabled efficient and orderly transfer of control from Cape Kennedy to the SFOF.

After the spacecraft was acquired by the Deep Space Network (DSN), flight control was assumed by the space flight operations director. Thereafter, the mission director moved from ETR to the SFOF and continued control of the mission. Control of spacecraft operations was delegated to the space flight operations director.

Control of the mission was centralized at the SFOF for the remainder of the mission. All commands to the spacecraft were coordinated by the spacecraft performance analysis and command (SPAC) and flight path analysis and command (FPAC) team of subsystem specialists and submitted to the space flight operations director for approval prior to being transmitted to the Deep Space Instrumentation Facility (DSIF) site for retransmission to the spacecraft. As a backup capability, each prime DSIF was supplied with a contingency capability (including predetermined commands and process tapes) to permit local assumption of the basic mission control function in the event of communications failures. On-line interpretation of efforts of all major operational areas was accomplished by the assistant space flight operations director on a 24-hour basis.

Mission IV was the most complex mission to date in that the mission profile required operation beyond the initial program requirements and, with few exceptions, each of the over 200 photo exposures required individual two- or three-axis spacecraft maneuvers. In addition, the priority readout mode was to be used to recover all significant photo data prior to Bimat cut. Additional environmental control problems were generated by the lack of Sun occultation periods to cool the spacecraft.

Detailed premission planning and mission design enabled scheduling photo requirements in a repetitive cycle occurring every two orbits, and planning programmer core maps to cover a complete 12-hour orbit. Except for the unexpected photo degradation resulting from control procedures initiated after the camera thermal door failure to open and the intermittent abnormal operation of the photo subsystem readout looper encoder, the preplanned sequence of events was followed. To recover the photo data degraded as a result of the camera door abnormalities, several photos were planned and taken of these areas when they were properly illuminated, near the end of the mission, from near apolune.

3.3.1 Spacecraft Control

The flight operations team was divided into three teams (designated red, white, and blue) to provide 24-hour coverage of mission operations at the space flight operations facility. Overlap was scheduled to allow detailed coordination between the oncoming and offgoing system analysts. The operations team was essentially unchanged for Mission IV. Spacecraft control was maintained throughout the mission by the generation, transmission, and verification of commands and the transmission of executed tones from the Earth-based facilities. A total of 7,111 commands was generated and, with the exception of three instances, was properly executed.

Lunar Orbiter IV's mission requirement necessitated more extensive premission planning to provide adequate assurance of accomplishing the objective. Several new operational and programming procedures were incorporated to superimpose the changes caused by spacecraft anomalies on the already complicated mission. The 12-hour orbit period made it possible to plan the programmer core maps to include one complete orbit. The combination of a 12-hour orbit and 8-hour shifts resulted in each of two command programmer teams attending preliminary and final command conferences, and the command sequences for one of the two orbits each day. This left the third team available for programmer updates, nonstandard sequences, and general functions. As the mission progressed, this capability became increasingly important.

There were three incidents late in the mission in which command programming resulted in the spacecraft initiating incorrect sequences. These were the initiation of a photo processing rather than the attitude update sequence, premature termination of a photo maneuver by a real-time command, and comparison of a commanded photo time with the time of the next photo. Corrective action was employed to initiate the proper sequence by real-time commands and by shifting the location of subsequent photographs to include the areas not photographed.

Failure of the camera thermal door to open by stored program command necessitated a change in control procedures which, in turn, produced undesirable results requiring additional actions. When it was found that the door could not be opened reliably by either stored program or real-time commands, a decision was made to leave it open. To prevent condensation in the photo subsystem windows, the spacecraft was oriented so that solar energy would be used to maintain the window temperature above the dew point. This procedure placed direct illumination on the photo subsystem light baffles and resulted in light fogging the exposed but unprocessed film during the period between photography and processing. This was corrected by elimination of the direct solar illumination on the window, but resulted in condensation on the window. Photograph quality was degraded by the flare introduced into the image. This latter effect was verified by some special light-leak tests conducted during the flight on an available photo subsystem retained at Cape Kennedy. Results of these tests were forwarded to Spacecraft Control for information.

Through a series of tests conducted with the flight spacecraft, it was determined that the camera door could be partially closed and opened in response to a series of individual commands. The control procedure was then modified to close the camera thermal door by stepping pulses to maintain the window temperatures above the dew point. This procedure was effective in controlling the temperature and eliminating the light leakage. Over a period of time, the condensation evaporated and good photographs were obtained for the remainder of the mission. A plan was developed and successfully implemented for rephotographing the areas covered by the degraded photographs near the end of the mission when the illumination was acceptable.

Photo processing and film handling problems were encountered during the latter portion of the mission. An extensive series of command sequences were developed and implemented to re-establish control of these functions so that the mission could be completed. Except for the processing problem which required Bimat cut shortly before the planned time, the alternate procedures were effective in recovering all of the desired photographic data obtained during the mission. During this period, the most tedious task was to advance all of the processed film through the system to the readout gate in the presence of a "readout looper empty" signal. The procedure developed was to inch the film along for readout and takeup for approximately 12 frames until unprocessed film was indicated at the readout position.

Although several abnormal situations were encountered during the mission, the problems were evaluated and corrective action initiated such that a minimum effect was felt on the quality and quantity of data recovered. On several occasions the early evaluation of the performance data indicated that the photo mission might be prematurely terminated. However, by using the inherent flexibility of the flight programmer, the alternate control modes and procedures restored the interrupted functional operation, thus permitting the mission to be satisfactorily completed. The overall photo mission was completed, with few minor exceptions, as outlined in the premission plans and the photographic objectives were accomplished.

3.3.2 Flight Path Control

The Lunar Orbiter trajectory was controlled during the boost phase and injection into cislunar orbit by a combination of the Atlas guidance and control system at AFETR and the on-board Agena computers. After acquisition

by the Deep Space Station at Woomera, Australia, trajectory control was assumed and maintained by the space flight operations facility in Pasadena, California. During the first 6 hours of the mission following injection, the Deep Space Network performed orbit determination calculations to ensure DSS acquisition. Guidance and trajectory control calculations for controlling mission trajectories were performed by the Lunar Orbiter Operations group.

Lunar Orbiter flight path control is the responsibility of the flight path analysis and command (FPAC) team located at the space flight operations facility (SFOF) in Pasadena, California. Flight path control by the FPAC team entails execution of the following functions.

- Tracking Data Analysis – Assessment of tracking data (doppler and range) and preparation of DSS tracking predictions.
- Orbit Determination – Editing of raw tracking data and determination of the trajectory that best fits the tracking data.
- Flight Path Control – Determination of corrective or planned maneuvers based on orbit determination results and nominal flight plan requirements.

FPAC activities during the mission were divided into the following phases.

- Injection through midcourse;
- Midcourse through deboost;
- Lunar orbit.

Each of these phases is discussed in the following sections.

Injection through Midcourse – Unlike previous missions, the midcourse guidance maneuver was required to rotate the injection point, in the plane of the Moon, from a 21-degree descending-node orbit to an 85-degree ascending-node orbit. This function was accomplished by:

- Calculation of the optimal orbit injection point;
- Selection of the cislunar trajectory that satisfied the injection constraints;
- Determination of the required midcourse maneuver.

DSS-51, Johannesburg, South Africa, acquired the spacecraft 1.5 minutes prior to spacecraft-Agena separation. The tracking period lasted only 8 minutes because of a ground antenna tracking speed limitation. As noted previously, DSS-41 (Woomera, Australia) acquired the spacecraft in one-way lock 45 minutes after launch and was acquired in two-way lock 3.5 minutes later. FPAC control was transferred from the DSN to the Lunar Orbiter Project FPAC personnel 2.75 hours after launch. A trajectory data arc length of 10 hours; 5 minutes was used to support the decision on the midcourse maneuver magnitude and time of execution. By varying the arrival time for a selected midcourse execution time, the FPAC software programs automatically optimized the deboost and midcourse ΔV. On the basis of these computations, the midcourse maneuver was set for 16:45 GMT May 5, with the spacecraft in view of both Madrid and Goldstone tracking stations.

The midcourse maneuver consisted of a 78.34-degree roll, a 67.26-degree pitch, and a velocity change of 60.85 meters per second (engine burn time 53.8 seconds). This maneuver was selected from 12 possible two-axis maneuvers based on:

- Maintaining Sun lock as long as possible;
- Minimizing total angular rotation;
- DSS line-of-sight vector not passing through an antenna null.

Figure 3-10 shows the encounter parameters for the booster targeted aiming point, the computed pre-midcourse encounter point, and the desired midcourse aiming point. The large shift in the encounter aiming point was the result of a change in the type of mission to be flown after the launch vehicle boost trajectory had been programmed into the computer. The booster was programmed to inject the spacecraft into a cislunar trajectory to support a photographic mission similar to Mission III. Thus, rather than delay the launch date, the decision was made, based on computer studies, that the midcourse maneuver could produce the required change with no degradation of the overall velocity changes required for the rest of the mission. The predicted doppler shift for the midcourse maneuver was 366 H_z and the actual value was 359.9 $\pm$0.5 H_z.

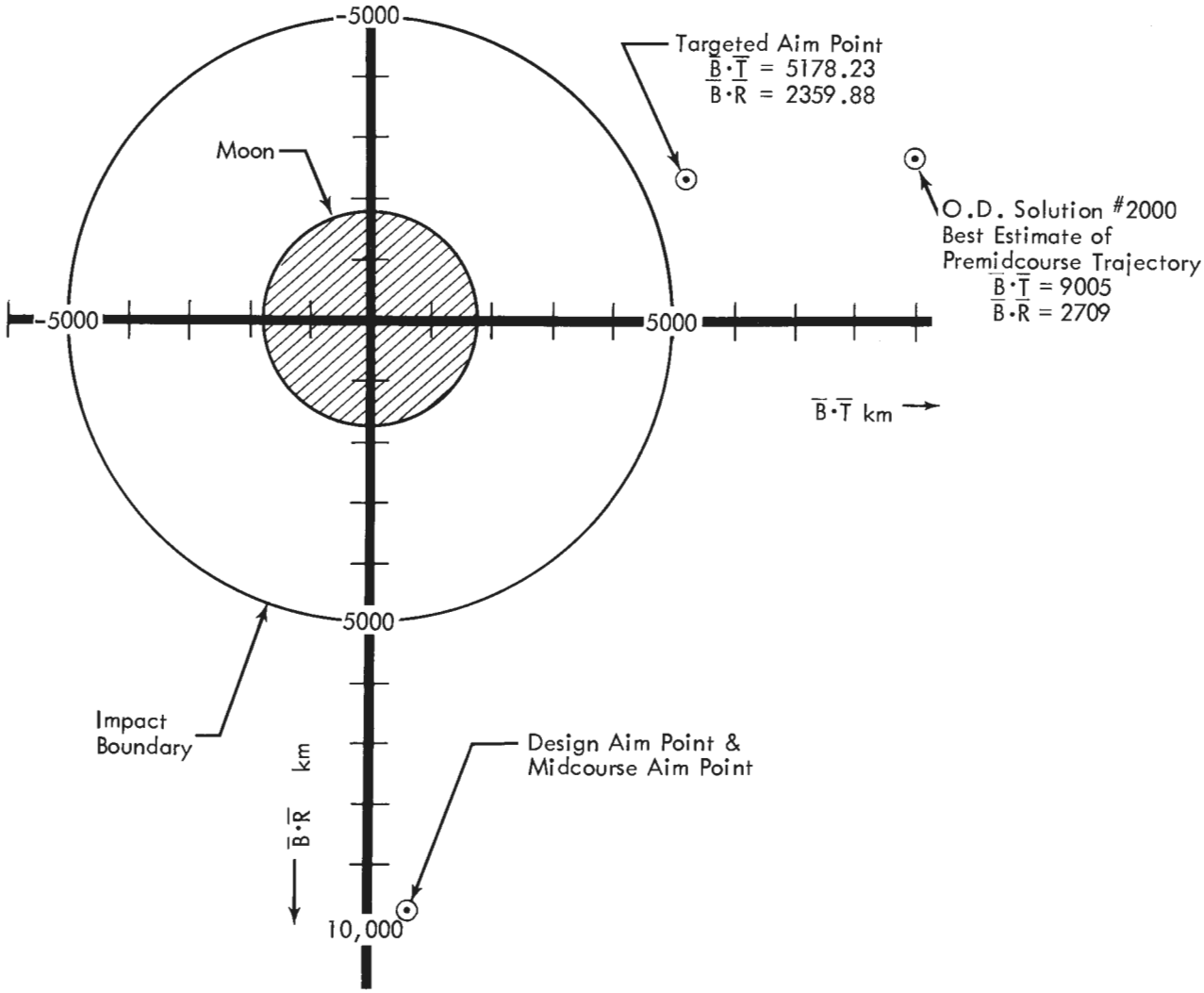

Figure 3-10: Pre-Midcourse Encounter Parameters

Midcourse through Deboost – The first orbit determination results were available for evaluation approximately 5 hours after the midcourse maneuver execution. Although a large midcourse maneuver was executed, the results showed that a 1.2 meter-per-second velocity change would be required by a second midcourse maneuver. Since this change was below the minimum engine burn period, and the error could be compensated for during the injection maneuver, a decision was made that the second midcourse correction would not be performed.

Some difficulties were encountered on previous missions by the dispersion in predicting "time of closest approach." New procedures were implemented during this mission that included:

- Solving for the state vector only using the doppler and ranging data.
- Solving for the state vector, Earth gravitational constraint, and station locations using an a priori covariance matrix and doppler data only.

These new procedures were effective in obtaining compatible results and a small dispersion in predictions of "time of closest approach." Mission IV data dispersion was near 10 seconds while Missions II and III were 40 and 30

seconds, respectively. A summary of the encounter parameters computed during the cislunar trajectory is shown in Table 3-6.

Final design of the deboost maneuver was based on 57 hours of ranging and two-way doppler data. The design predictions were compared with the orbit determination result using the last 10 hours of tracking data (best estimate) prior to the deboost maneuver, which showed that $\overline{B}\cdot\overline{R}$ was within 3.5 km, $\overline{B}\cdot\overline{T}$ was within 2 km, and the time of closest approach was within 2.6 seconds. The design philosophy was to guide the spacecraft from its approach trajectory into an elliptical orbit satisfying the following parameters in the order indicated.

- Longitude of ascending node;
- Perilune radius;
- Orbit inclination;
- Apolune radius;
- Argument of perilune.

The Langley Research Center lunar model of November 11, 1966, was used in calculating the deboost maneuver.

Engine ignition for the deboost maneuver was scheduled to occur at 15:08:46.7 GMT on May 8. The spacecraft maneuver commanded to inject the spacecraft into the elliptical lunar orbit was:

- Sunline roll -29.47 degrees
- Pitch -96.13 degrees
- ΔV 659.62 meters per second
- Estimated burn time 501.9 seconds

This maneuver was selected from 12 possible two-axis maneuvers based on the same general criteria employed for the midcourse maneuver correction.

A series of flyby maneuvers was also designed to be used in the event of a velocity control engine failure. A series of photos along the lunar terminator were to be taken at 12- to 15-minute intervals. Successful completion of the injection maneuver caused these plans to be cancelled.

Lunar Orbit Phase – The 85-degree orbit inclination eliminated the Earth occultation period immediately after the deboost maneuver as experienced in previous missions. The first orbit determination calculation was based on nearly 2 hours of tracking data from the first orbit. Table 3-7 compares the orbit parameters used in the design with the first and best estimates obtained from tracking data.

For the remainder of the mission, a data arc of one orbit (12 hours) provided near-optimum results. To avoid apolune and perilune and to provide complete coverage of all photo sites for subsequent analysis, the data arc epochs were placed at a true anomaly of about 245 degrees. All orbit determination computations converged rapidly as a probable result of the high apolune and perilune altitudes, which made the effects of the lunar gravitational field very small.

Perilune photography required computation of spacecraft maneuvers based on a celestial

Table 3-6: Summary of Encounter Parameters

Elements	Midcourse Design	Best Estimate
$\overline{B}\cdot\overline{T}$ km	723.2	725.5
$\overline{B}\cdot\overline{R}$ km	9,811.1	9,807.5
Time of Closest Approach (seconds after 15:36 GMT, May 8)	1.1	3.8

Table 3-7: Lunar Orbit Parameter Summary			
Orbital Element	Deboost Design	First OD Estimate	Best Estimate
Perilune Altitude (km)	2700.7	2706.2	2706.3
Apolune Altitude (km)	6110.8	6110.8	6114.3
Inclination (degrees)	85.48	85.48	85.48
Ascending Node Longitude (degrees)	131.0	131.0	131.0
Argument of Perilune (degrees)	1.49	1.17	1.17

orientation for the first exposure in an orbit. Subsequent spacecraft maneuvers were computed as an additional maneuver increment from the previous orientation. Apolune photography maneuvers were based on a celestial reference orientation. During the photographic mission, 161 different photo maneuvers requiring 383 single-axis spacecraft maneuvers were determined and executed. An additional six photo maneuvers requiring 15 single-axis maneuvers were designed, but not performed, at the time of Bimat cut in Orbit 36.

Photo maneuvers were designed on the concept that perilune photos for successive orbits were taken at specific latitudes (±72.0, ±42.5, +14, -14.5 degrees). The longitude coordinate was specified as a differential from the orbit trace for the specified latitudes. These differential longitudes were updated periodically to maintain the most favorable illumination.

During the mission, an operational decision was made to rephotograph areas between 50 and 90° E longitude because the perilune photos of this area were degraded by window fogging and light streaking. As the mission progressed, this area rotated into view for apolune photography and was properly illuminated. Photos were taken at ±34° latitude on five successive orbits, beginning on Orbit 29 to recover the desired photo data, but with a decrease in static resolution.

Orbit Phase Kepler Elements – Lunar Orbiter IV orbit characteristics are presented in Figures 3-11 through 3-14, time histories of perilune altitude, orbit inclination, argument of perilune, and ascending-node longitude. To show the long-term effects, each parameter covers the period from injection into lunar orbit on May 8 to the end of the photo mission 48 orbits later on June 1, 1967.

3.4 GROUND SYSTEM PERFORMANCE

The Lunar Orbiter ground system provided the facilities and equipment required to receive, record, and transmit data and commands between the space flight operations facility and the spacecraft. In addition, all facilities necessary to sustain mission operations were provided by a complex consisting of three primary deep space stations (DSS), the space flight operations facility (SFOF), and the ground communications system (GCS) which provided voice and data between all locations. Separate facilities were provided at Eastman Kodak, Rochester, New York, and at Langley Research Center, Hampton, Virginia, to process, copy, and evaluate the photos and data obtained.

All of these facilities provided the required support during the photographic mission and only minor irregularities were encountered. Each area is separately discussed in the following sections.

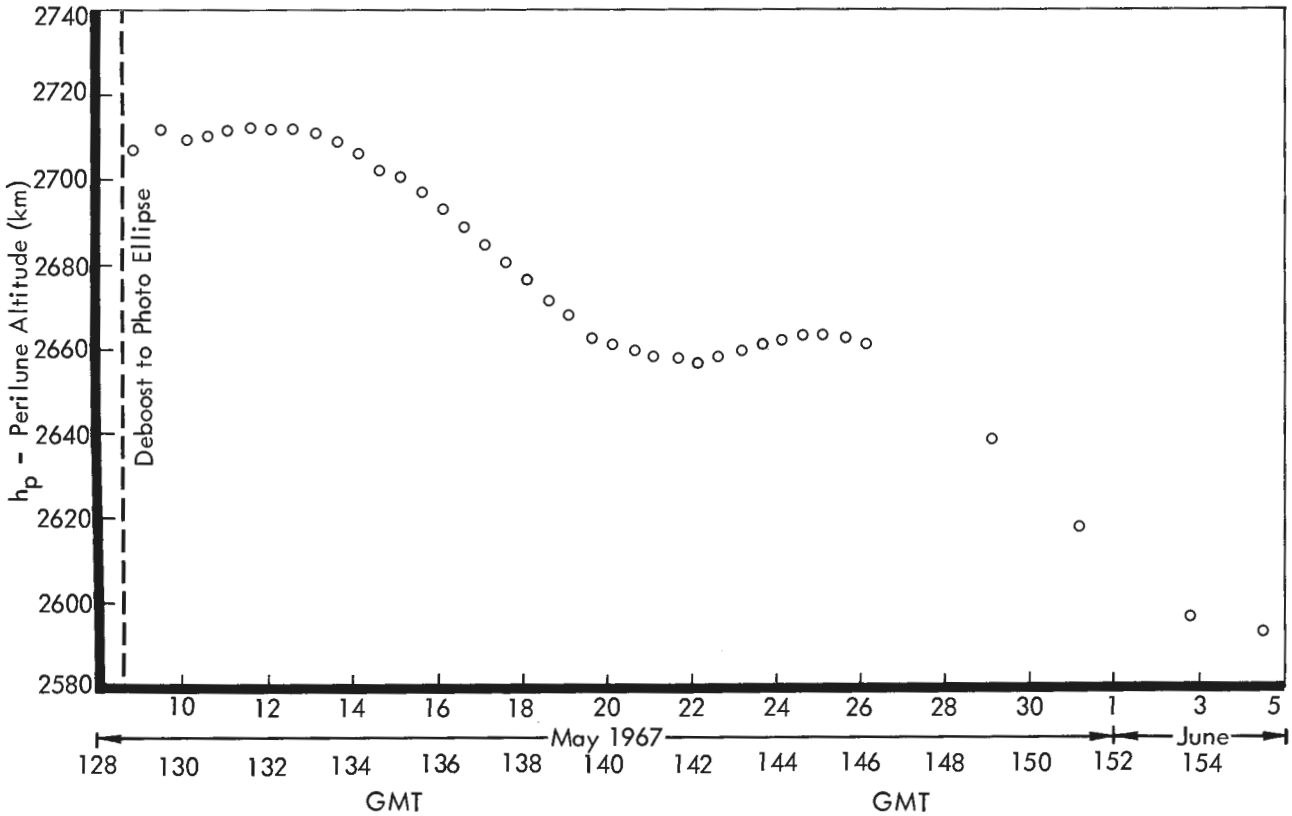

Figure 3-11: Perilune Altitude History

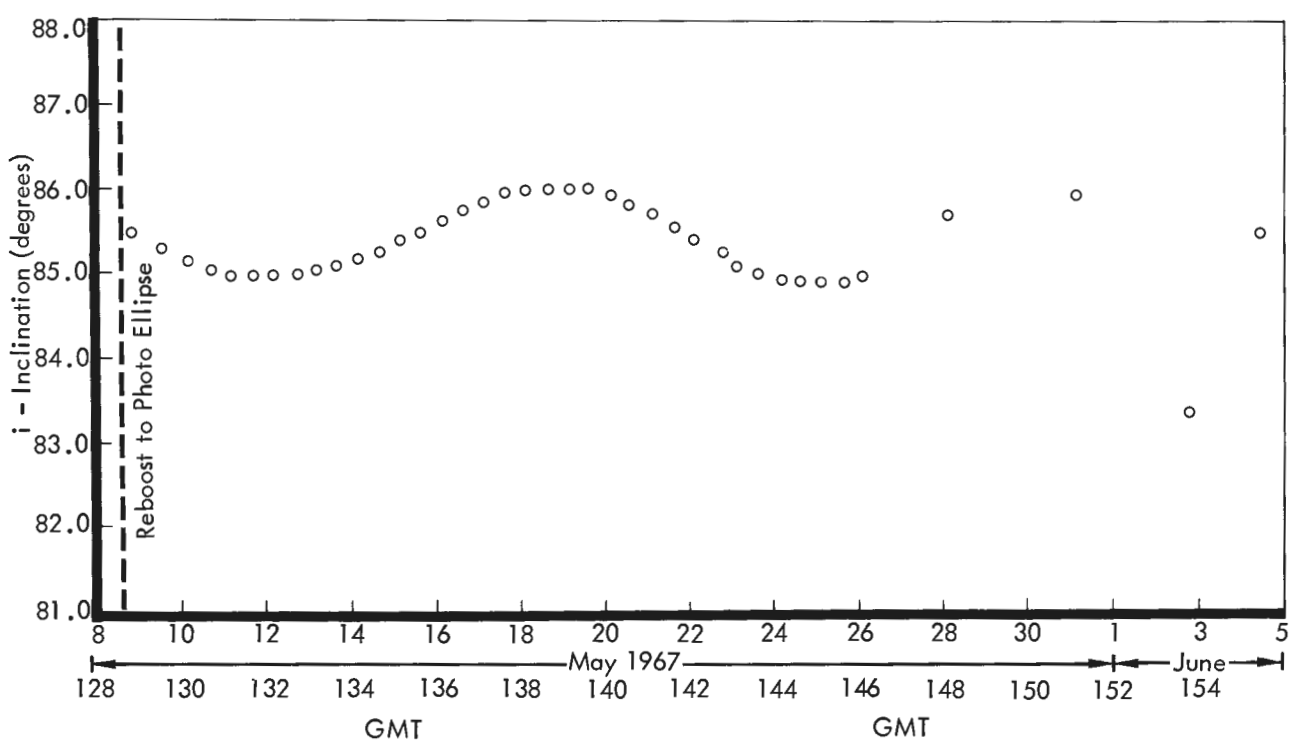

Figure 3-12: Orbit Inclination History

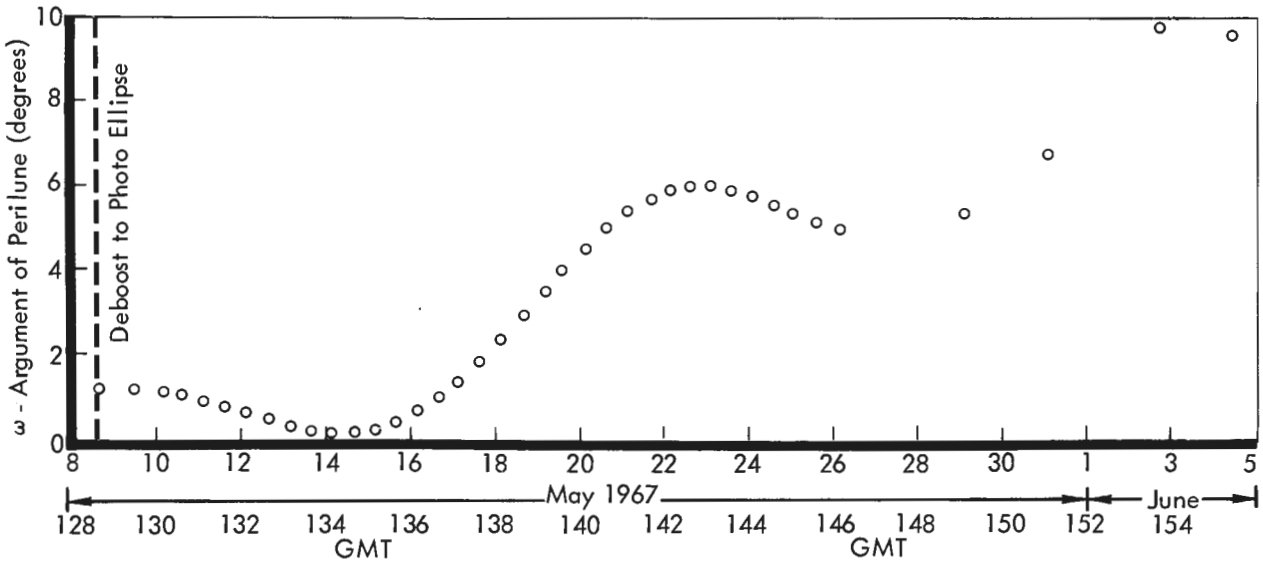

Figure 3-13: Argument of Perilune History

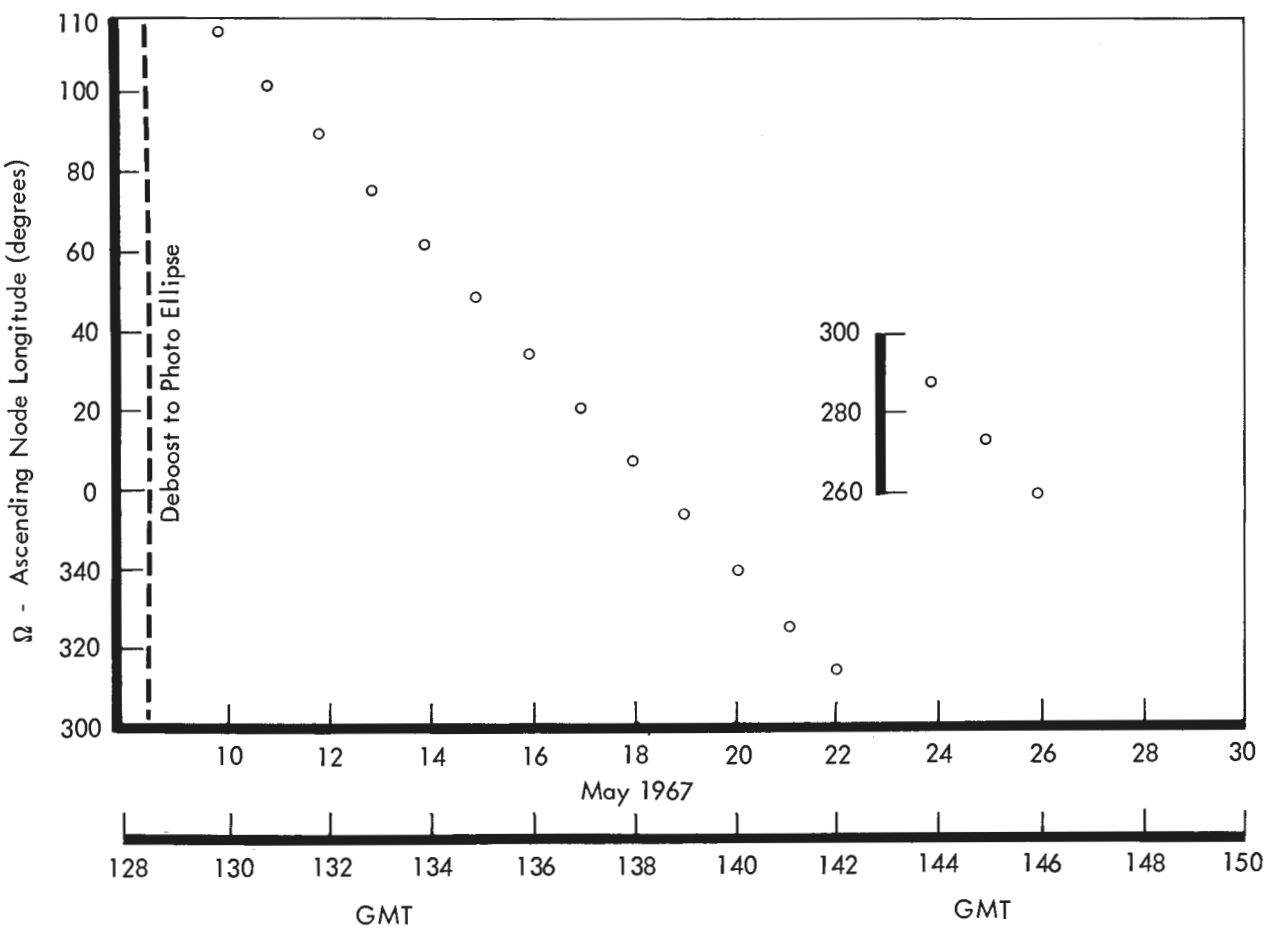

Figure 3-14: Ascending Node Longitude History

3.4.1 Space Flight Operations Facility (SFOF)

The space flight operations facility provided the mission control center, as well as the facilities to process and display data to support operational mission control. The entire system performed very well.

The telemetry processing station and the internal communications system provided telemetry and tracking data from the high-speed data line and teletype lines for use by the SFOF computers and the subsystem analysts in the operations areas. The central computing complex consists of three computer strings, each of which contains an IBM 7094 computer coupled to an IBM 7044 input-output processor through an IBM 1301 disk file memory and a direct data connection. All three computer strings were used to support Mission IV for the periods indicated. A dual Mode 2 configuration was used to support all critical phases of the mission.

Computer String	Total Hours	Mode 2 (Hours)
X String	613	96
Y String	211	94
W String	28	10
Total	852	200

During the first 6 hours, the DSN was responsible for both orbit and data quality determination. For the entire mission, the DSN was responsible for the history of data quality and analysis. Jet Propulsion Laboratory personnel performed the first orbit determination after cislunar injection. The orbit was determined within the allowable time and showed a nominal injection that was subsequently verified by later orbit determination computations.

Changes were made in the SPAC computer programs to expand the capability of the thermal program status reporting and plotting. Numerous changes were made in the FPAC computer programs for Mission IV to accommodate the high orbit inclination and high-altitude photography. In addition, changes were required to compute the nonstandard photo maneuver sequences to conserve the attitude control nitrogen gas. Minor changes were made in computation routines to facilitate the determination of photo supporting data predictions. All of these changes were verified during premission training exercises and operated satisfactorily throughout the mission.

The 14 SPAC programs were executed a total of 2,735 times, of which 2,652 were successfully completed. Of the 83 failures to execute, 32 were attributed to input errors and the remaining 51 contained software and hardware errors.

Addition of closed-circuit TV monitors of selected 100-word-per-minute printers and changes in the internal communications network were provided for this mission. This increase in visibility enabled the assistant space flight operations directors to follow the mission performance in greater detail and more effectively respond to the mission anomalies.

3.4.2 Deep Space Stations (DSS)

The Deep Space Stations (Goldstone, California; Woomera, Australia; and Madrid, Spain) supported the Lunar Orbiter IV mission by:

- Receiving and processing telemetry and video data from the spacecraft;
- Transmitting commands to the spacecraft;
- Communicating and transmitting both raw and processed data to higher user facilities.

Real-time tracking and telemetry data were formatted for transmission to the SFOF via the ground communications system. Video data were recorded on video magnetic tapes and, by mission-dependent equipment, on 35-mm film. All physical material, such as processed films, video tapes, logs, and other reports, were sent to the appropriate destinations via air transportation. All commitments were met and the incidence of error was low.

To avoid communication interference between the three spacecraft orbiting the Moon, a procedure for multiple spacecraft operation was

developed and implemented. Transmissions to Lunar Orbiter IV were made on the best lock frequency for the transponder. This frequency was measured at various times during the mission and compared with previous data. An offset frequency of 330 H_Z was used for most of the mission, and 380 and 400 H_Z were used to a lesser extent. Except for minor problems during the first two tracks and the first handover, the procedure was successfully implemented.

On May 9, when the solar eclipse occurred, the line of sight between the spacecraft and DSS-62 approached within 0.1 degree of the edge of the Sun's disk. A rise in system noise (approximately 19 db) was noted and the station was unable to obtain ranging data on the pass. There was no indication of the expected transmitter element heating from the focusing of the Sun's rays by the antenna. Evaluation of the data obtained during this period can extend the operational range of the Deep Space Network in tracking spacecraft in the vicinity of the Sun.

Special procedures were developed to compensate for the slight image distortion caused by scan line tilt and image degradation caused by window fogging and flare in the spacecraft. To compensate for the mechanical or electrical tilt of the spacecraft optical-mechanical scanner, the kine tube of each GRE was rotated slightly. An effort was also made to increase the amount of photo data recovered from the early photos which were degraded during the camera thermal door control problem period. One GRE at each site was set up by normal procedures while the gain on the second GRE at each site was adjusted to give maximum recovery of data in the overexposed and light-struck areas. This procedure increased the data recovered from these degraded photos.

3.4.3 Ground Communications System (GCS)

Ground communications between the DSS and the SFOF consist of one high-speed-data line (HSDL), three full duplex teletype (TTY) lines, and one voice link. Communication lines to overseas sites are routed through the Goddard Space Flight Center at Greenbelt, Maryland. Performance telemetry data was normally transmitted via the HSDL while the tracking data was transmitted via a TTY line. Telemetry performance data can be transmitted via teletype lines with a reduction in the amount of data transmitted in real time.

Overall performance of the ground communication system was very good. Less than 0.04% of the telemetry data was lost due to ground communication system problems. Table 3-8 summarizes the "downtime" in percent for each transmission mode and station.

Table 3-8: Transmission Mode Downtime (Percent)

	HSDL	TTY	Voice
DSS-12	0.01	0.10	0.02
DSS-41	2.44	0.39	0.19
DSS-62	1.79	0.52	0.34

There was one HSDL outage at DSS-12 which lasted for 2 minutes. The outage period for DSS-41 ranged from 2 to 27 minutes. At DSS-62 there were four occasions (a total of 16 minutes) when the HSDL and backup TTY lines were both down. Other HSDL outages ranged from less than 10 minutes to a maximum of 65 minutes.

3.4.4 Photo Processing

Photo processing at Eastman Kodak included printing negative and positive transparencies by successive-generation contact printing from the original GRE 35-mm transparencies. There were no machine-reassembled 9.5- by 14.5-inch subframes made for this mission. All reassembled photos were made from manually reassembled GRE film by the Army Map Service and NASA Langley Research Center.

GRE 35-mm film was printed on Type 5234 Eastman Fine-Grain Duplicating Film. Processing goals were to have a density (D) of 0.50 to reproduce on the copy at a value of 2.00 and a density of 2.00 to reproduce at a value of 0.50 (where a density of 0.50 corresponds to white and 2.00 corresponds to black). The inverse of densities is the normal result of the film transparency copy process in which white areas on the original produce black areas on the copy.

These densities were within ± 0.10 density of the received D-maximum and within ± 0.05 density of the received D-minimum.

Density measurements were made on the GRE film processed from the sites and actually used to make the GRE copies. Measurements were made of the test bar pattern in the edge data format pre-exposed on the spacecraft film prior to flight. Results of these measurements are shown in Table 3-9, where D max and D min are the maximum and minimum densities, respectively.

A processing and priority schedule was developed for the 35-mm film to satisfy the urgent requirements for film copies within the daily output capacity (30,000 feet per day) of the assigned facilities. During the final readout period, the copying schedule was modified to process the long-readout-period (up to 830 feet) film rolls. Previous mission processing was based on a nominal two-frame readout period which produced about 400 feet of GRE film.

3.4.5 Langley Photo Data Assessment Facility

The primary functions accomplished at the Photo Data Assessment Facility at Langley Research Center were to make:

- A duplicate copy of the original video tape;
- An analog tape copy containing only the video data;
- One GRE film for each analog tape;
- Two additional GRE films as priority permitted;
- Compensation for image distortion by employing line scan tube tilt capability.

A total of 263 video tapes was received during the mission. These tapes were used to produce:

- 1,555 rolls of 35-mm GRE film;
- 307 analog tape duplicates (many in multiple copies).

Table 3-9: Measured GRE Film Density

Station	GRE	Average D Max	2σ	Average D Min	2σ
Goldstone	03	1.96	0.10	0.48	0.08
	04	1.96	0.12	0.49	0.08
Woomera	05	2.00	0.10	0.44	0.04
	06	1.95	0.06	0.43	0.04
Madrid	07	1.97	0.08	0.45	0.06
	08	2.04	0.10	0.50	0.08
Overall Average		1.98	0.09	0.46	0.06

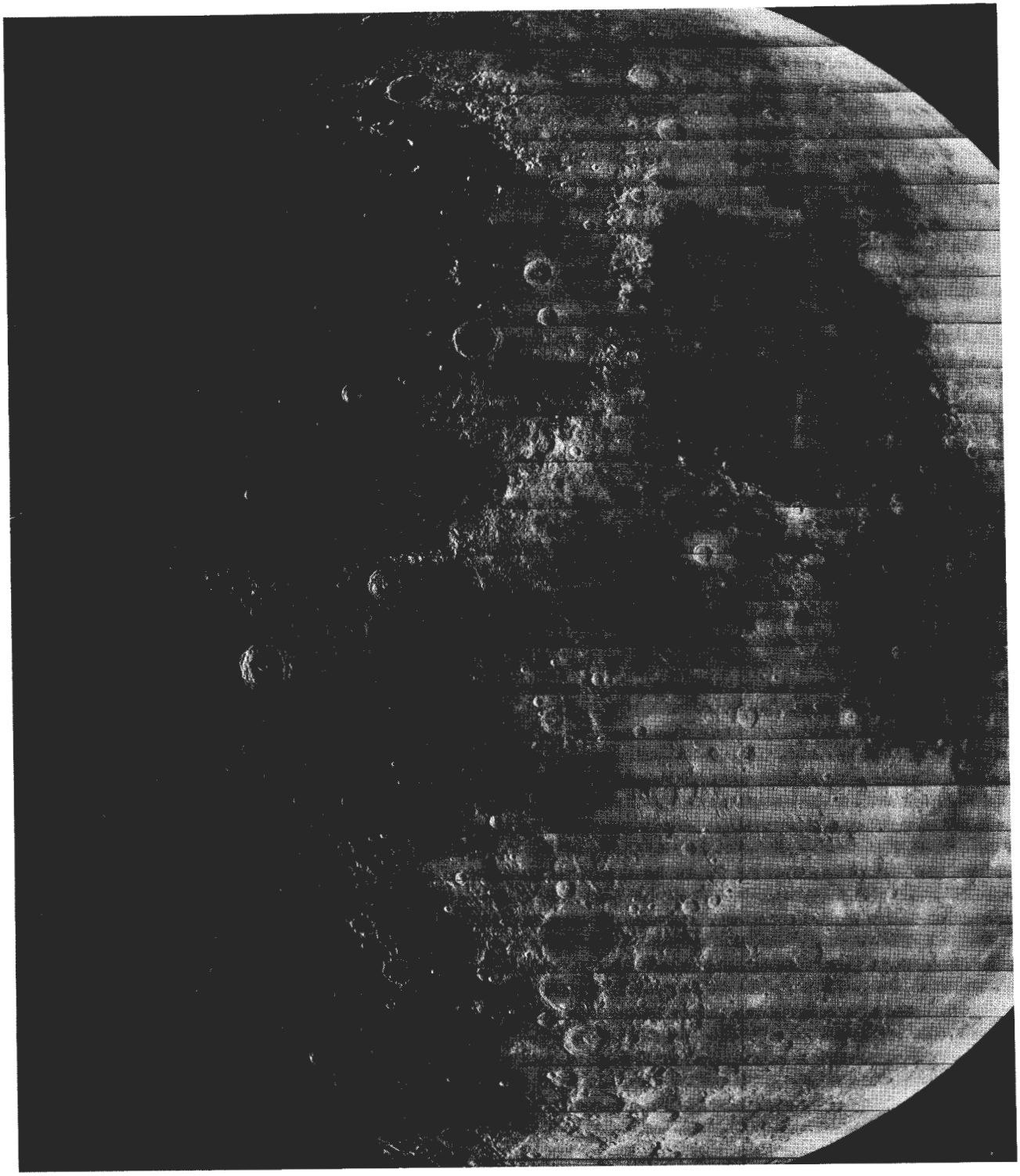

Wide-Angle Frame 109, Site IV20C
Centered at 3.5° W, 14.0°N;
includes Archimedes, Copernicus, Palus Putredinus, and Appenine Mountains.

4.0 Mission Data

An objective of each Lunar Orbiter mission has been to provide four types of data – photographic, lunar environmental, tracking, and performance. The photographic data varied with the specific mission as defined in the NASA specifications and requirements. These objectives were fulfilled by the data obtained during the 28-day photographic mission.

One hundred sixty-five of the total of 199 dual-frame exposures were made to provide approximately 99% areal coverage of the visible side of the Moon. The remaining exposures were used for film set and farside photographs. The photographs obtained provide information and detail at least 10 times better than Earth-based observation. The photo mosaics obtained will be employed for years as the basic lunar terrain reference.

The secondary objective of providing a spacecraft to be tracked by the Manned Space Flight Network (MSFN) to evaluate the Apollo Orbit Determination program will be accomplished during the extended mission. Each type of data is discussed, in turn, in the following sections.

4.1 PHOTOGRAPHIC DATA

A total of 398 telephoto and wide-angle photographs (199 dual exposures) was taken during this broad systematic lunar mapping mission essentially as planned. Seventeen of these photos were not developed because "Bimat cut" was commanded earlier than planned. Mission planning provided for periods of processing and readout so that virtually all of the photos were read out in the priority mode. As a result of deviations to this plan, to resolve the camera thermal door operation and film handling problems, the planned final readout period was extended to recover the significant data missed in priority readout. Some of the early photographs skipped in priority readout were deleted from further consideration in the final readout because they contained overlapping data (Orbit 6 photographs) or were severely degraded by light fogging.

Photographs taken during Orbits 7 through 10 (Exposures 27 through 51) were severely degraded by light fogging or flare from camera window condensation while developing an effective procedure of controlling the camera thermal door and the photo subsystem window temperatures. To recover the maximum amount of this last data, the photo sequences near the end of the mission were revised to rephotograph the area from near apolune with an accompanying reduction in resolution. The combination of perilune nearside and apolune nearside (recovery) photographs provided more than 99% coverage of the visible half of the lunar surface.

Perilune photography was taken at four latitude positions (+42.5, −42.5, +14, and −14.5 degrees) on each of 30 consecutive orbits. The telephoto photographs taken from 42.5° latitude were taken from altitudes of 2,880 to 3,000 kilometers and included the surface area from about 26 to 60° latitude. A typical telephoto photograph included an area about 275 x 1,100 kilometers (302,500 square kilometers). Similarly, the 14-degree-latitude telephoto photographs were taken from altitudes of 2,680 to 2,740 kilometers and covered an area 250 x 1,010 kilometers (252,500 square kilometers).

Perilune photography also included coverage of the North and South Polar regions taken on alternate orbits. These photos were taken from ± 72° latitude from altitudes between 3,340 and 3,610 kilometers. Each of the photos covered a latitude band from 50 to 90 degrees. Surface coverage of a typical telephoto photograph was 330 x 1,300 kilometers (429,000 square kilometers).

Apolune photography was planned to increase the farside coverage obtained on the previous three missions and to satisfy photo subsystem operational constraints. Lunar photographs were taken on every fourth orbit from an altitude range of 6,108 to 6,149 kilometers. During the intervening three orbits, film-set photographs were taken with the camera thermal door closed. Degradation of the original photograph taken between 60 and 90°E longitude, caused by light leak and condensation on the camera window, was minimized by a minor change in the photo

plan. Apolune and film-set photography was modified to take pictures of the northern and southern latitude bands from near apolune beginning in Orbit 29. Even though these photographs were taken from nearly twice the altitude of perilune photography, the resolution of the photographs was considerably better than Earth-based photographs of the same areas.

Data from the photo subsystem of Lunar Orbiter IV showed that a line-scan tube tilt of 0.78 degree existed. A procedure was developed at Langley to compensate for this condition by developing electronic circuitry for use with the FR-900 tape playback system, which measured the tilt of each scan line and applied the measured correction to the next scan line.

Film handling control logic abnormalities were encountered on several occasions during priority readout and ultimately required transmission of the "Bimat cut" command earlier than planned. These abnormalities resulted in shortening the readout periods and other film advance problems beginning with the readout of Wide-Angle Exposure 108. Several alternate control procedures were developed that moved all of the developed film through the readout process prior to the initiation of final readout. These procedures were operationally effective and there were no short or interrupted readout periods during final readout.

The photo subsystem was exposed to radiation during transit through the Van Allen belt and during a solar flare on May 23. Table 4-1 shows the total radiation dose received by the spacecraft film prior to processing. During exposure the maximum rate of change was 5.7 rads per hour. Examination of the gray scales in the pre-exposed edge data pattern showed no evidence of change in the white level density on the GRE film, thus confirming that the radiation level encountered did not fog the film.

To aid in evaluating Mission IV photos, reseau marks illustrated in Figure 4-1 were pre-exposed on the spacecraft film at the same time as the edge data. The fixed orientation, which is the same pattern employed on Mission III, can help the photo analyst detect and compensate for distortions introduced after imaging by the camera lens.

Table 4-1: Spacecraft Film Radiation Dosage

Frame	Total Dose (rads)
4-170	6.25
171	7.25
172-176	8
177-178	13
179-183	23
184-185	45
186-190	49
191	30
192-194	20
195-196	10

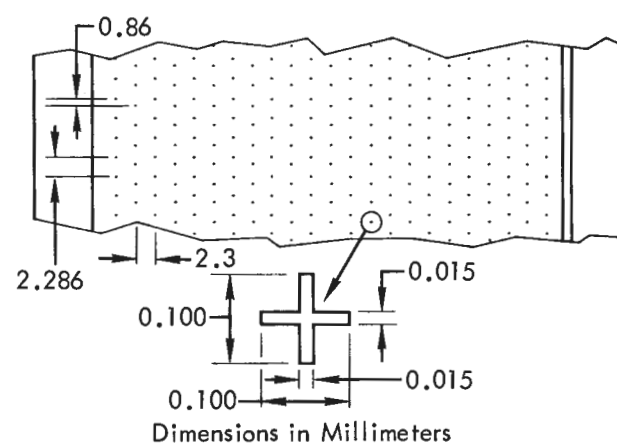

Figure 4-1: Pre-Exposed Reseau Mark Characteristics

4.1.1 Mission Photography

Analysis and assessment of mission photography was based on visual examination of second-generation GRE positive transparencies and paper prints made from manually reassembled GRE film using a 10 to 30X zoom macroscope.

A sampling technique was employed for examination of selected photos within each zone.

Lunar orbital photography was made particularly difficult by uncertainties in knowledge of the Moon's surface characteristics and its photometric function, both of which are critical to photography. The Moon has unique reflectance characteristics unlike any encountered in terrestrial photography. The wide range of reflectance can and did produce photographic images in adjacent areas having a density range that exceeded the capability of the spacecraft readout system (thus obliterating detail in areas of density extremes) while exhibiting excellent detail in the surrounding areas. Experience gained during previous missions was used to refine the selection of photographic parameters needed to determine the required exposure settings.

Other photographic problems were encountered on Mission IV as a direct result of the type of mission performed. The relatively high photographic altitude and near-polar orbit resulted in each photo covering a wide range of surface and reflective characteristics. Exposure control was selected using the predicted spacecraft film densities computed by the Photo Quality Prediction (QUAL) program. Factors included in this computation included surface albedo illumination geometry and radiation levels. Many areas were photographed for the first time; therefore, the albedo charts provided by the U.S. Geological Survey were revised based on the experience gained on previous missions. Several photographs were exposed to provide detailed information of a specific feature within the photograph at the possible expense of less desirable exposure of the surrounding areas. All of the wide-angle photographs cover an area that extends beyond the terminator at one extreme to severe overexposure toward the bright limb at the other. Figure 4-2 shows the view angles of the wide-angle and telephoto lens for the nominal photographic altitude of 2800 km.

Near-vertical photography was possible for the equatorial bands, whereas camera axis tilt was required to obtain desired coverage of the temperate, polar, and recovery photos. The precession of the Moon in a 12-hour period was close to the surface track displacement on successive orbits, which made it possible to use a given set of spacecraft maneuvers as a design reference for several orbits. Reference maneuvers changes were designed for use on Orbits 6, 14, 24, 32, and 35. Figure 4-3 illustrates the relationship of orbit track, spacecraft position at time of perilune photography, and location camera aiming point (principal point).

The relative position of the Sun and Moon at the time of apolune photography was such that the area of the Moon directly under the spacecraft was beyond the terminator. This required tilting the camera axis approximately 7 degrees so that the telephoto exposure footprint would contain the illuminated lunar surface.

With the exception of those photos degraded by the effects of the camera thermal door and thermal control, mission photography was considered to be very good. Emphasis was placed on evaluation of nearside telephoto exposures because they provided the majority of the data obtained to support the primary objective. Lunar surface resolution of the telephoto photographs range from 60, 65, and 75 meters for the equatorial, temperate, and polar zones, respectively. In general, the resolution of all normal photos evaluated was near nominal and the wide-angle photos appeared to have slightly better resolution performance than the telephoto lens in terms of scan-lines spanning the smallest objects visible.

Processing marks which result from the intermittent processing schedule employed during the mission were evident in many of the wide-angle photos. The resulting local degradation was expected because operational control procedures required placing these effects in the wide-angle rather than the telephoto exposure. Other characteristic processing defects were present in varying degrees on the spacecraft film. Although tests and investigations have been made, they have failed to reproduce the "lace" or "bubble" effect observed on all flights; a complete explanation has not been found.

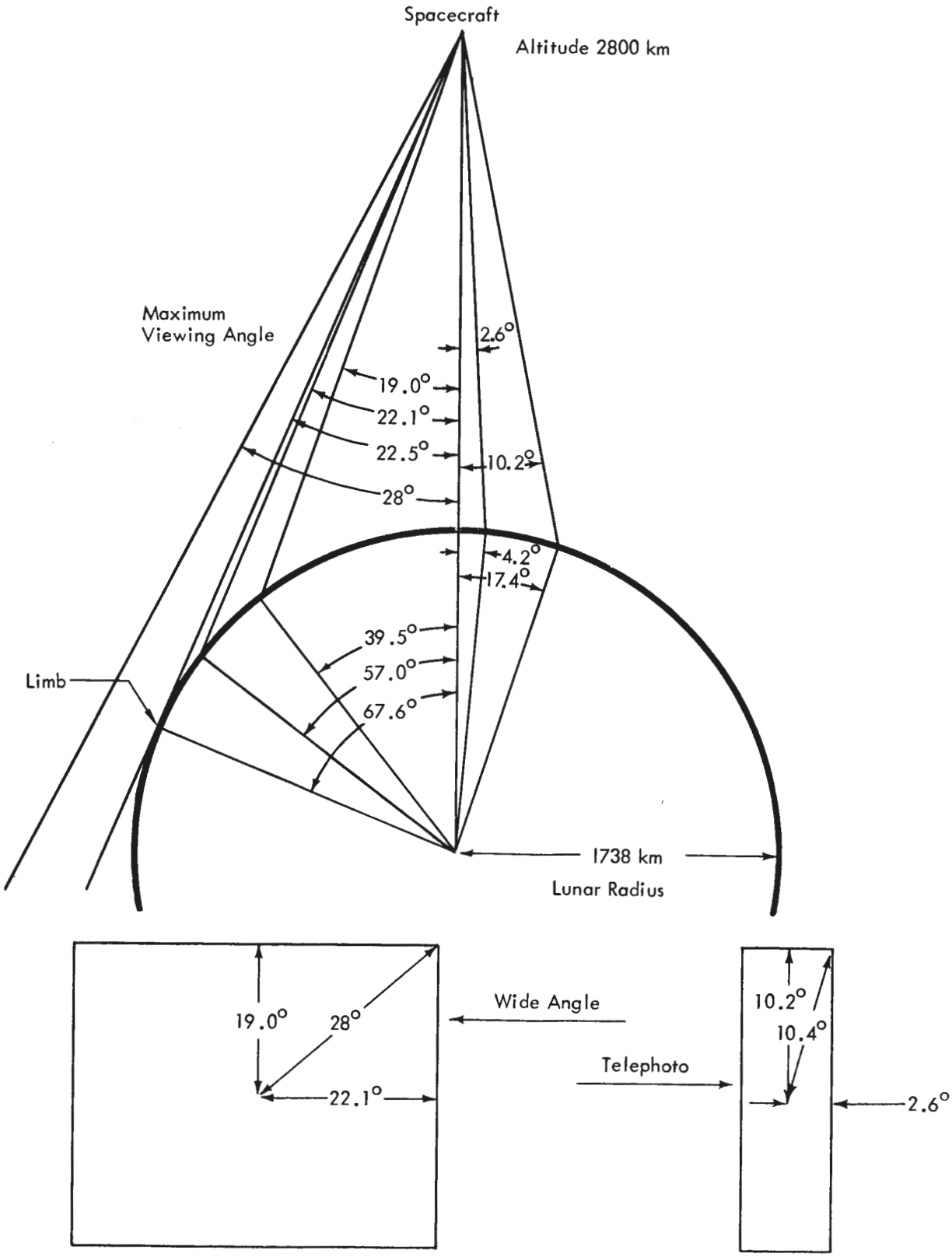

Figure 4-2: Field of View for Perilune Photography

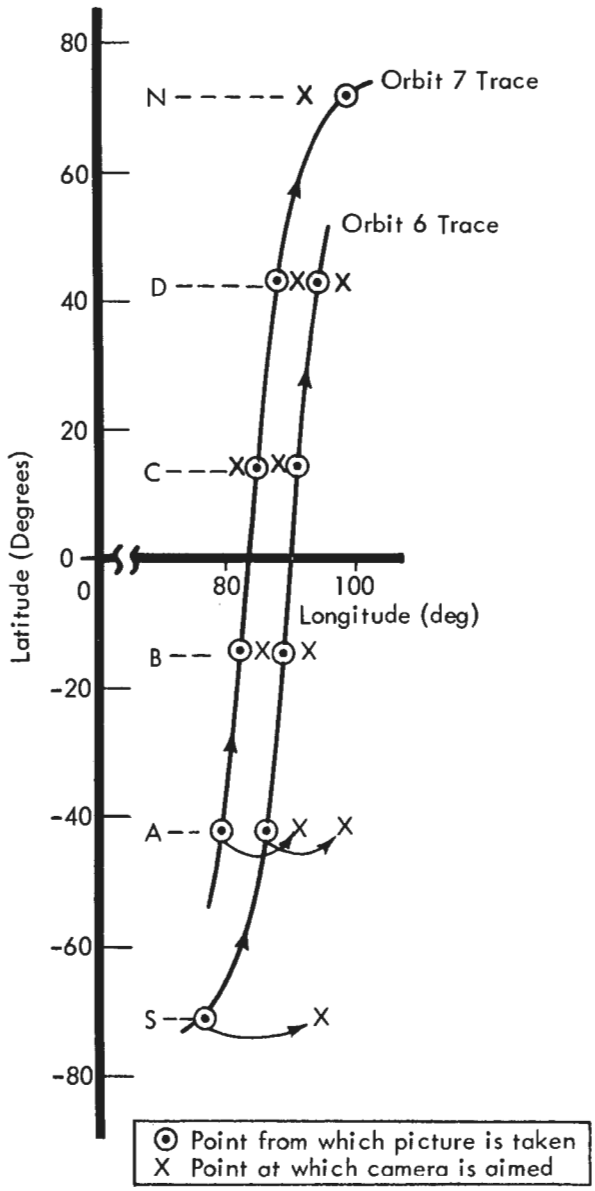

Figure 4-3: Perilune Photography Pointing Orientation

Nearside telephoto photography provided areal coverage of virtually the entire visible half of the lunar surface with resolution capability about 10 times better than the data obtained from Earth-based observations. Feature matching of the photo produced mosaics covering nearly the entire photo zone. In addition, the photos provided the first essentially vertical view of the entire nearside of the Moon, with the eastern and western limbs and the polar regions being of particular interest. The photo of the Orientale basin at the western limb – the details of which had never before been known – is of great scientific value.

Mission IV photography provided farside coverage that can be combined with the coverage of Orbiters I, II, and III to give a total of approximately 60% of the farside surface. The resolution capability of this farside coverage is better than that obtainable of the nearside from Earth.

Although telephoto stereo coverage was not included in mission planning, an evaluation of the photo shows that limited telephoto stereo coverage was obtained. The side overlap and orientation of the zone A, D, and polar region photos provided the limited stereo coverage with complete coverage at latitudes greater than 45 degrees, thus providing additional information of the areas where visibility from Earth-based observations begins to degrade.

4.1.2 Photo Coverage

The primary objective of Lunar Orbiter IV was to conduct a broad systematic survey of the lunar surface. Therefore, the discussion of photo coverage has been arranged to support the general mapping concepts. One hundred and ninety-two exposures were taken and processed during the mission as follows:

- Nearside perilune 158 frames
- Nearside apolune 7 frames
- Farside apolune 9 frames
- Film set (blank) 18 frames

A direct comparison of the coordinates of the photos with existing lunar charts cannot be made over the entire visible surface. Matching of individual photos with the most recent lunar charts indicates varying degrees of agreement. Some contributing factors are: the photo orbit did not pass directly over all sites, variations in lunar surface elevations, uncertainties in the mathematical model of the Moon, and uncertainties in spacecraft attitude based on accumulative effect of photo maneuvers without intervening celestial reorientation. In addition, a secondary objective of the Lunar Orbiter program is to

obtain tracking data from which to refine the mathematical model of the Moon. To compute the photo supporting data and predicted photo locations, the best available estimates for these parameters must be used in the orbit determination routines. Therefore, some discrepancies can be expected in coordination of the computed photo location with the maps made from Earth-based observations. Other errors in locating the photos stem from spacecraft attitude variations within the ±0.2-degree control deadband and the lunar surface elevation changes. It must also be remembered that considerable effort is required to transfer the data from the unrectified, nonorthographic projection photographs to the Mercator projection maps. In general, the lunar feature matching between the photos and lunar charts indicates that the predicted photo locations are generally consistent with the chart "reliability diagram." Continued analysis and comparison of photos obtained from each photo mission will result in more accurately defining the lunar surface, and reducing the positioning error in subsequent lunar charts. In addition, the capability of discerning surface features or formation detail from Earth-based observations falls off rapidly as the limbs and polar regions are approached. Prior to the Lunar Orbiter and Ranger photos, lunar mapping efforts were generally concentrated within ±10 degrees of the equator with limited and decreasing effort in the other regions.

Photo site designations for Mission IV are defined in Table 4-2. The complete site identification also includes the photo orbit number (i.e., 8A is the south temperate photo taken in Orbit 8). For Orbit 6 only, a 1, 2, 3, or 4 follows the zone symbol letter, which represents the exposure number in the four-frame sequence taken at each of the first five sites. Figures 4-4 and 4-5 show the nesting of photos taken on successive orbits for Zones A and B, and C and D, respectively, by spacecraft frame number. Figures 4-6 and 4-7 present the corresponding information for the polar regions. Also shown in the figures are those exposures that were seriously degraded by condensation and light streaking.Figures 4-8 and 4-9 show the nesting of the apolune photos of the northern and southern latitude areas obtained by the recovery photography of Orbits 29, 31, 32, and 33. It must be noted that the grid reference has been rotated by 70 degrees to provide the best display of the data.

Table 4-2: Photo Zone Identification (Lunar Orbiter IV)

Symbol	Nominal Latitude of Principal Point	Zone
A	42.5°S	South temperate
B	14.5°S	South equatorial
C	14.0°N	North equatorial
D	42.5°N	North temperate
S	72.0°S	South polar
N	72.0°N	North polar
F	0°	Film set (Including farside and blanks)
G	33.8°N	North latitudes (recovery)
H	33.8°S	South latitudes (recovery)

Table 4-3 summarizes major photographic parameters of Mission IV photography and provides significant supporting data for each zone. The orbits have been grouped in each band to include all the photos taken with the same design reference spacecraft maneuvers. Geometric parameters of photography are illustrated in Figure 4-10. The angle of incidence is defined as the angle between the Sun's rays and the normal to the lunar surface. The phase angle is the angle between the camera axis and the Sun's rays. The angle and altitude ranges are for the first and last frames of the group, respectively. The angle "alpha" is defined as the angle between the projection of the surface normal and the camera axis, measured in

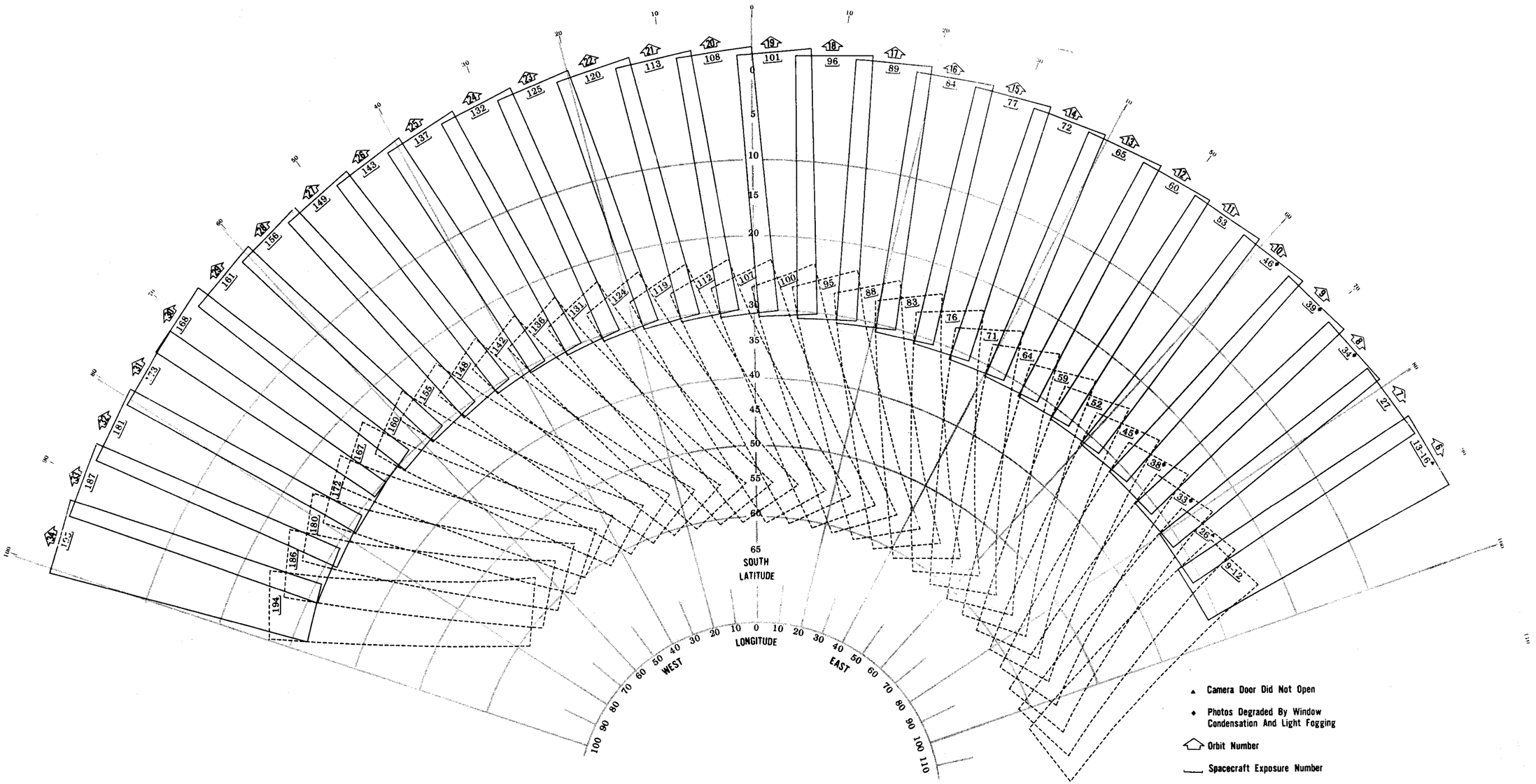

Figure 4-4: Photo Zones A and B Telephoto Footprints

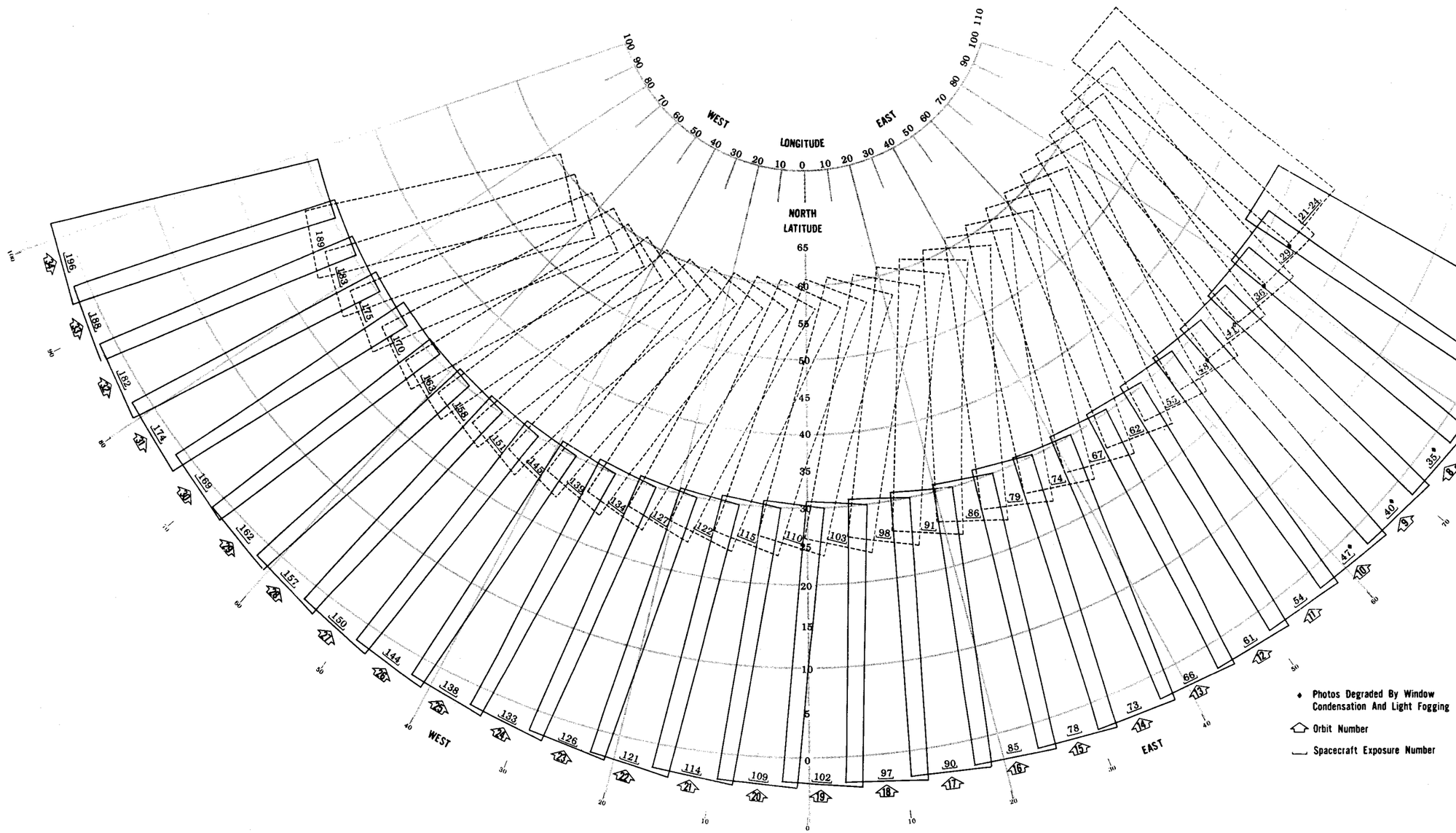

Figure 4-5: Photo Zones C and D Telephoto Footprints

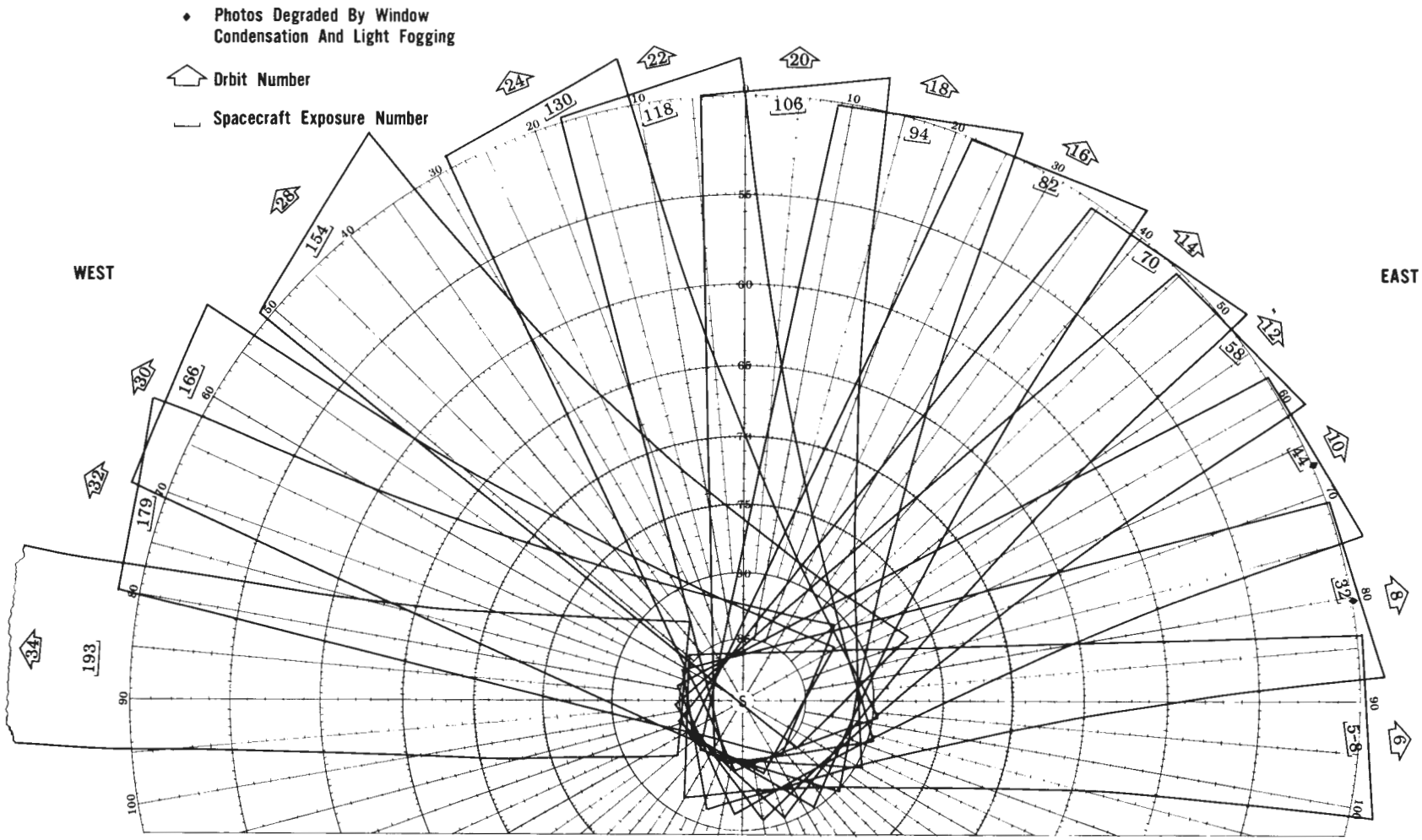

Figure 4-6: Photo Zone S Telephoto Footprints (South Polar)

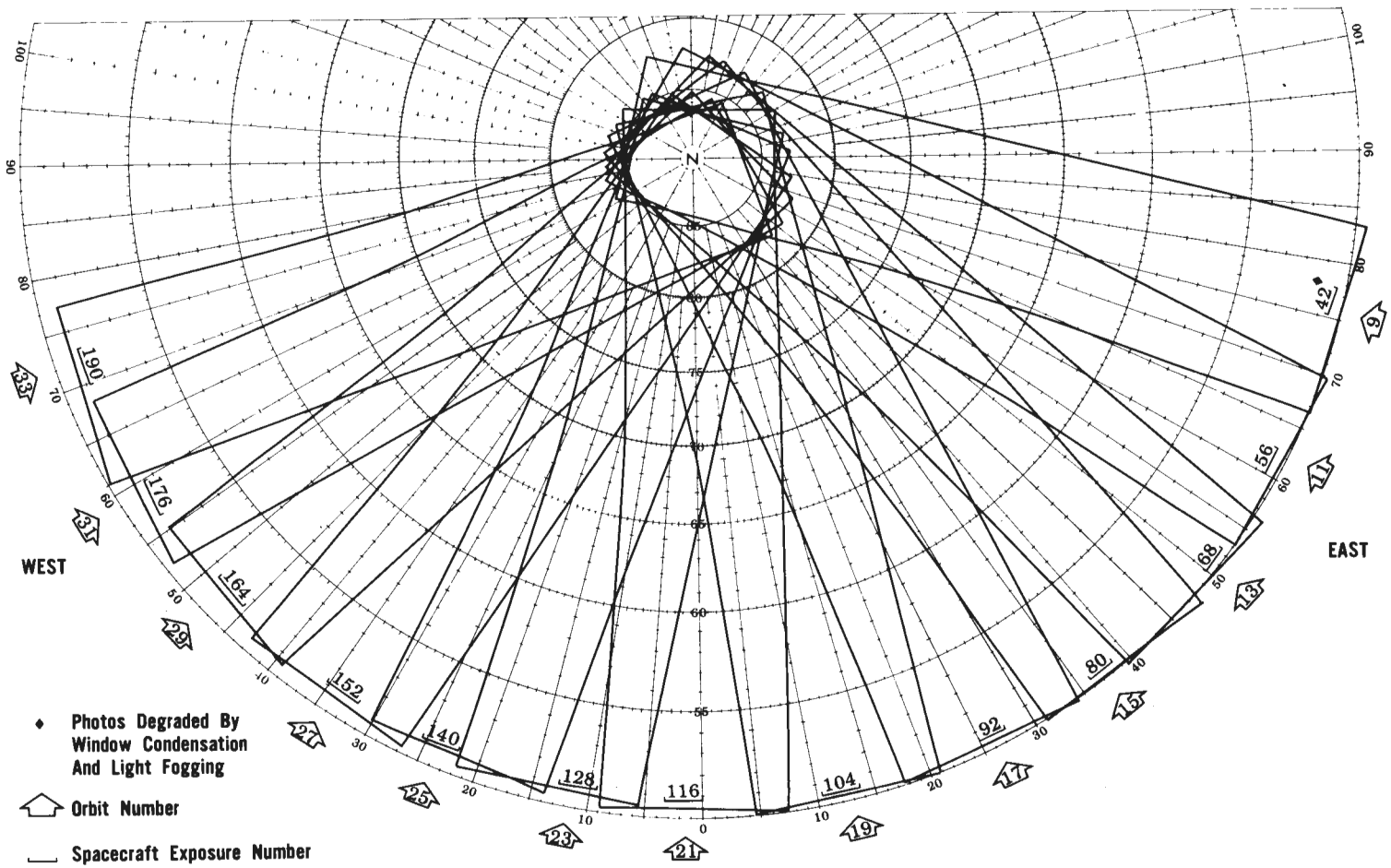

Figure 4-7: Photo Zone N Telephoto Footprints (North Polar)

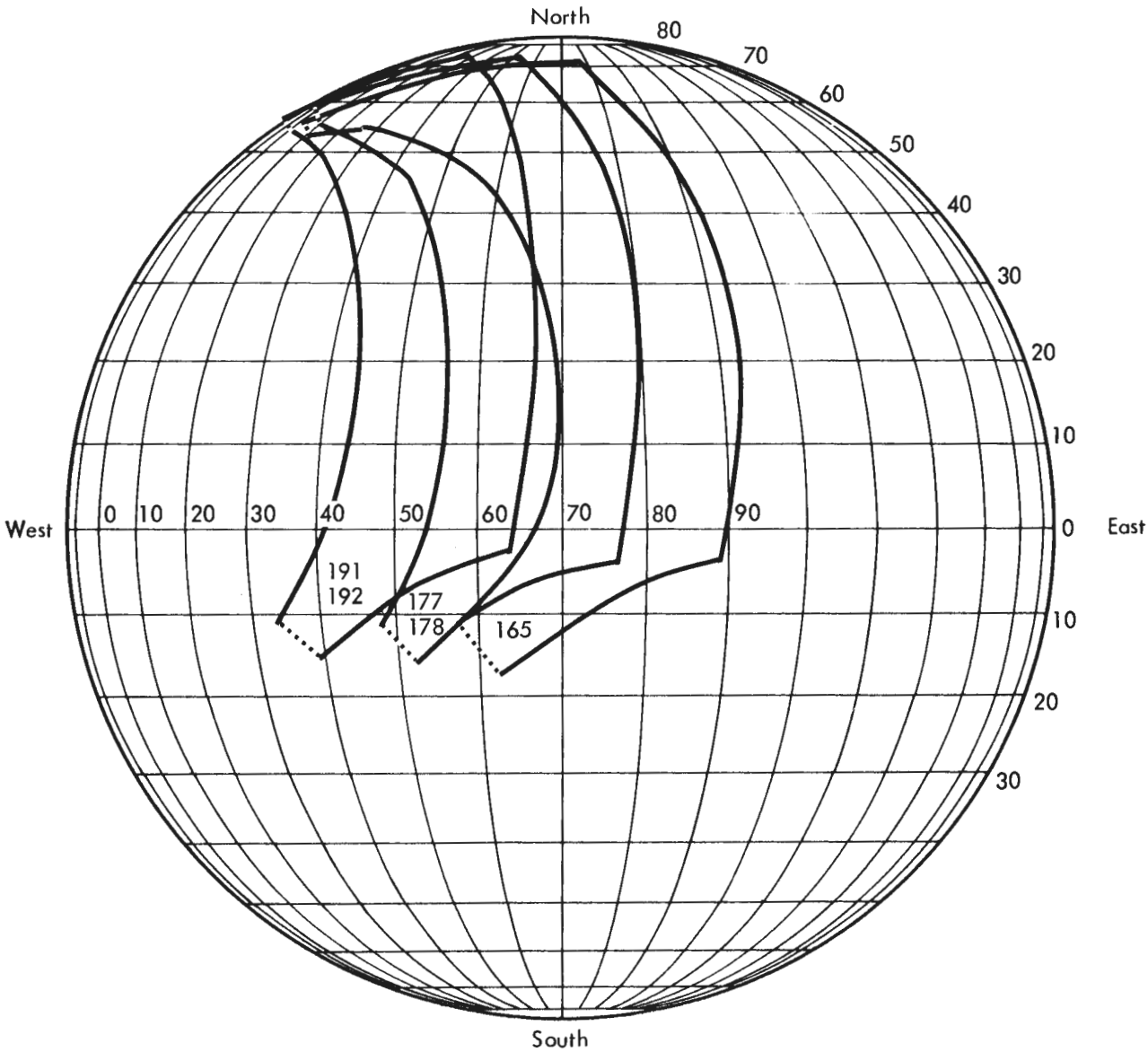

Figure 4-8: North Latitude Zone Recovery Photo Footprints

the phase angle (camera-Sun-principal point) plane. The slant distance is defined as the distance between the camera and the principal ground point (the intersection of the projected camera axis and the lunar surface). Tilt angle is defined as the true angle between the camera axis and the local vertical through the spacecraft. Tilt azimuth is the clockwise angle from lunar north to principal ground point measured from the vertical projection of the spacecraft on the lunar surface. Since the photos were taken from relatively high altitudes including the employment of cross-axis camera tilt, the lunar surface scale factor changes throughout the photo. The relationship between the distance covered on the lunar surface for a telephoto framelet is given by the expression

$$D_{km} = 0.004164 \times h_{(km)}$$

where h represents the straight line distance from the spacecraft camera to the point of interest on the lunar surface. Correspondingly, the wide-angle photo relationship is

$$D_{(km)} = 0.03175\, h_{(km)}$$

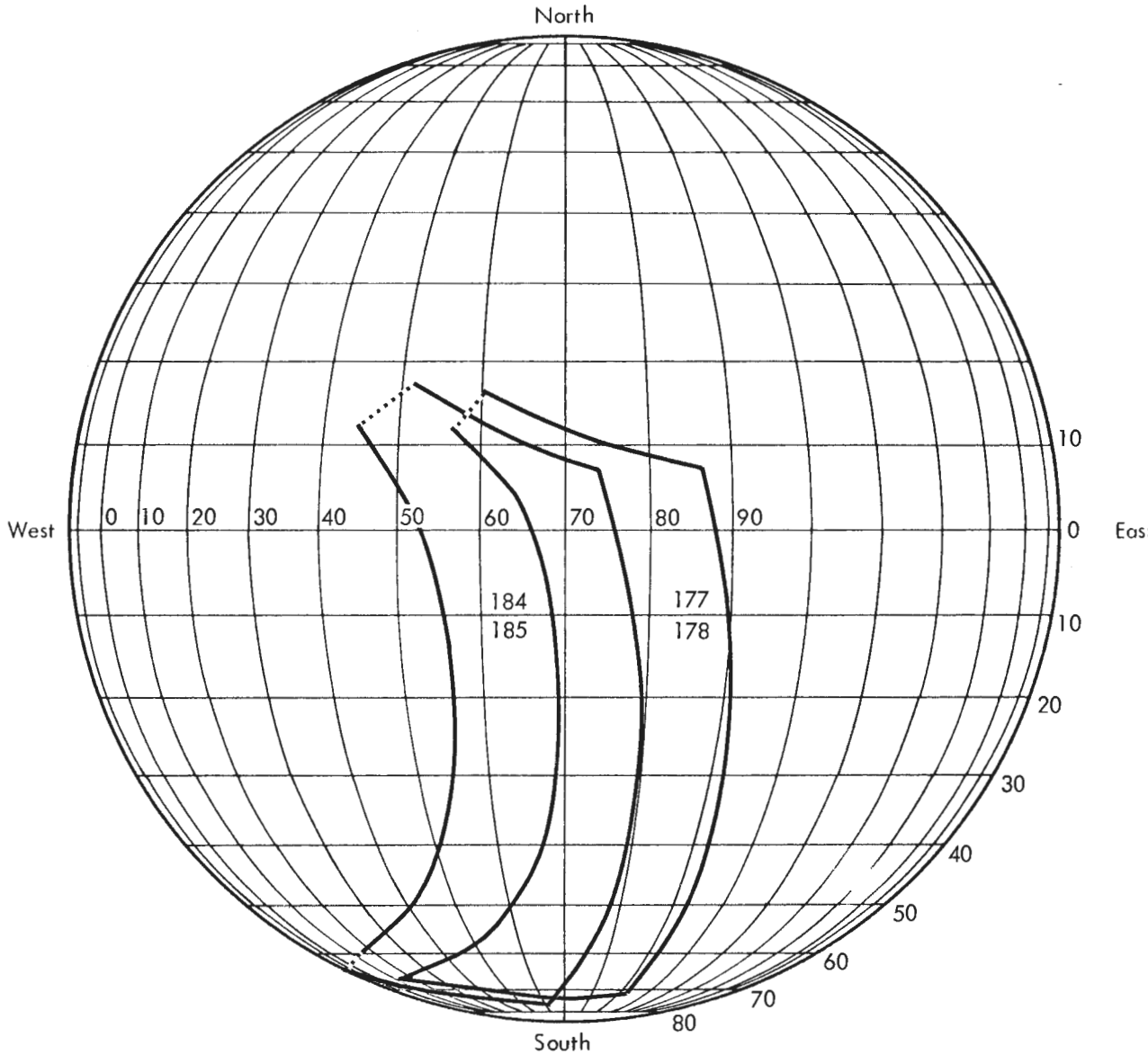

Figure 4-9: South Latitude Zone Recovery Photo Footprints

Figure 4-11 shows this relationship for the altitude and slant range distances applicable to Mission IV telephoto photography.

The following photographs, Figures 4-12 through 4-41, are representative of Mission IV photography. Samples were selected from each of the four frontal zones, two polar zones, and the recovery photographs. In general, the wide-angle photograph and a section of the corresponding telephoto photograph are shown. A broken line outlines the complete telephoto frame while the solid line indicates the coverage of the section selected. Each photograph contains an appropriate descriptive caption.

Figures 4-13 and 4-14 show wide-angle photographs of the same latitude bands but taken three orbits apart, and show the amount of the Moon's precession during the intervening 36-hour period. Figures 4-15 through 4-18 are wide-angle photographsof successive frames of Zones A, B, C, and D taken on Orbit 31. The areal coverage is near the western limb and shows nearly pole to pole coverage.

Table 4-3: Photo Supporting Data

Photo Zone	Photo Orbits	Spacecraft Exposure No.	Shutter Speed sec	Coordinates of Coverage				Spacecraft		Phase Angle deg	Alpha deg	Angle of Incidence deg	Camera Axis Tilt	
				NW	NE	SE	SW	Altitude km	Slant Range km				Angle deg	Azimuth deg
A	6-13	9-12, 26, 33, 38,	0.02	38.9°E	94.9°E	121.8°E	61.3°E	2987-2980	3015-3010	76.5-77.8	-12	64.8-65.5	5	96
		45, 52, 59, 64		27.3°S	22.2°S	55.9°S	61.3°S	2977-2971	3007-3001	78.1-79.1	-12	65.8-66.7	5	96
	14-23	71, 76, 83, 88, 95	0.02	27.1°W	41.9°E	70.3°E	4.1°W	2971-2974	3000-3004	79.4-80.7	-13	67.0-68.1	5	97
		100, 107, 112, 119, 124		27.1°S	23.9°S	55.8°S	61.2°S	2976-2993	3006-3019	81.0-82.5	-13	68.5-69.9	5	96
	24-31	131, 136, 142, 148	0.04	80.5°W	24.1°W	4.6°E	58.6°W	2997-3009	3027-3038	83.0-84.4	-13	70.3-71.6	5	95
		155, 160, 167, 172		26.8°S	23.4°S	55.5°S	61.4°S	3007-3010	3026-3040	83.5-86.2	-9- -13	74.4-73.4	5	96
	32-34	180, 186, 194	0.04	100.3°W	77.5°W	49.4°W	78.5°W	3007-3001	3037-3031	86.7-87.5	-13	73.8-74.6	5	96
				26.9°S	23.3°S	55.9°S	61.5°S							
B	6-13	13-16, 27*, 34, 39	0.02	37.8°E	92.5°E	96.1°E	40.3°E	2746-2743	2746-2743	63.4-64.9	-1	62.9-64.1	0	NA
		46, 53*, 60, 65*	0.01*	2.0°N	4.2°N	30.9°S	31.7°S	2741-2733	2741-2733	65.4-66.8	-1	64.6-66.0	0	NA
	14-23	72, 77, 84, 89, 96	0.02	28.3°W	39.6°E	43.5°E	25.5°W	2731-2720	2731-2720	67.3-69.1	-1	66.5-68.3	0	NA
		101, 108, 113, 120, 125*	0.04*	2.0°N	2.5°N	31.0°S	31.5°S	2719-2715	2719-2715	69.5-71.4	-1	68.8-70.7	0	NA
	24-31	132, 137, 143, 149	0.04	81.2°W	26.6°W	22.5°W	79.0°W	2716-2720	2716-2720	72.0-73.6	-1	71.2-72.8	0	NA
		156, 161*, 168*, 173*	0.02*	2.1°N	2.7°N	30.6°S	31.4°S	2720-2722	2720-2722	74.1-75.7	-1	73.3-74.9	0	NA
	32-34	181, 187*, 195	0.04	101.1°W	79.5°W	75.9°W	98.9°W	2722-2719	2722-2719	76.2-77.3	-1	75.4-76.4	0	NA
			0.02*	2.1°N	2.7°N	30.8°S	31.5°S							
C	6-13	17-20, 28, 35, 40,	0.02	39.9°E	96.6°E	91.9°E	36.9°E	2737-2738	2738-2740	59.4-60.7	3	62.3-60.3	1	277
		47, 54*, 61*, 66	0.01*	31.3°N	31.6°N	3.2°S	2.5°S	2736-2729	2738-2730	61.2-62.7	3	64.4-65.9	1	276
	14-23	73, 78, 85, 90. 97	0.02	26.5°W	42.9°E	38.7°E	29.0°W	2724-2709	2726-2711	63.3-65.2	3	66.4-68.5	1	274
		102, 109, 114, 121, 126		31.0°N	30.1°N	3.3°S	2.1°S	2697-2680	2699-2681	65.7-67.1	3	68.9-70.4	1	274
	24-31	133, 138*, 144, 150*	0.04	78.8°W	23.5°W	27.5°W	82.0°W	2671-2668	2673-2669	68.0-69.4	3	71.2-72.6	1	275
		157, 162, 169, 174	0.02*	31.1°N	30.0°N	2.7°S	1.9°S	2667-2671	2668-2673	69.8-71.3	3	73.0-74.5	1	277
	32-34	182, 188, 196	0.02	98.7°W	76.0°W	80.4°W	101.8°W	2672-2673	2674-2675	71.8-72.8	3	75.0-76.0	1	277
				31.0°S	29.9°S	2.8°S	2.0°S							
D	6-13	21-24, 29, 36, 41	0.02	54.4°E	119.3°E	96.2°E	39.6°E	2977-2981	2980-2983	67.1-67.9	-4	63.3-64.6	1	95
		48, 55, 62, 67		61.5°N	58.2°N	23.4°N	26.0°N	2981-2973	2983-2975	68.3-69.5	-3	65.0-66.2	1	95
	14-23	74, 79, 86, 91, 98	0.02	12.8°W	63.6°E	42.6°E	26.4°W	2968-2935	2970-2937	69.5-71.5	-3	66.5-68-2	1	96
		103, 110, 115, 122*, 127*	0.04*	61.0°N	57.1°N	23.3°N	26.5°N	2924-2884	2926-2886	71.9-73.2	-3	68.5-69.8	1	95
	24-31	134, 139, 145, 151	0.04	64.0°W	3.8°W	23.6°W	78.8°W	2876-2864	2878-2866	73.5-74.3	-3	70.1-70.8	1	95
		158, 163, 170, 175		60.8°N	57.0°N	24.2°N	26.8°N	2863-2869	2865-2872	74.5-75.4	-3	71.1-71.9	1	95
	32-34	183, 189*	0.04	77.3°W	55.4°W	76.1°W	92.1°W	2872-2876	2874-2878	75.7-76.1	-3	72.3-72.6	1	96
			0.02*	60.9°N	56.6°N	24.2°N	26.8°N							

* Shutter Speed change

Table 4-3: (Continued)

Photo Zone	Photo Orbits	Spacecraft Exposure No.	Shutter Speed sec	Coordinates of Coverage NW	NE	SE	SW	Spacecraft Altitude km	Slant Range km	Phase Angle deg	Alpha deg	Angle of Incidence deg	Camera Axis Tilt Angle deg	Azimuth deg
S	6, 8, 10, 12	5-8, 32*, 44, 58	0.04 0.02*	44.8°E 50.2°S	100.6°E 47.8°S	148.1°W 81.4°S	92.5°W 84.7°S	3511-3492	3522-3505	88.1-89.1	-7	81.0-81.5	3	105
	14, 16, 18, 20, 22	70, 82, 94, 106, 118	0.04	17.4°W 49.8°S	51.8°E 49.1°S	160.6°E 80.4°S	165.8°W 84.8°S	3495-3553	3512-3571	89.7-90.7	-9	80.9-81.5	3	104
	24, 28, 30	130*, 154, 166	0.04 0.02*	70.2°W 48.3°S	11.1°W 48.0°S	96.8°E 79.8°S	164.7°E 84.2°S	3575-3612	3596-3653	91.5-94.2	-10, -14	79.8-83.5	4	104
	32, 34	179, 193*	0.02 0.04*	92.6°W 39.7°S	62.6°W 47.7°S	48.3°E 80.5°S	132.0°W 83.4°S	3590-3517	3615-3553	94.1-94.5	-11 & -14	82.8-81.0	4	106
N	7, 9, 11, 13	30, 42, 56*, 68	0.04 0.02*	86.4°W 83.8°N	97.8°E 66.1°N	90.1°E 13.4°N	39.7°E 49.8°N	3307-3492	3425-3493	76.1-77.1	-9, -3	69.0-79.9	9 & 1	198 & 288
	15, 17, 19, 21, 23	80, 92, 104, 116*, 128	0.04 0.02*	140.5°W 84.3°N	162.0°E 82.6°N	47.8°E 49.7°N	21.8°W 50.6°N	3477-3367	3477-3367	78.2-79.3	1	79.2-80.2	0	NA
	25, 27, 29, 31	140, 152*, 164, 176*	0.04 0.02*	163.4°E 85.3°N	94.9°E 83.1°N	13.7°W 50.5°N	68.6°W 51.0°N	3353-3344	3353-3344	80.1-80.2	-1	79.1-79.2	0	NA
	33	190	0.04	154.4°E 85.3°N	44.2°E 82.2°N	61.0°W 50.1°N	77.5°W 50.8°N	3371	3372	81.1	-3	78.4	1	105
F	6, 10	25, 50	0.04	96.1°W 44.3°S	87.4°W 43.2°S	86.8°W 42.3°N	95.5°W 43.6°N	6108-6112	6167-6124	115.2	17 & 8	132 & 123	4&2	91
	14, 18, 22	75, 99, 123	0.04	169.9°W 36.4°S	161.6°W 42.4°S	161.3°W 44.4°N	156.3°E 45.0°N	6125-6149	6125-6149	115.2 & 111.0	-2 & -10	113.7-104.7	0 & 2	275
	26	146, 147	0.04	163.9°E 36.1°S	140.0°E 43.6°S	105.0°E 37.3°N	129.4°E 45.0°N	6146-6147	6146-6147	109.0	0	108.9	0	NA
G	29, 31	165, 177	0.04	76.1°E 3.4°S	57.2°E 15.2°S	9.4°E 51.7°N	53.5°E 71.8°N	5484&5490	6147&5725	109.2 & 108.1	-34	74.6 & 73.8	8	279
	33	191, 192	0.04	63.4°E 3.4°S	31.6°E 16.6°S	17.5°W 50.7°N	39.0°E 71.8°N	5501	5735	107.2	-34	73.0	8	279
H	30, 31	178	0.04	91.6°E 72.8°S	17.2°E 65.9°S	58.7°E 15.9°N	85.3°E 7.8°N	5794	5918	112.1	-25	87.6	6	264
	32	184, 185	0.04	63.4°E 74.0°S	14.5°W 54.1°S	42.1°E 16.7°N	74.1°E 7.2°N	5788	5989	113.1	-32	81.7	7	262

* Shutter Speed change

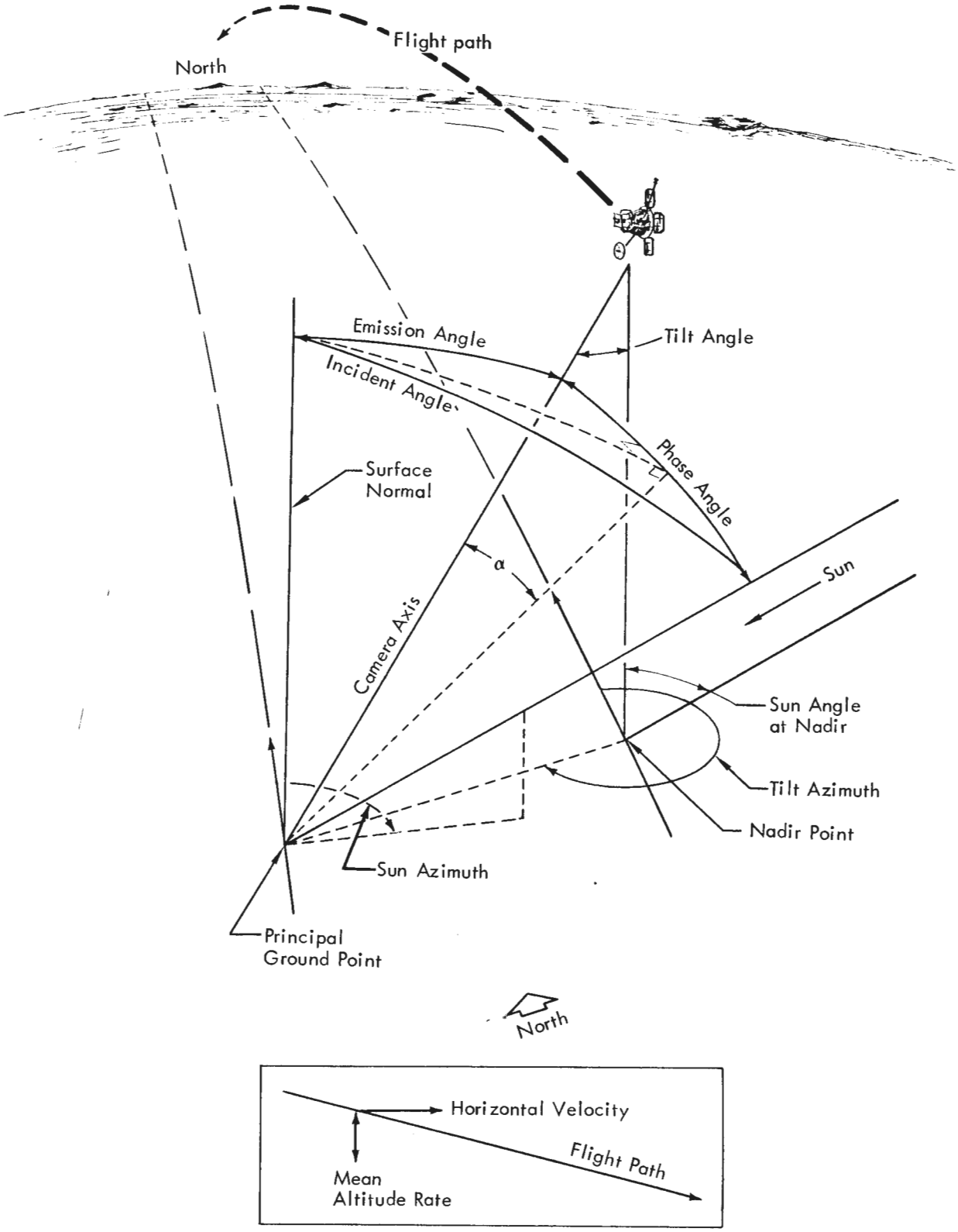

Figure 4-10: Geometrical Parameters of Photography

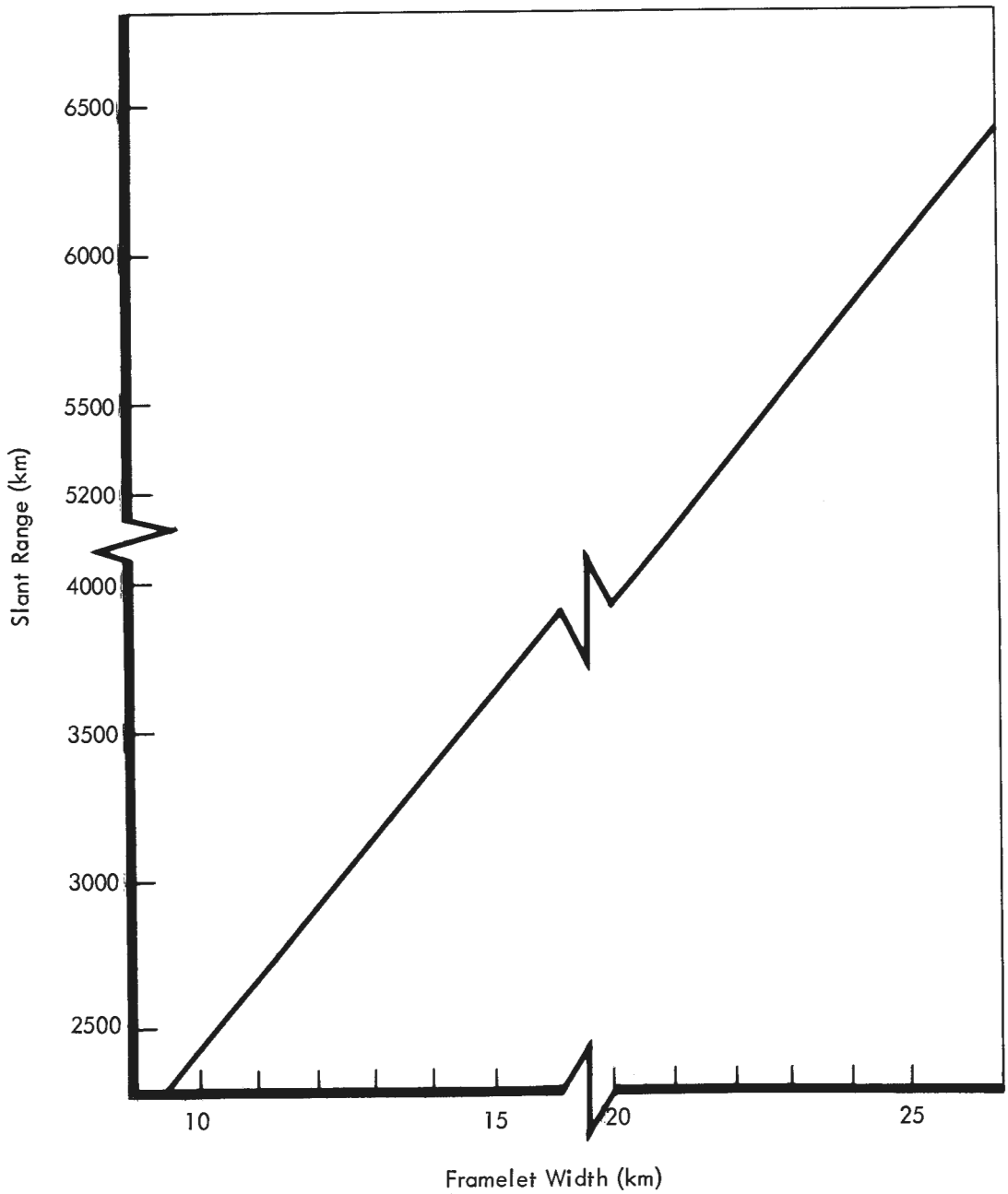

Figure 4-11: Slant Range vs Framelet Width (Telephoto Lens)

Figures 4-19 and 4-20 show the side overlap of telephoto photographs on successive orbits for equatorial (Zone C) photographs. The vertical overlap of successive telephoto photographs is illustrated in Figures 4-21 and 4-22.

Figures 4-23 and 4-24 show photo mosaics assembled by NASA Langley from the telephoto photographs of northern and southern regions greater than 30° latitude. The remaining photographs (Figures 4-25 through 4-41) were selected to illustrate lunar features and areas of scientific interest photographed during the mission.

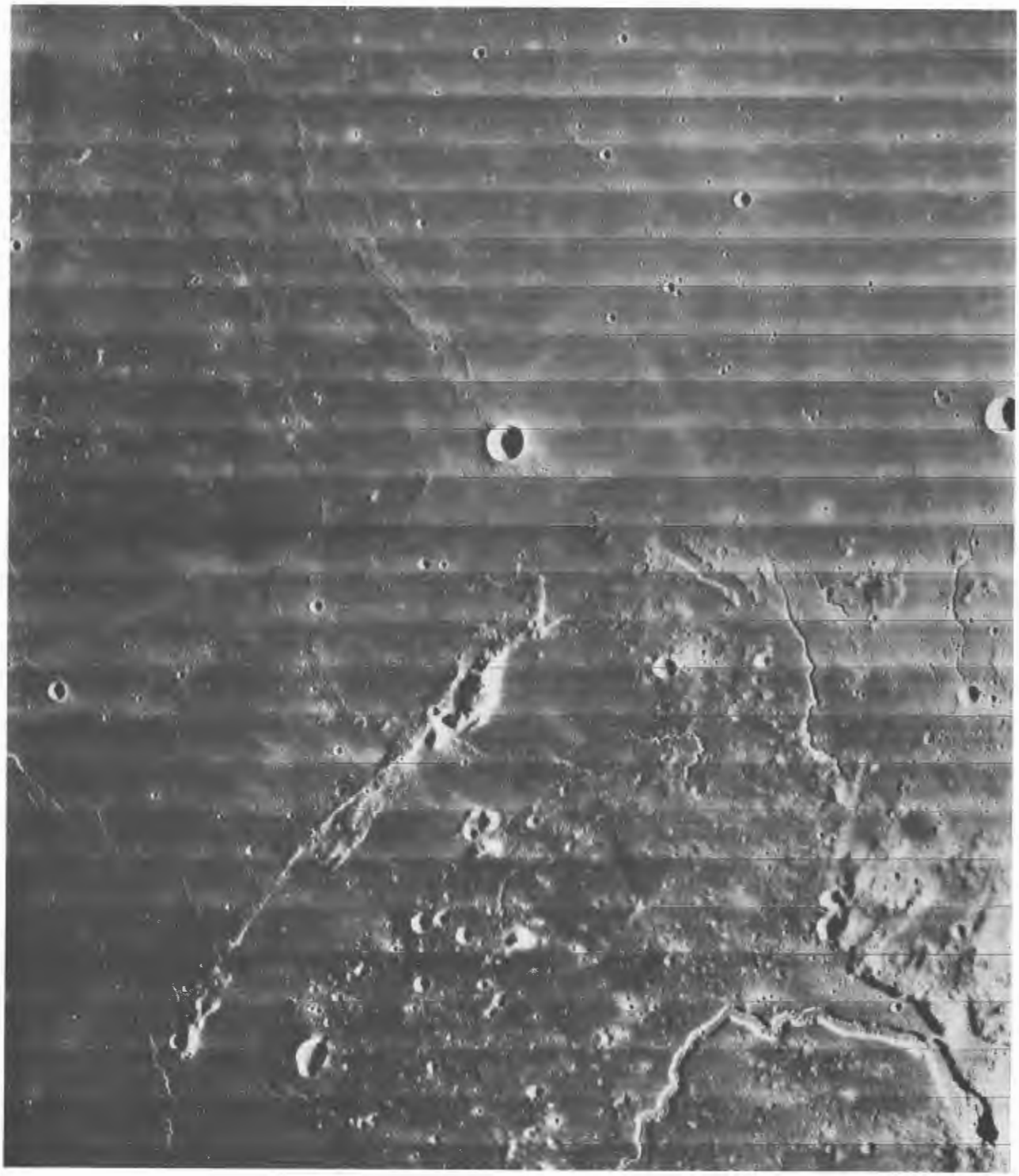

Schröter's Valley.

Figure 4-12: Portion of Telephoto Frame 158, Site IV28D

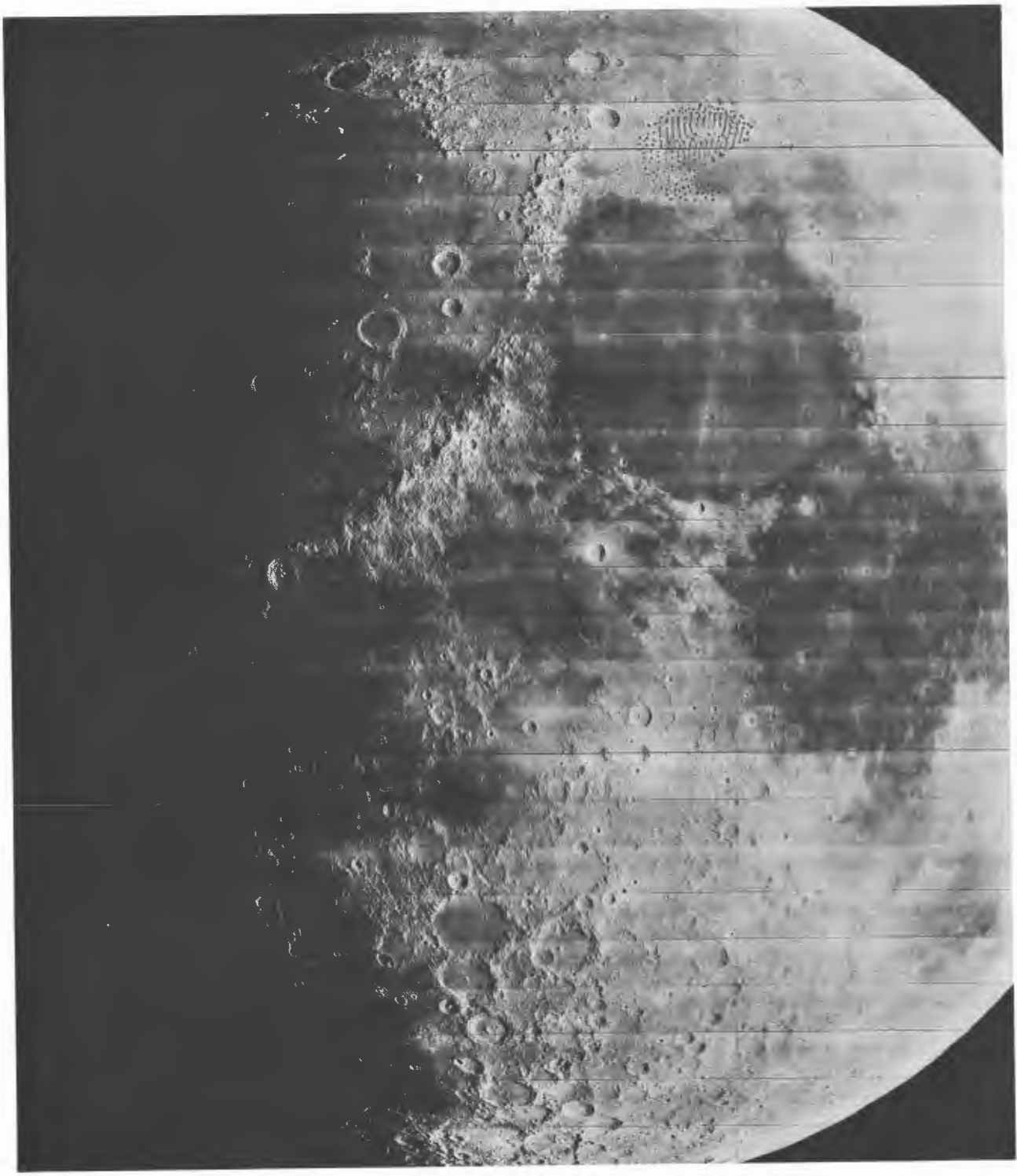

Centered near Mare Vaporum,
at 3.1°E, 14.0°N.

Figure 4-13: Wide-Angle Frame 102, Site IV19C

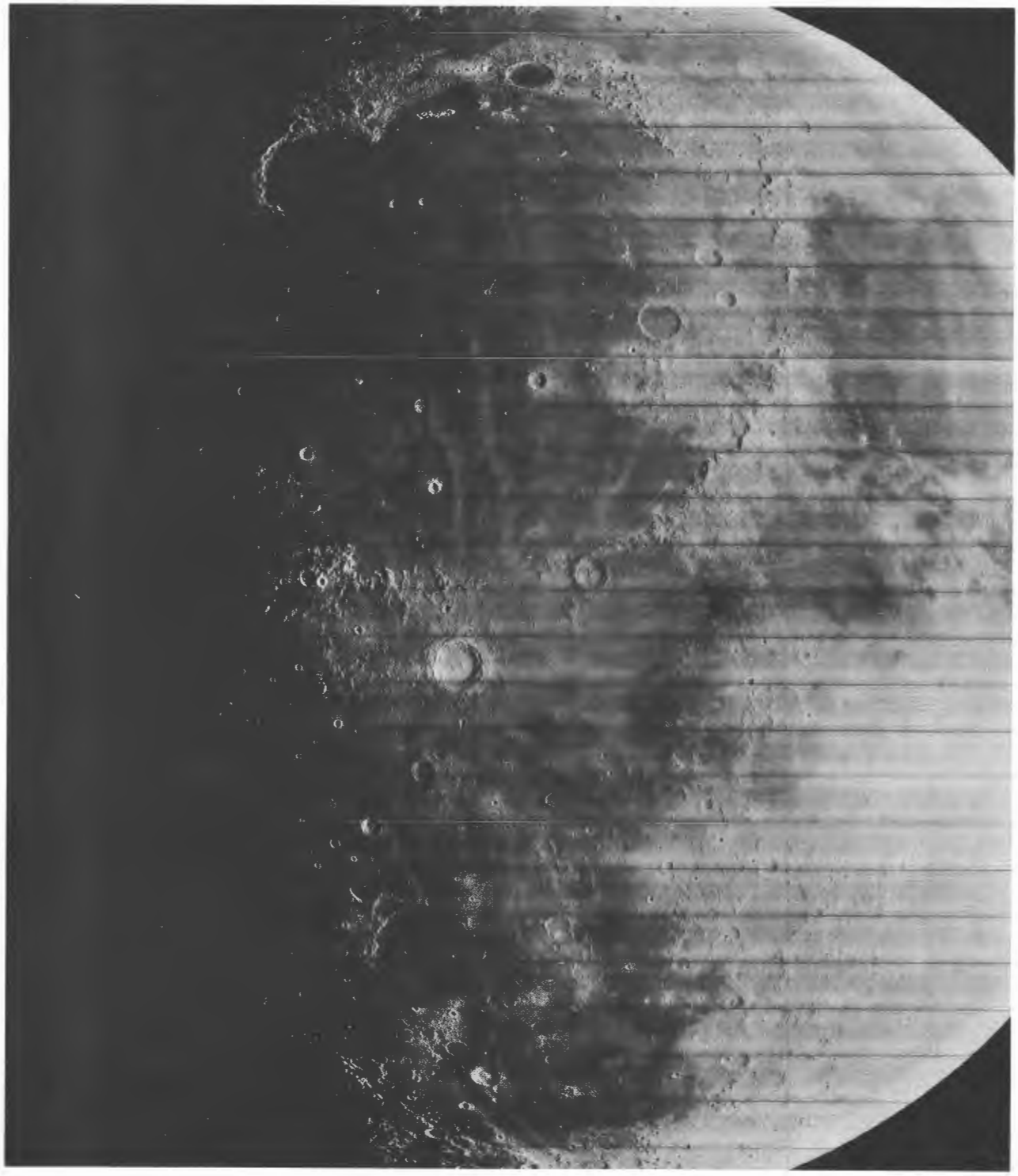

Centered near Copernicus and Eratothenes,
at 16.7°W, 14.0°N.

Figure 4-14: Wide-Angle Frame 121, Site IV22C

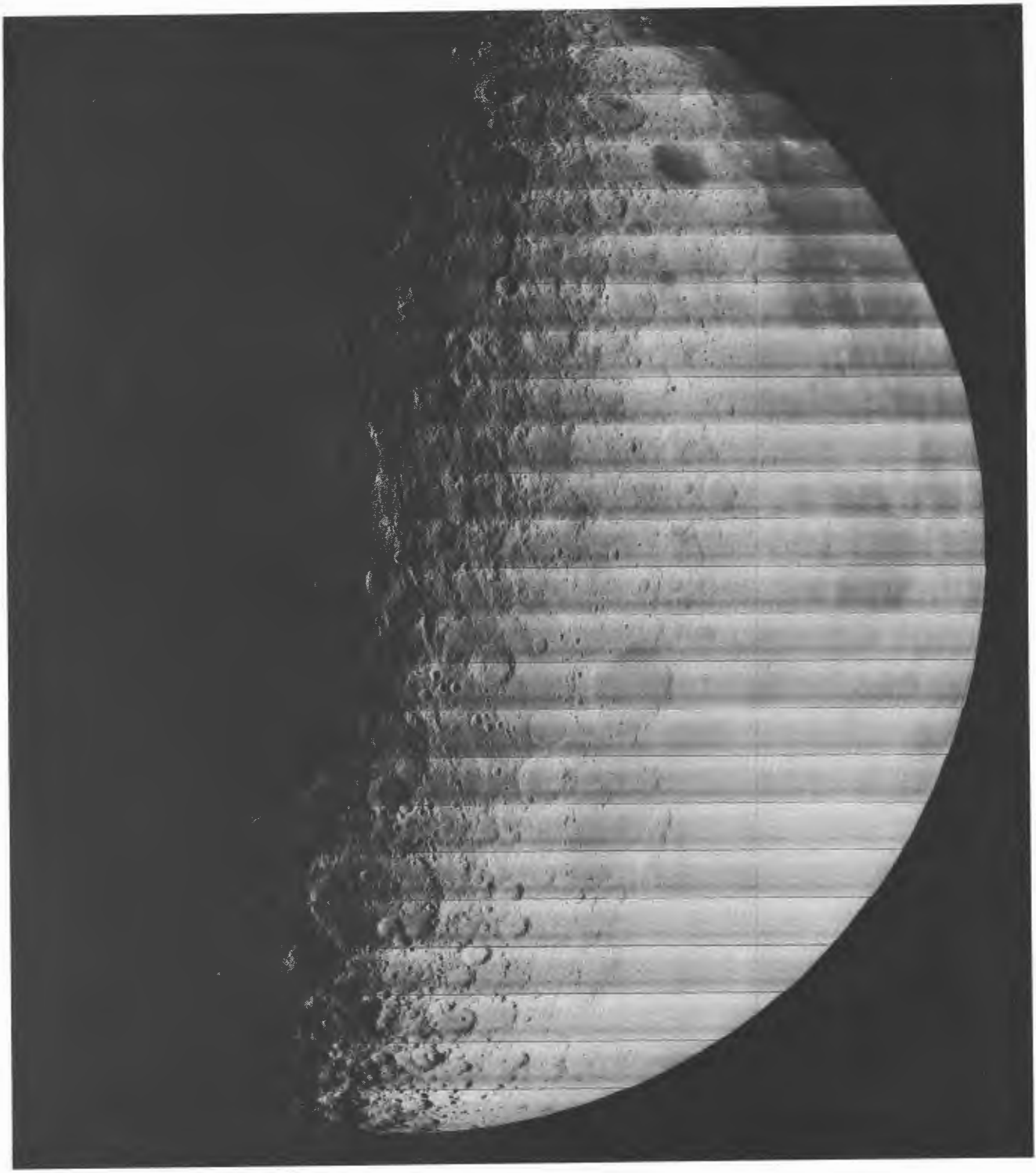

Centered near Southwestern limb,
at 67.8°W, 42.3°S.

Figure 4-15: Wide-Angle Frame 172, Site IV31A

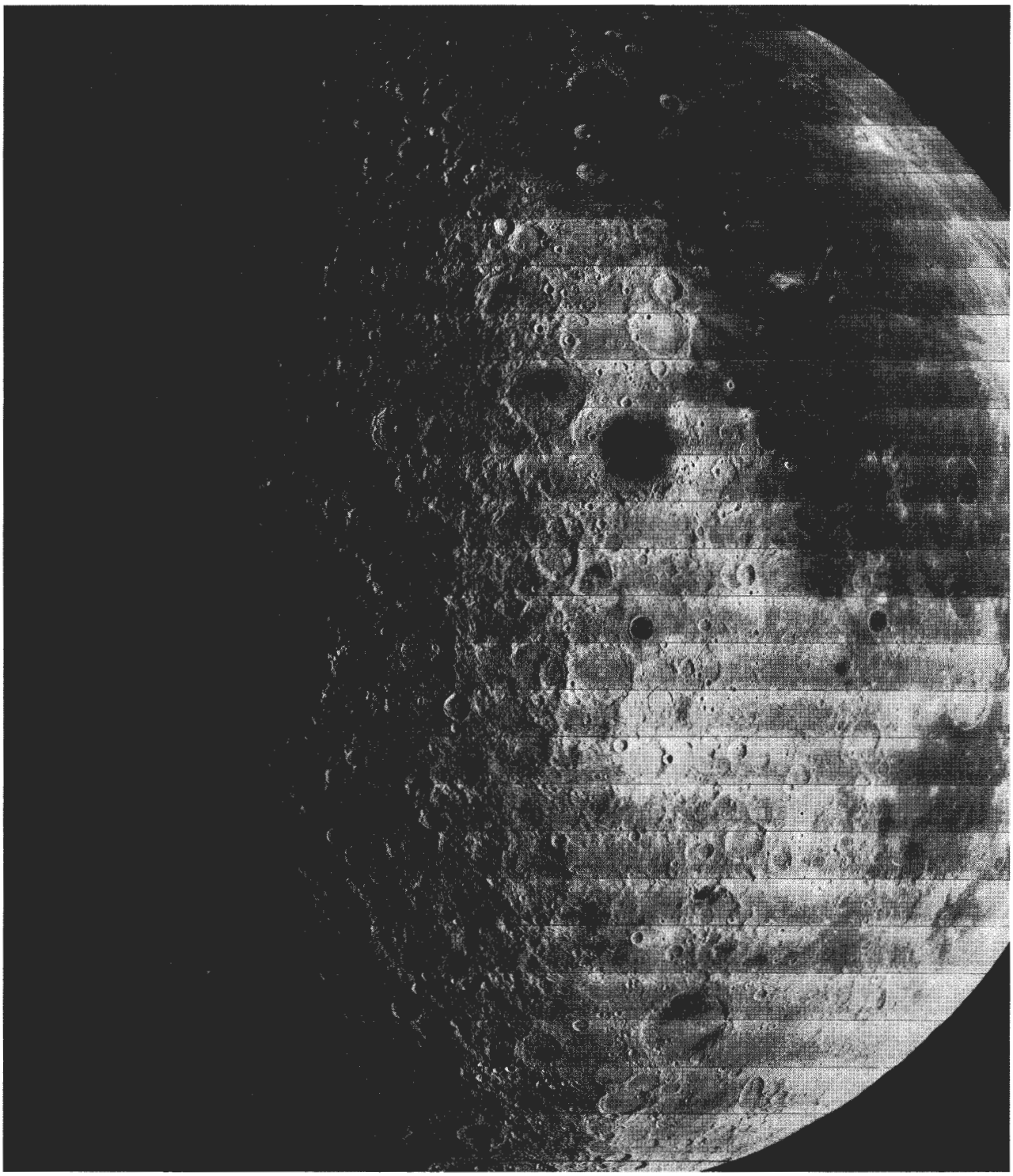

Centered southwest of Grimaldi;
Orientale Basin at left center.

Figure 4-16: Wide-Angle Frame 173, Site IV31B

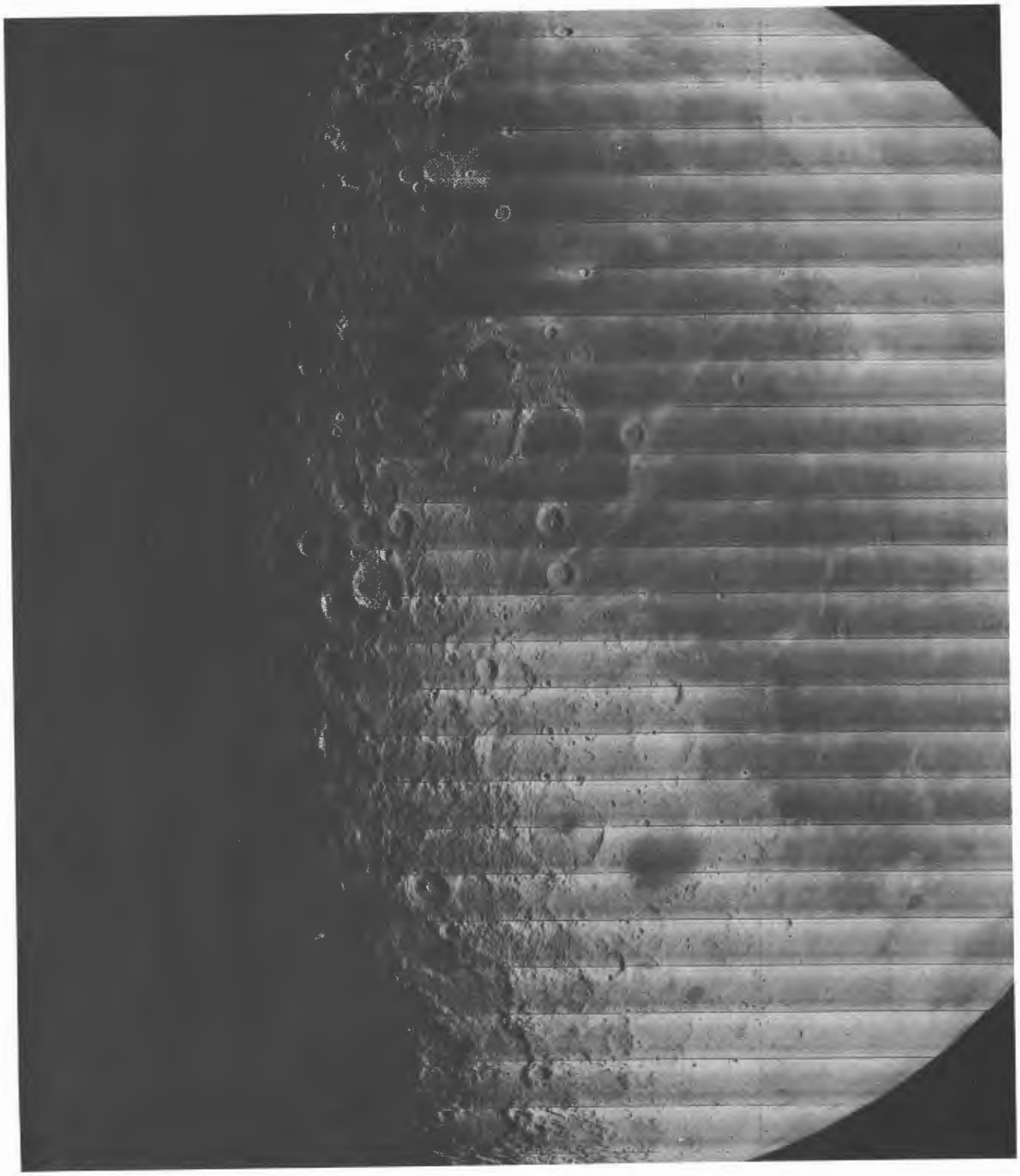

Centered at 75.9°W, 14.1°N;
Orientale Basin at bottom.

Figure 4-17: Wide-Angle Frame 174, Site IV31C

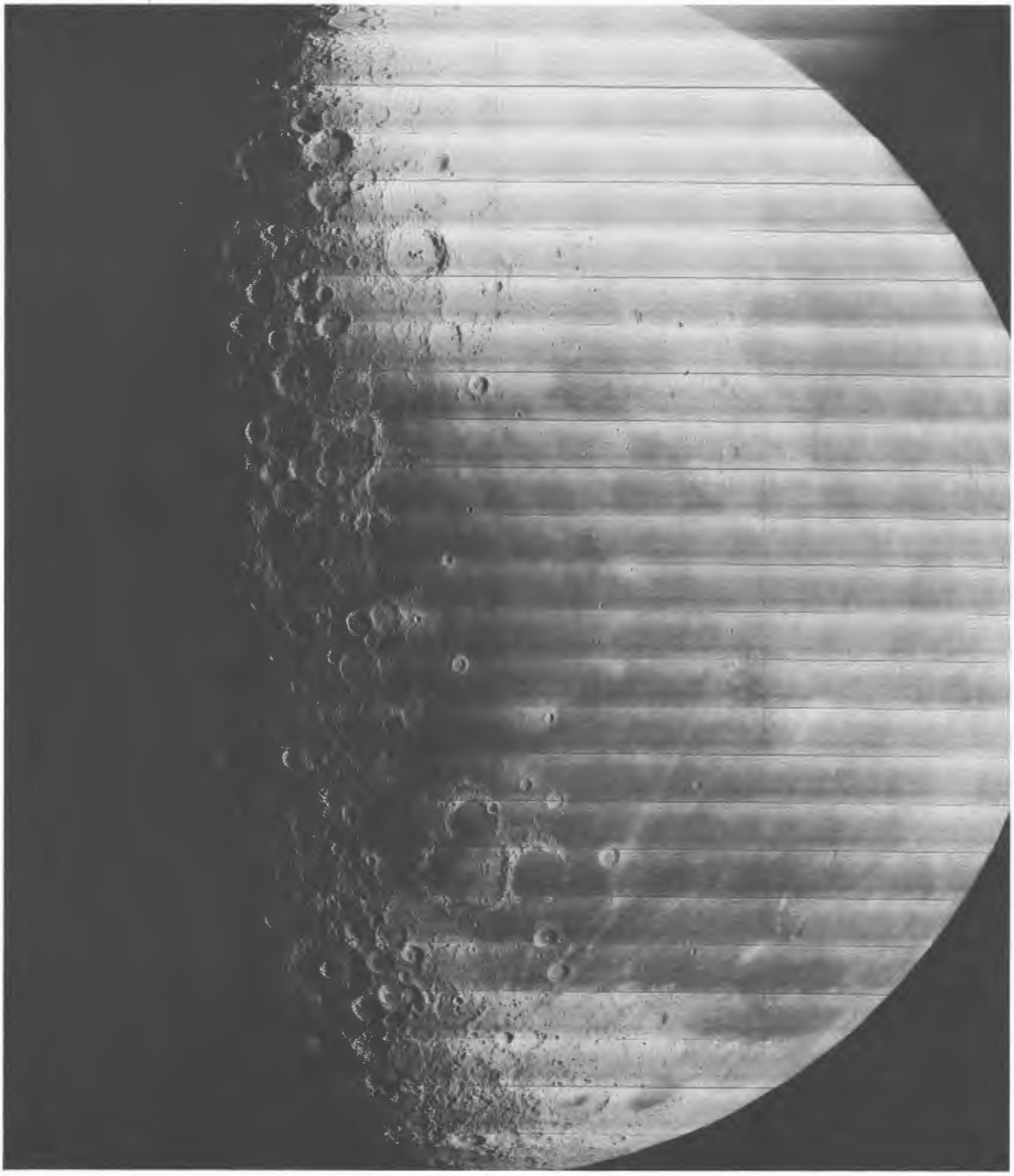

Northwestern Limb;
centered at 67.8°W, 42.6°N.

Figure 4-18: Wide-Angle Frame 175, Site IV31D

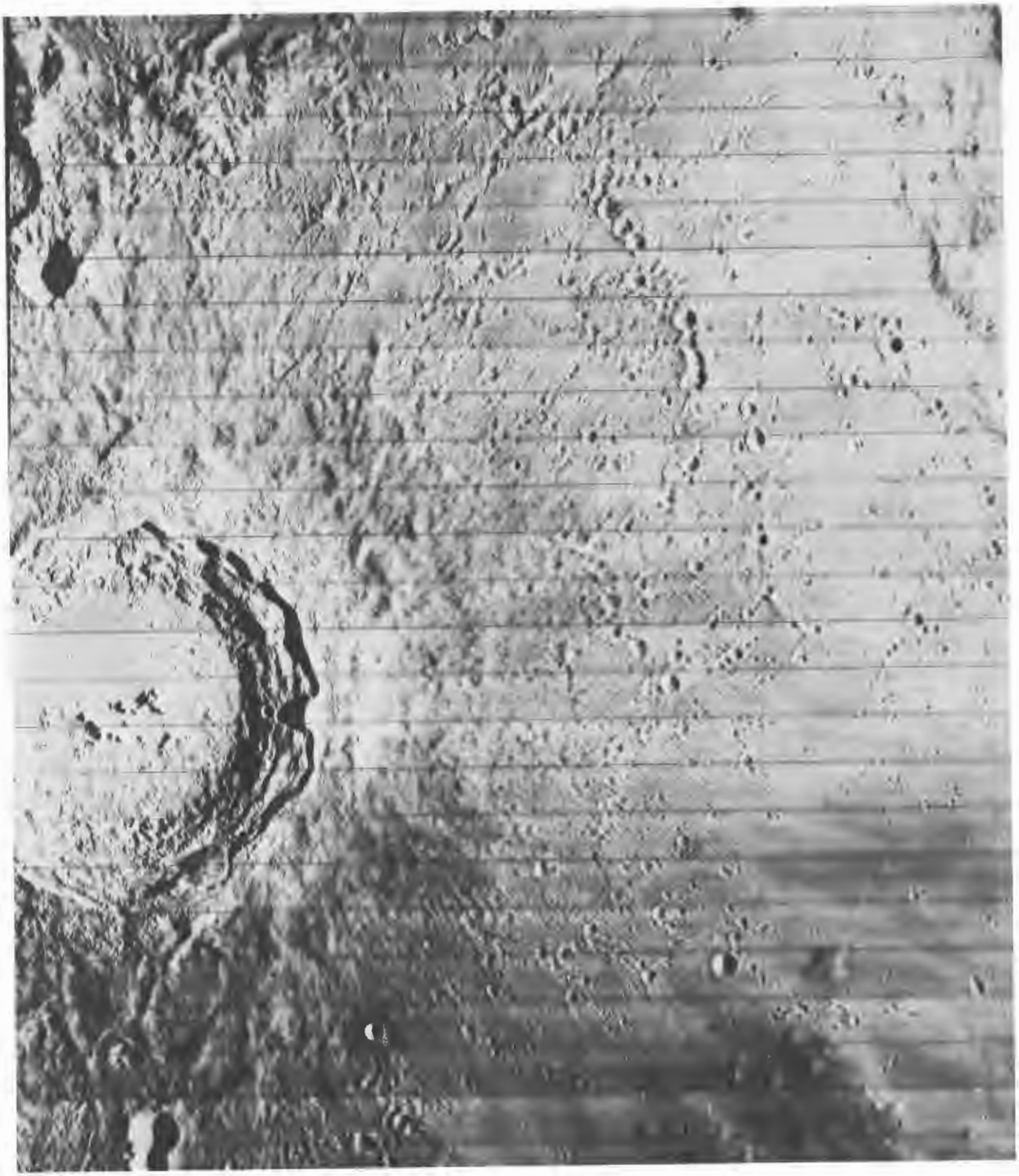

Copernicus and Eastern Appenine Mountains;
taken on orbit after Figure 4-20.

Figure 4-19: Portion of Telephoto Frame 121, Site IV22C

Centered near Eratosthenes and Appenine Mountains;
side overlap with Figure 4-19.

Figure 4-20: Portion of Telephoto Frame 114, Site IV21C

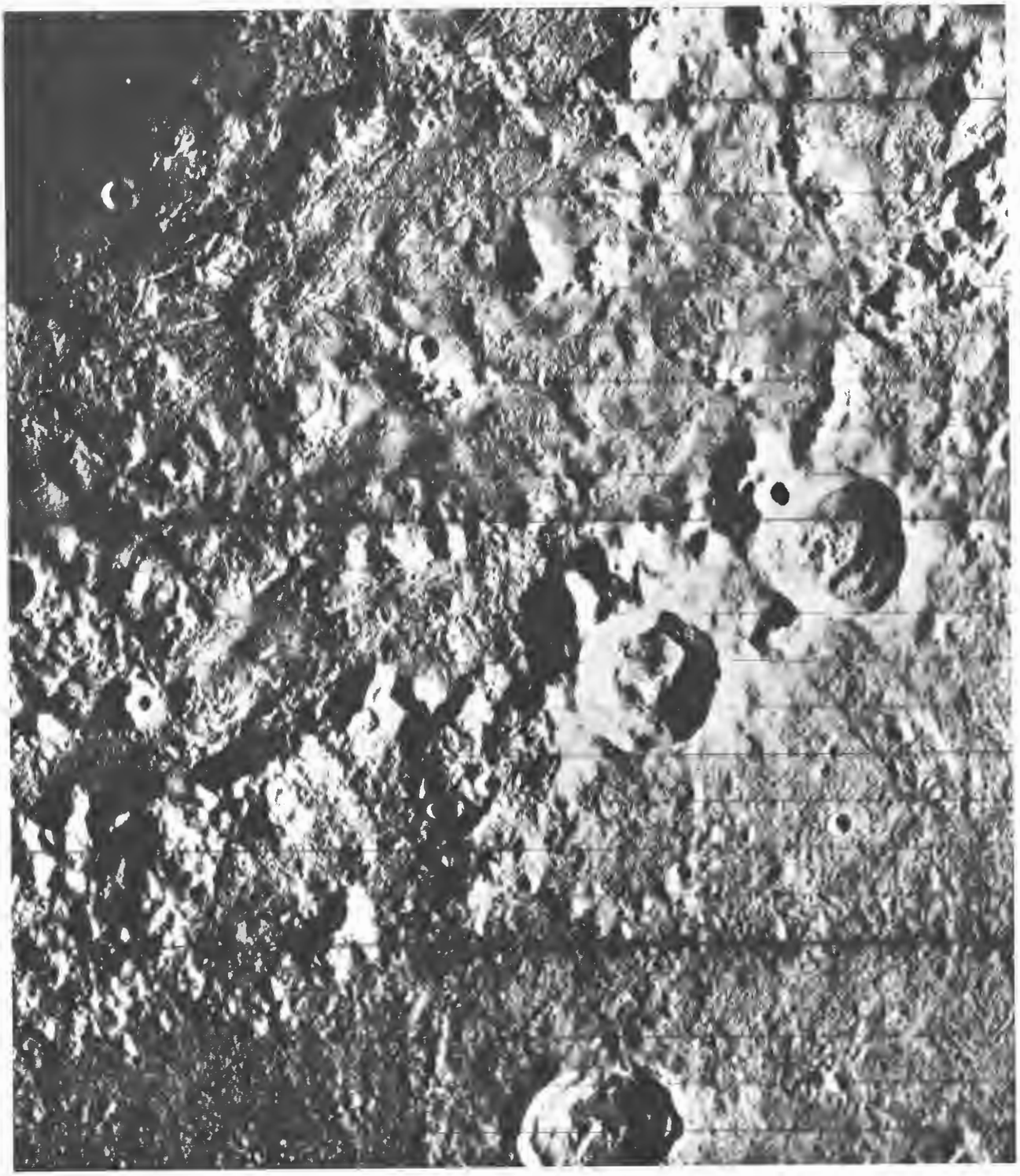

Southeast quadrant of Orientale Basin with outer rim;
vertical overlap with Figure 4-22.

Figure 4-21: South Portion of Telephoto Frame 187, Site IV33B

Southeast quadrant of center of Orientale Basin.

Figure 4-22: North Portion of Telephoto Frame 186, Site IV33A

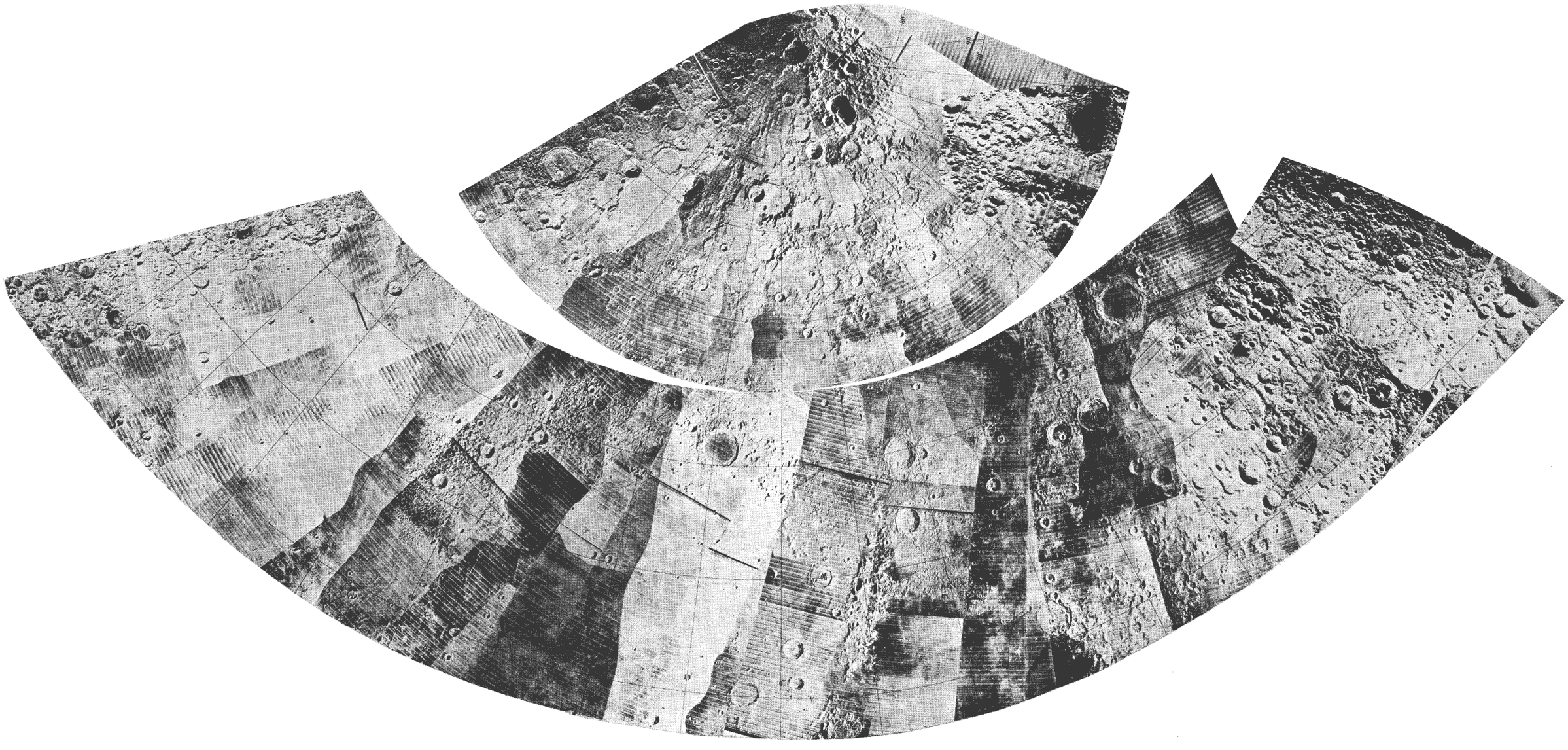

Figure 4-23:
Photo Mosaic of High Northern Latitudes

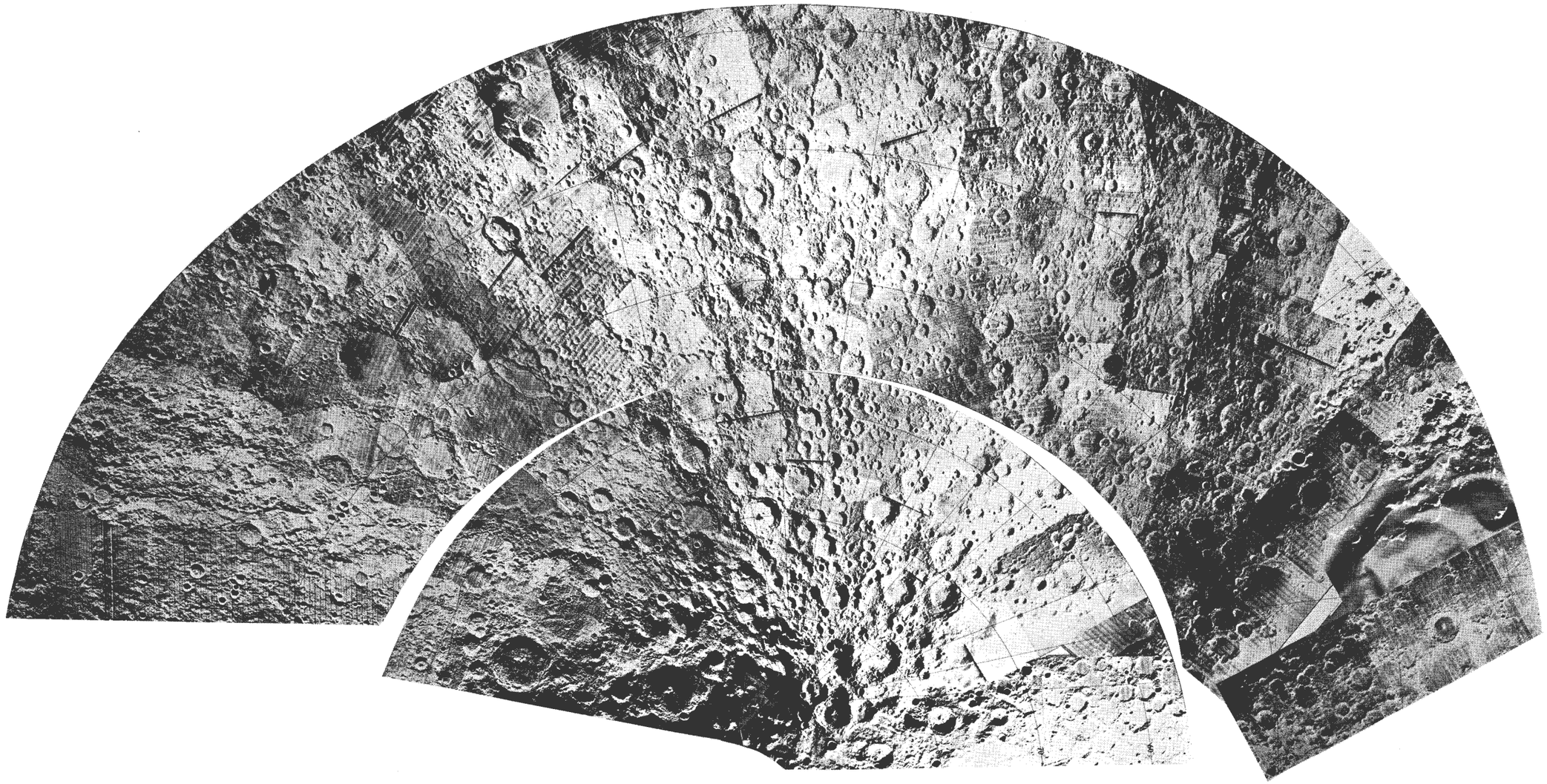

Figure 4-24:
Photo Mosaic of High Southern Latitudes

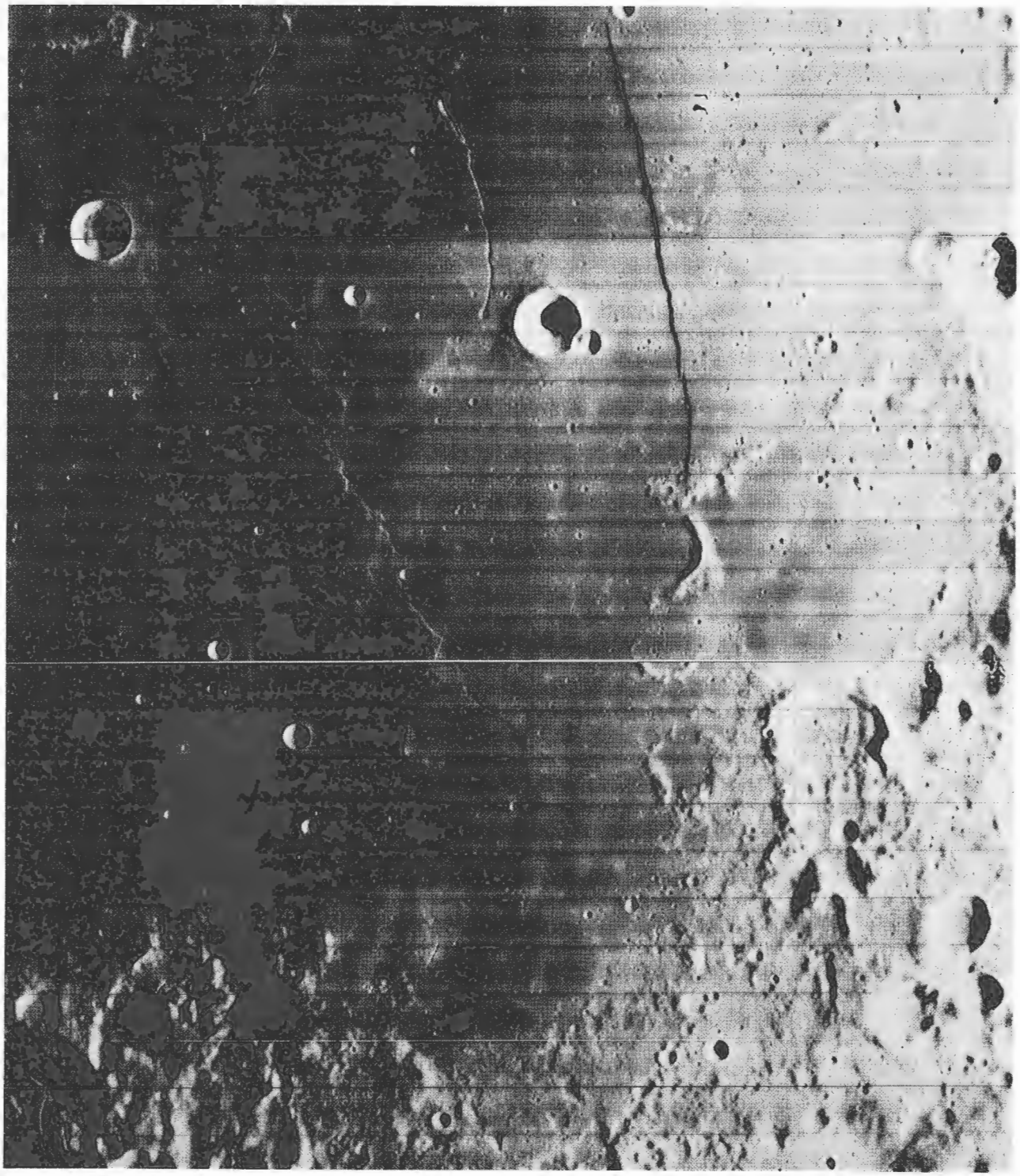

Rupes Recta.

Figure 4-25: Portion of Telephoto Frame 113, Site IV20B

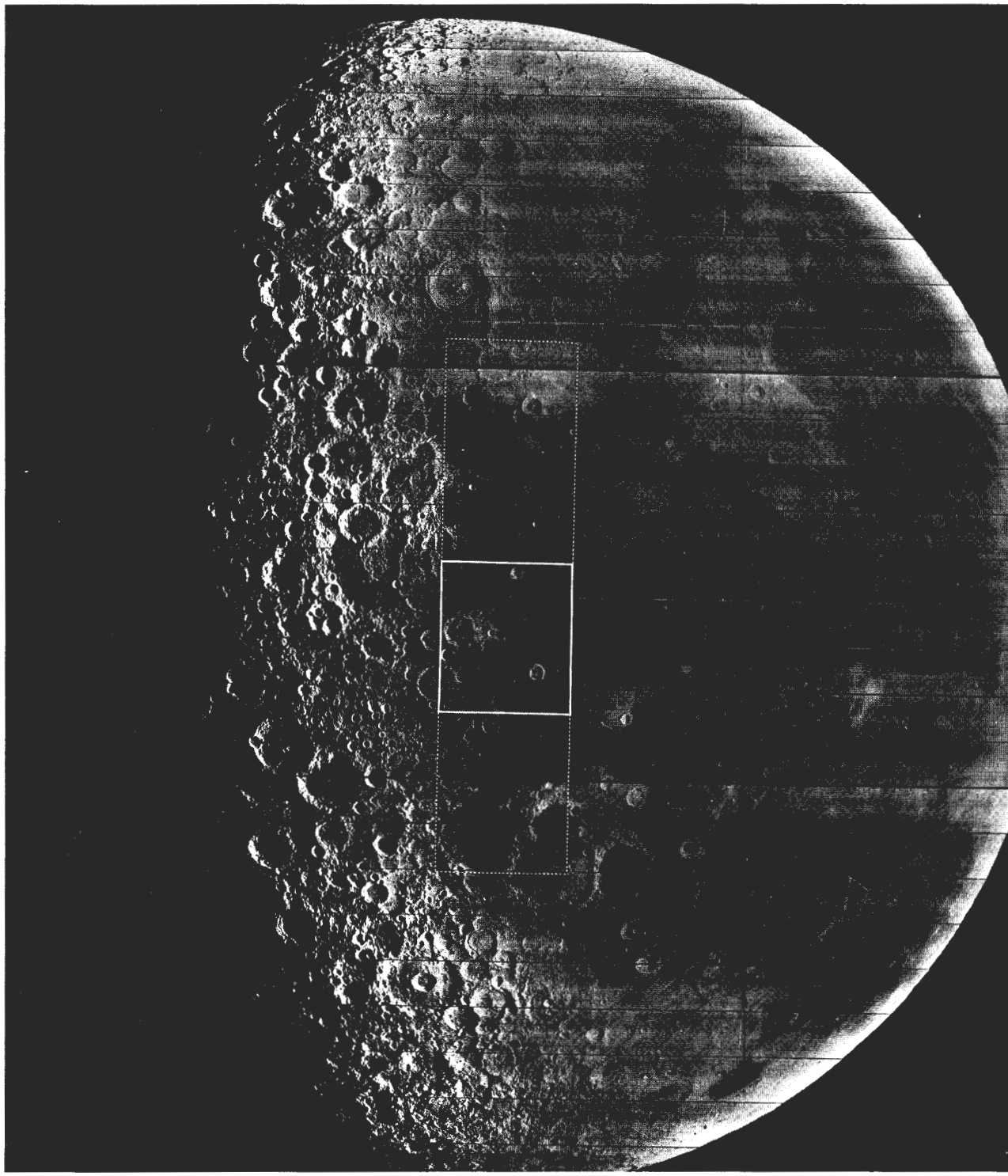

Centered at 74.4°W, 42.5°N;
outlined areas of complete telephoto coverage and
portion shown in Figure 4-27.

Figure 4-26: Wide-Angle Frame 183, Site IV32D

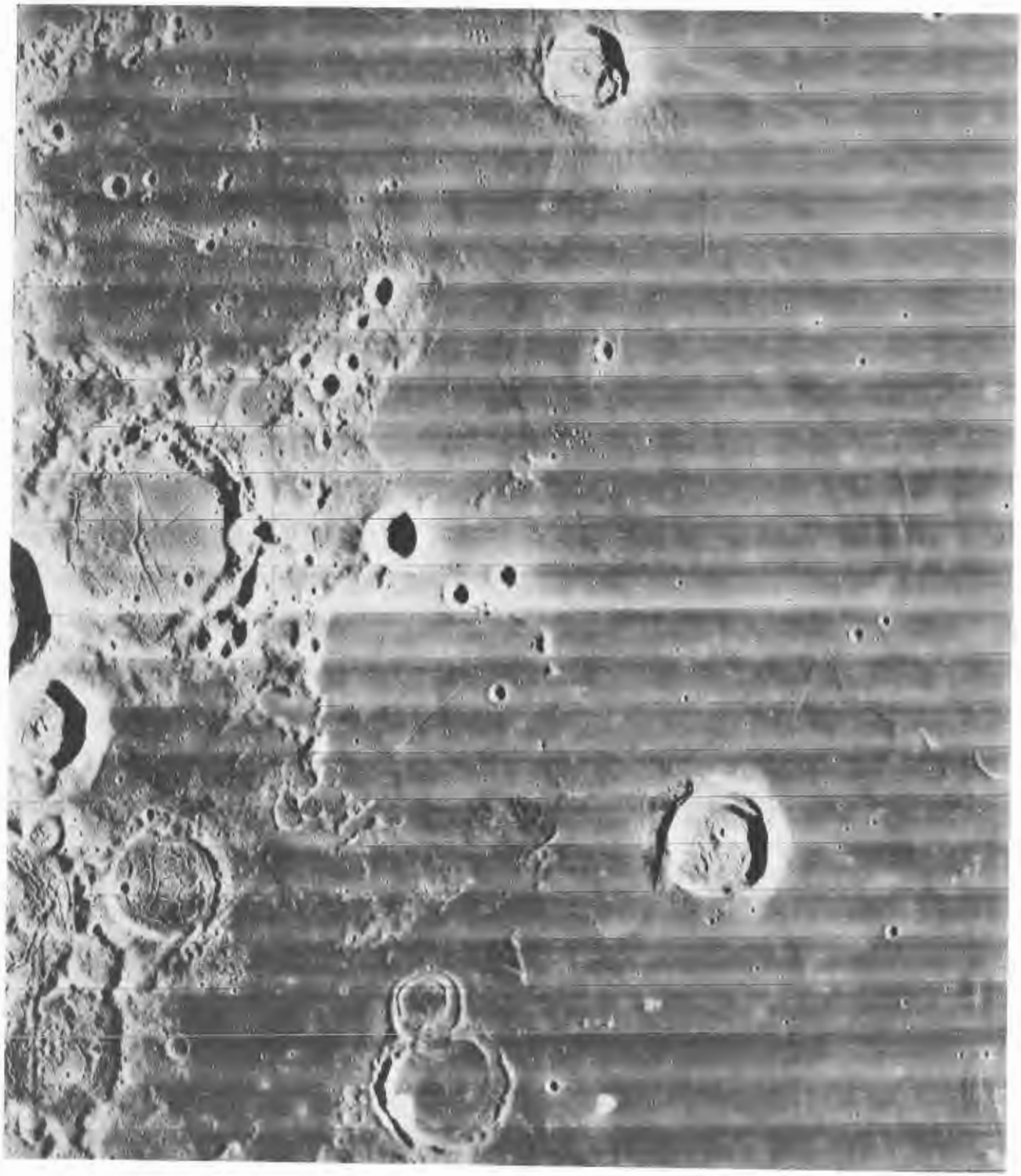

Northwest limb area outlined in Figure 4-26.

Figure 4-27: Portion of Telephoto Frame 183, Site IV32D

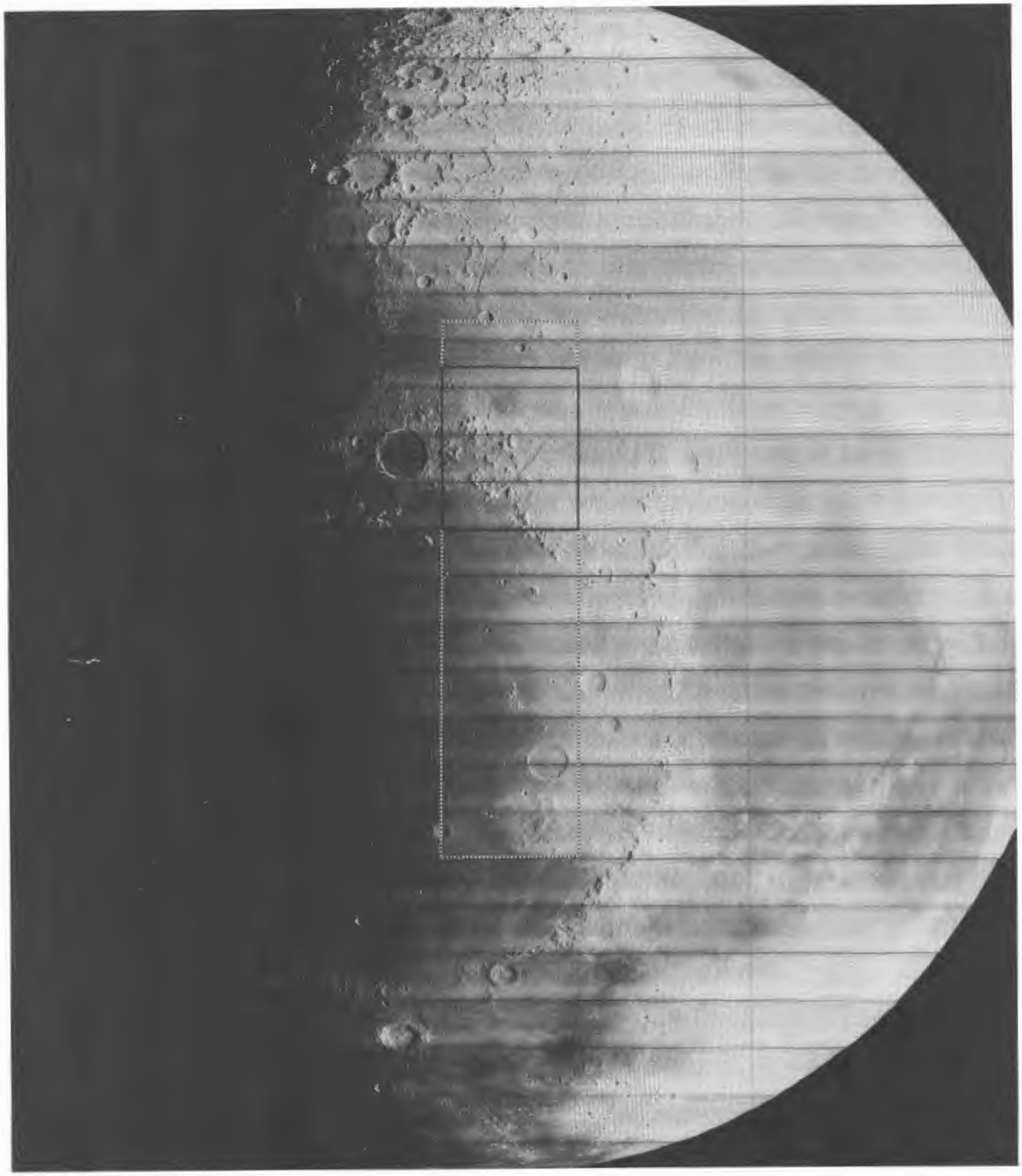

Centered at 2.8°W, 42.5°N.

Figure 4-28: Wide-Angle Frame 115, Site IV21D

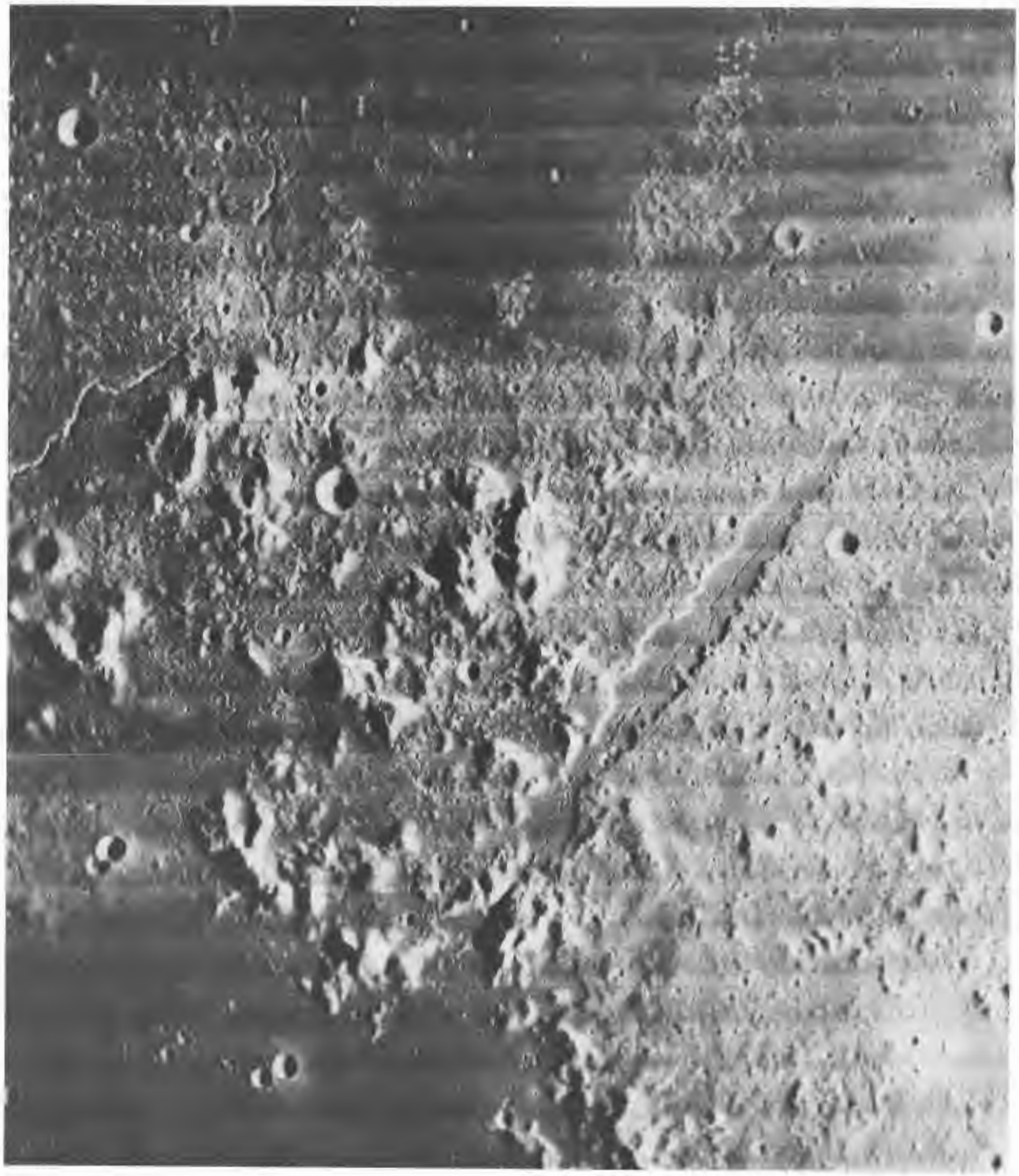

Alpine Valley.

Figure 4-29: Portion of Telephoto Frame 115, Site IV21D

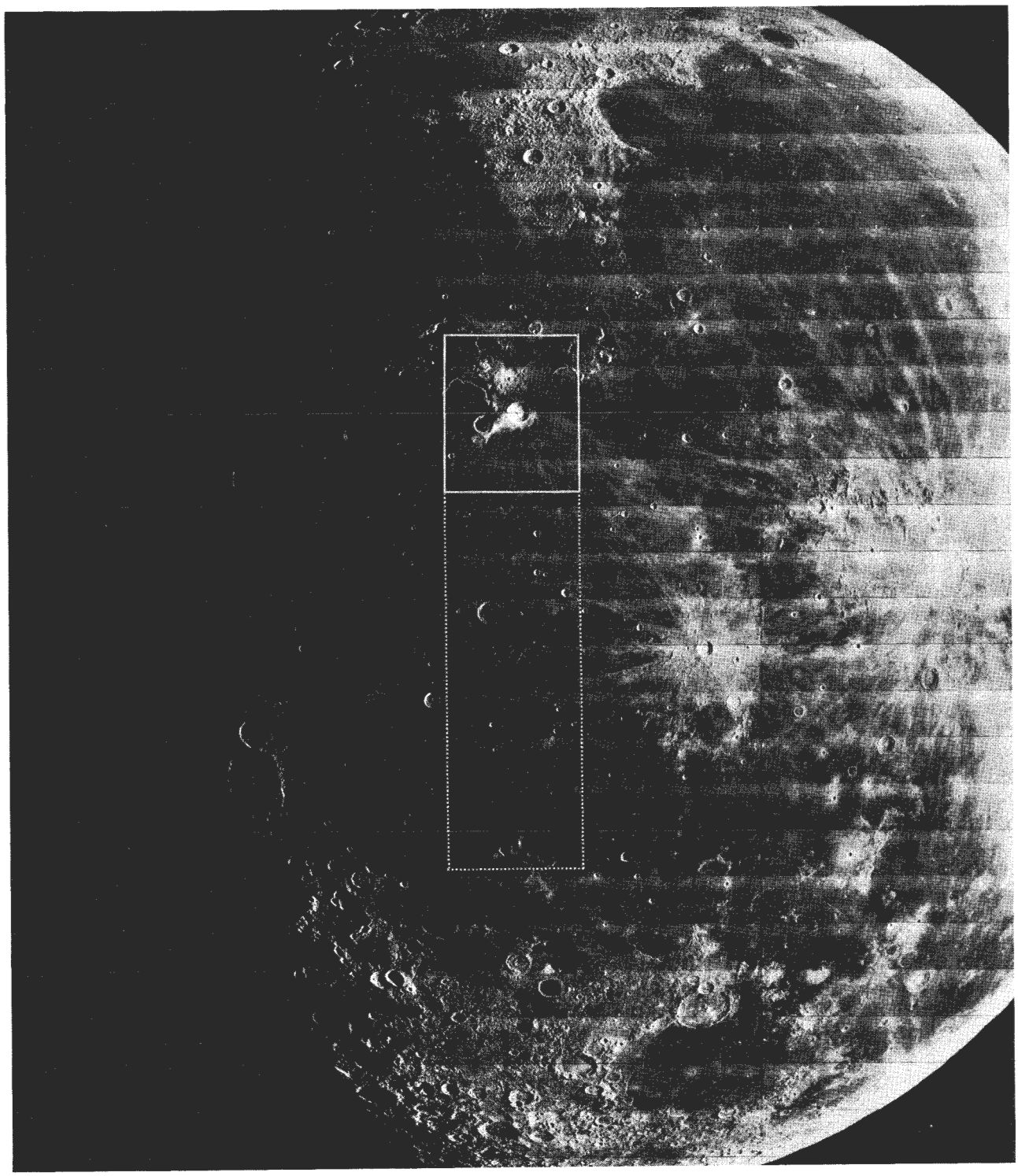

Centered at 49.6°W, 14.0°N.

Figure 4-30: Wide-Angle Frame 150, Site IV27C

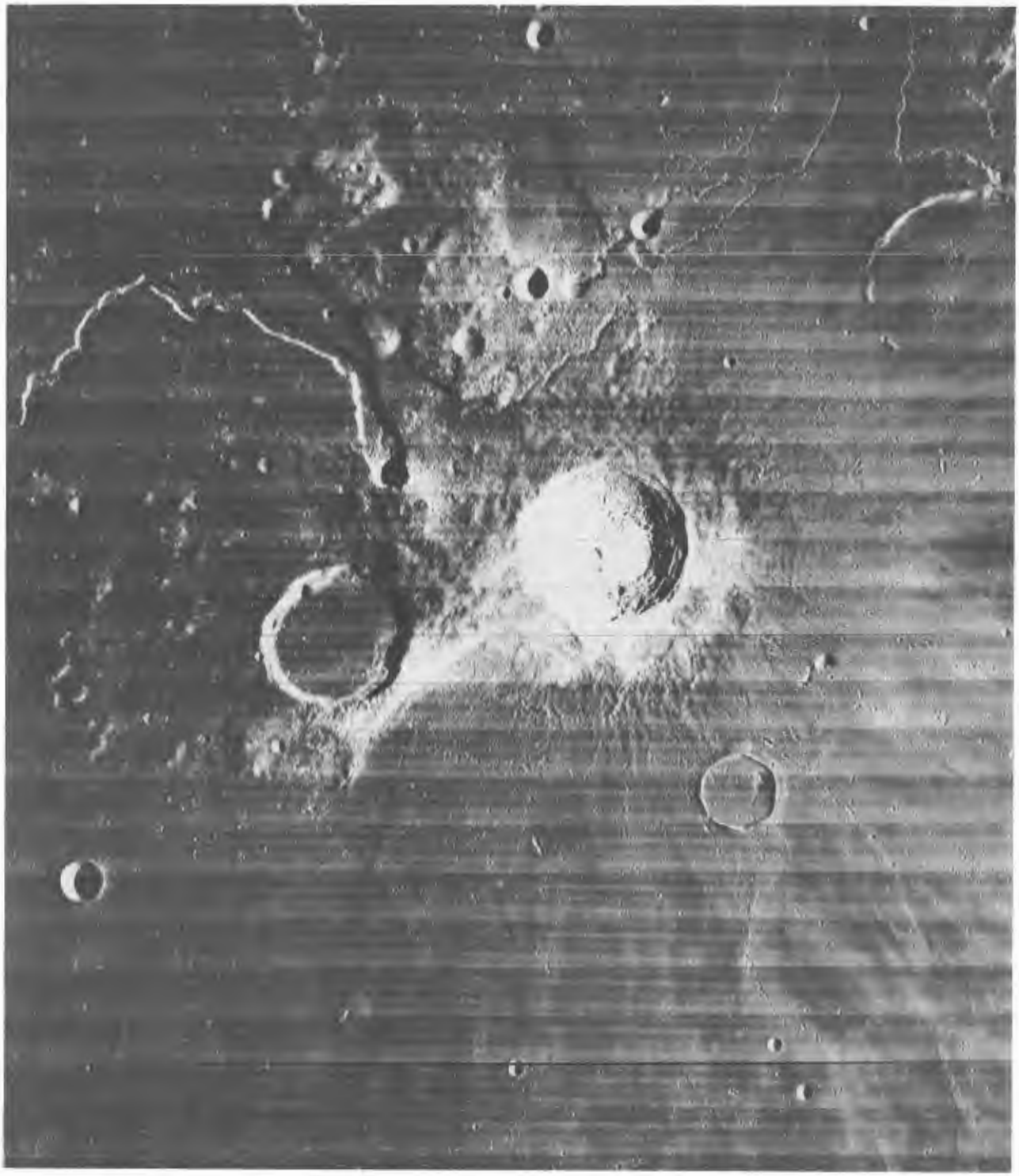

Aristarchus and Schröters valley.

Figure 4-31: Portion of Telephoto Frame 150, Site IV27C

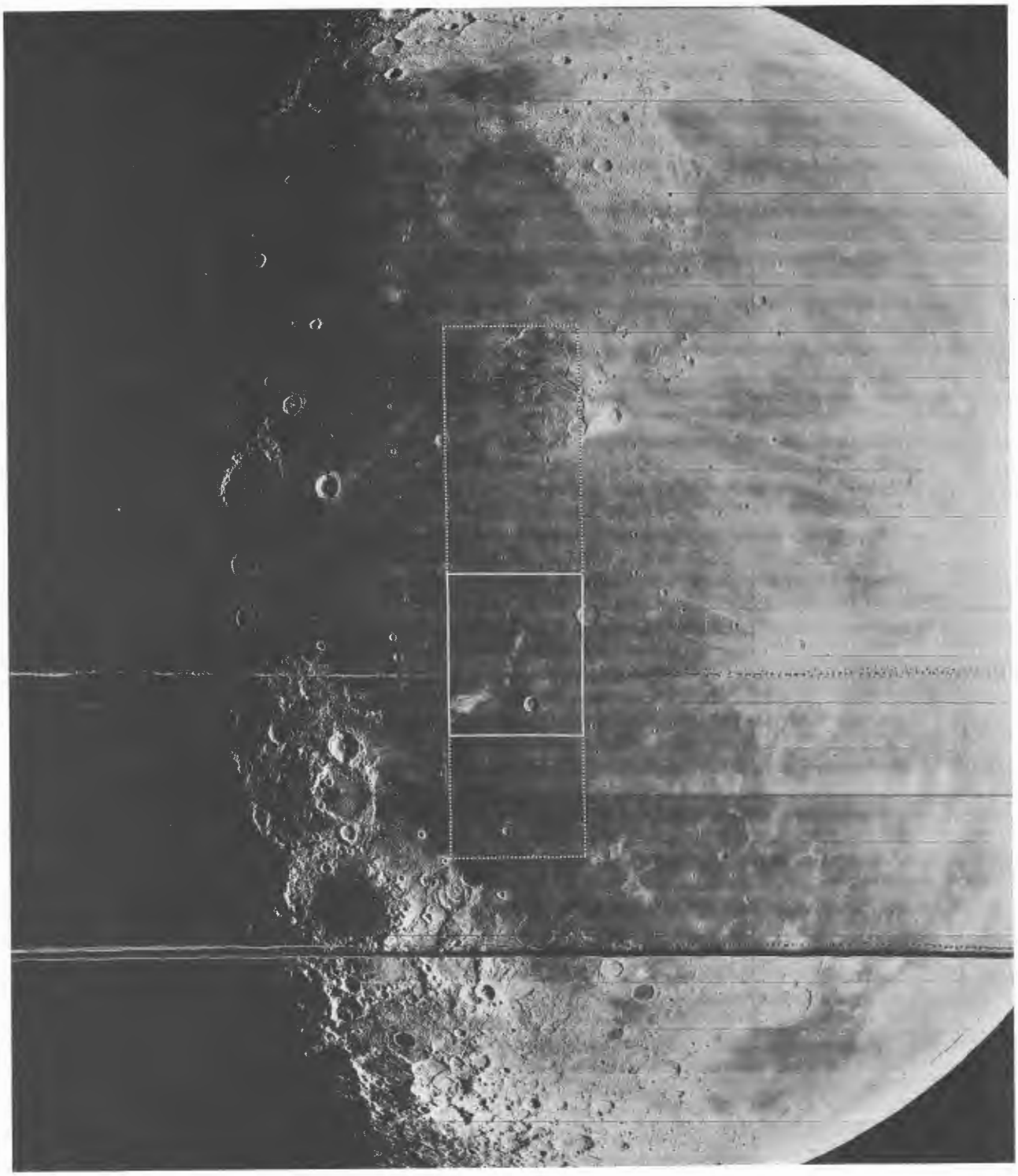

Centered at 56.1°W, 14.1°N.

Figure 4-32: Wide-Angle Frame 157, Site IV28C

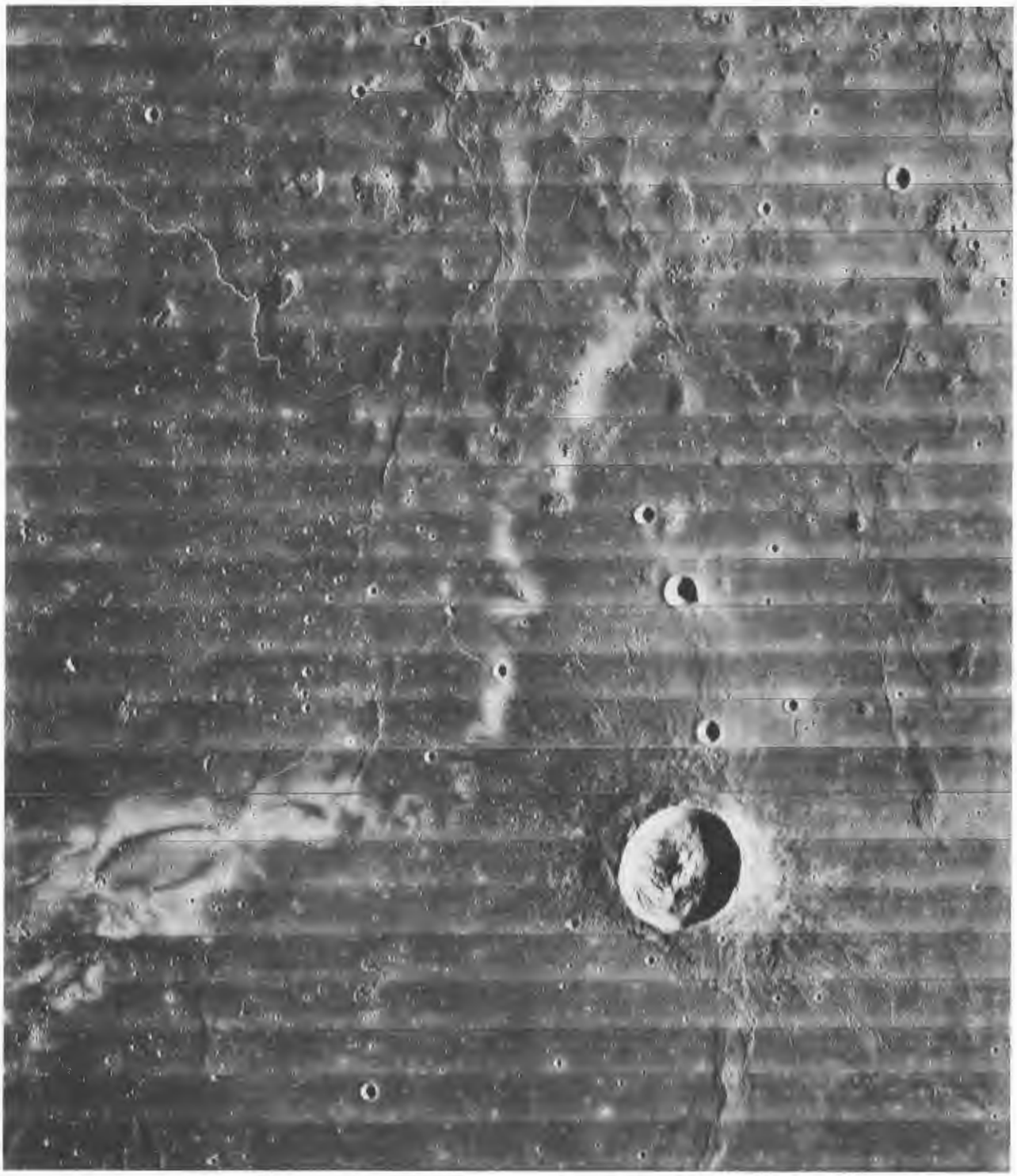

Marius Hills.

Figure 4-33: Portion of Telephoto Frame 157, Site IV28C

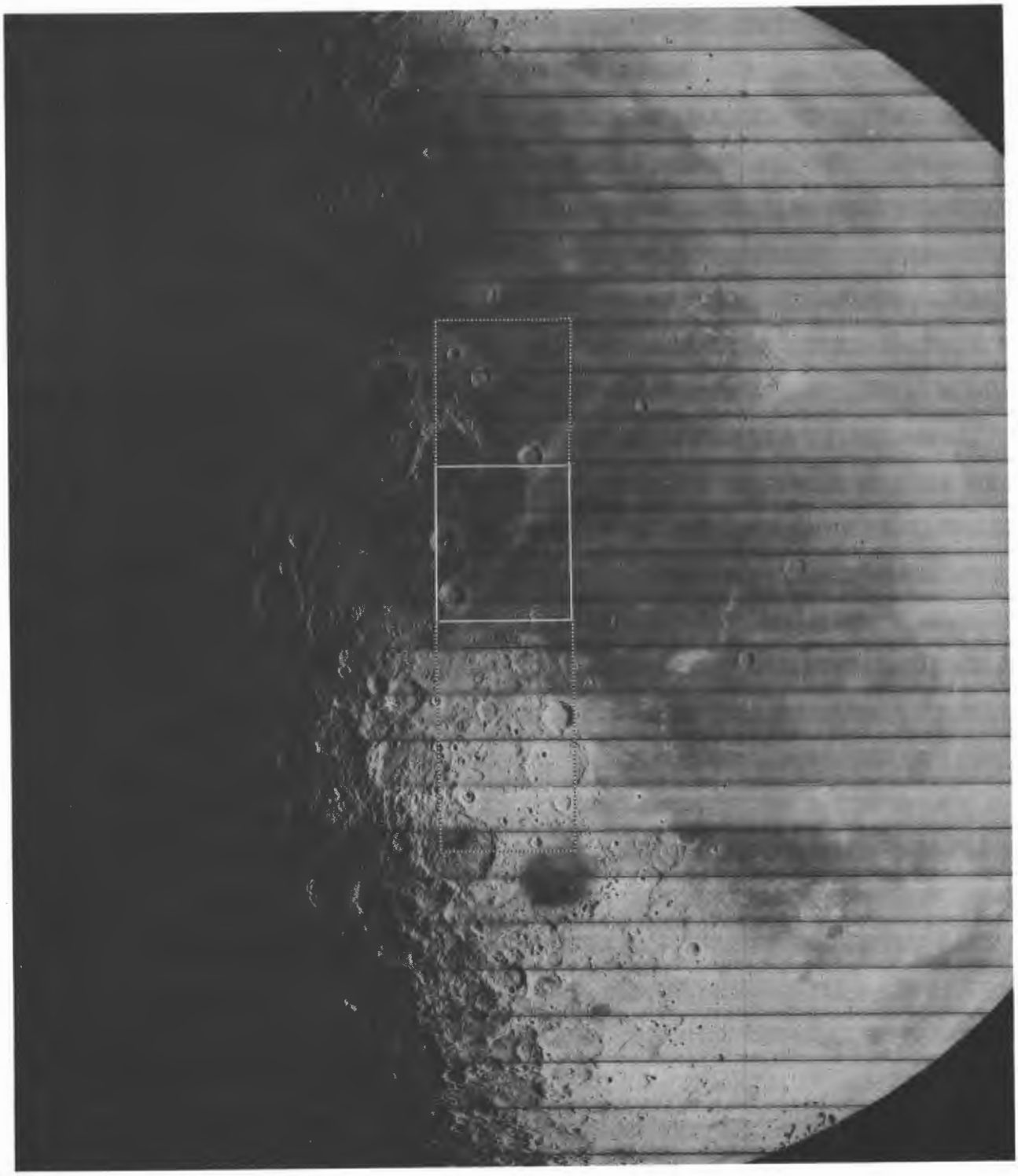

Centered at 69.2°W, 14.7°N.

Figure 4-34: Wide-Angle Frame 169, Site IV30C

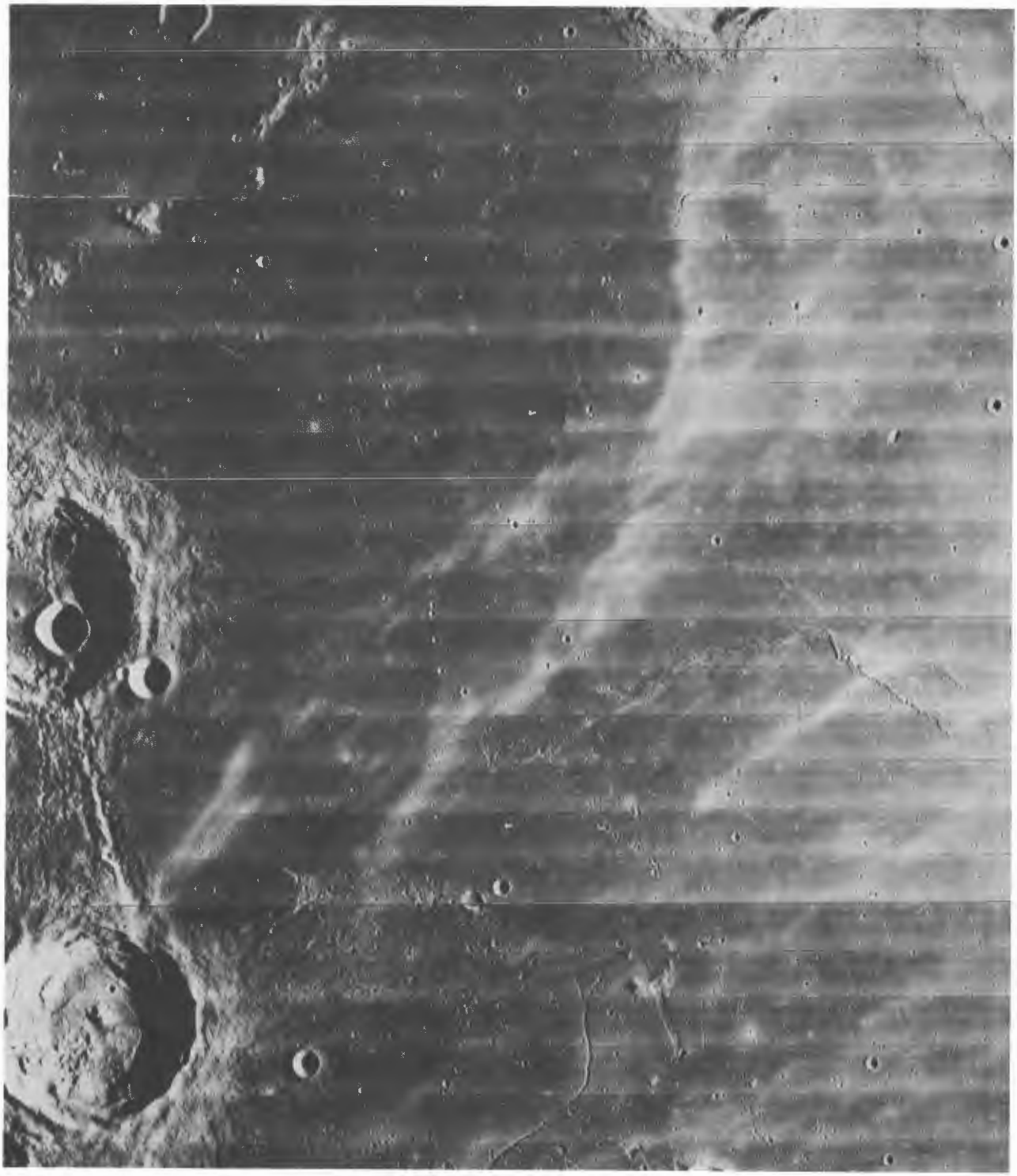

Includes crater Kraft.

Figure 4-35: Portion of Telephoto Frame 169, Site IV30C

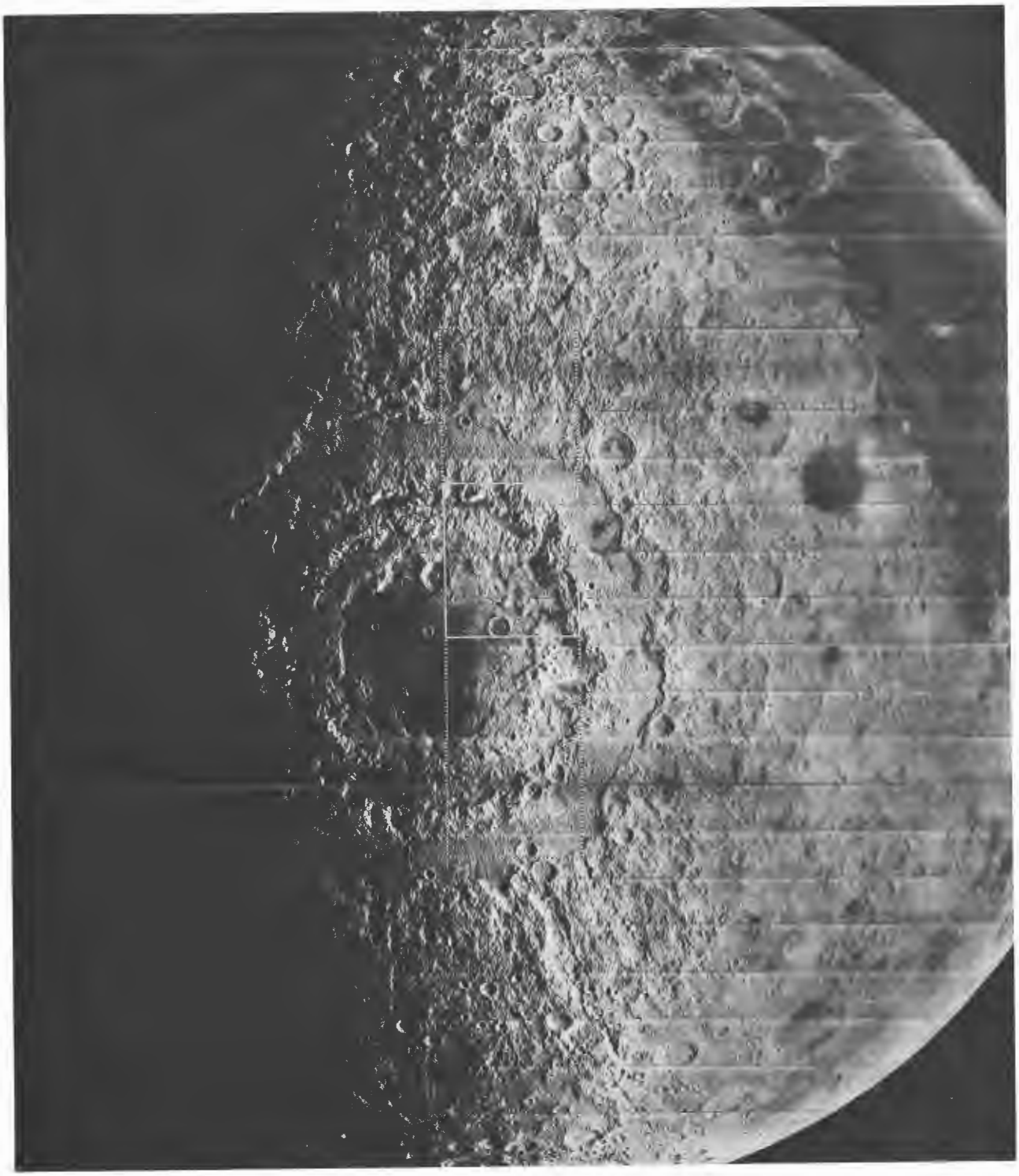

Centered at 89.0°W, 14.3°S.

Figure 4-36: Wide-Angle Frame 187, Site IV33B

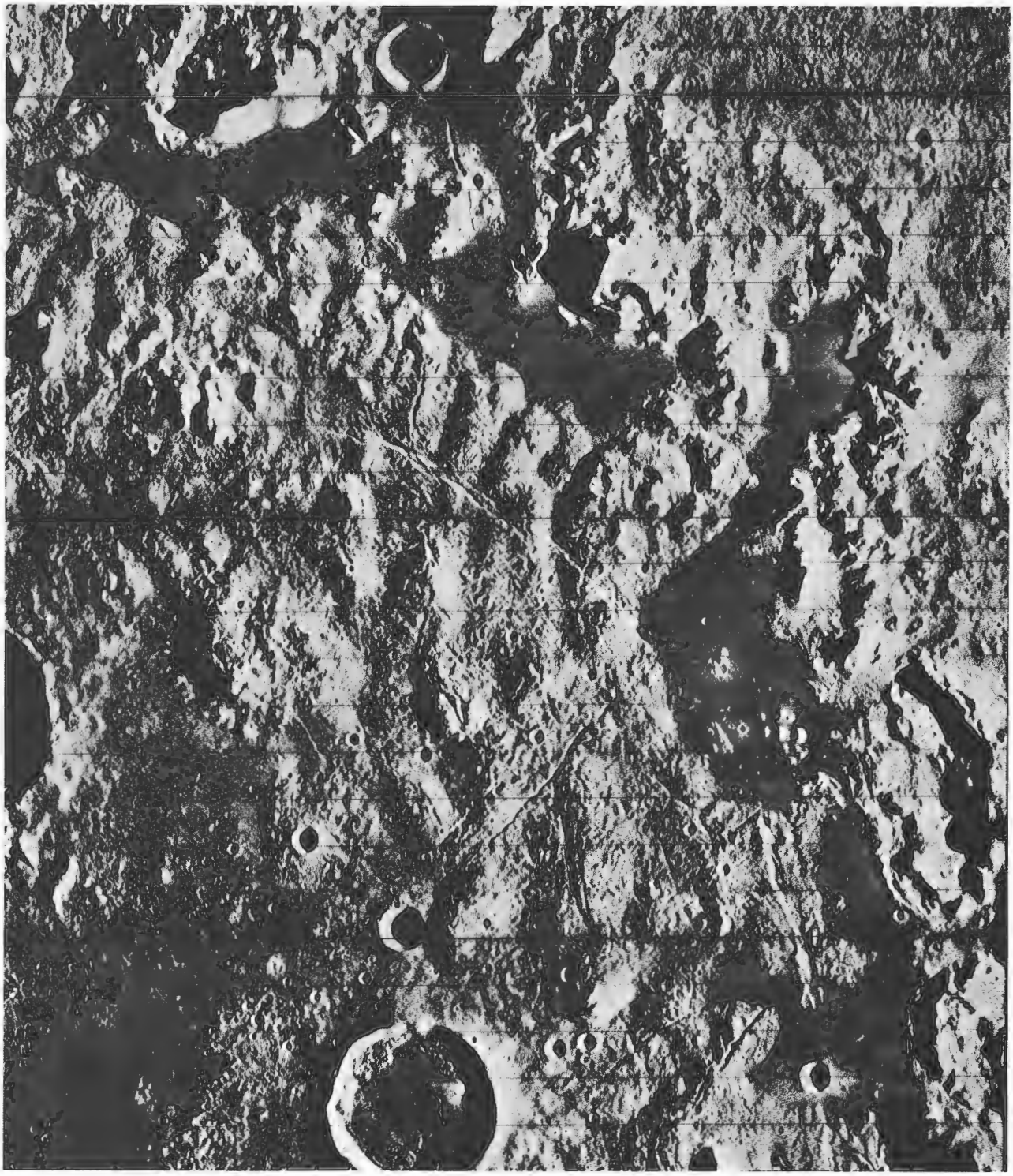

Northeast quadrant of Orientale Basin.

Figure 4-37: Portion of Telephoto Frame 187, Site IV33B

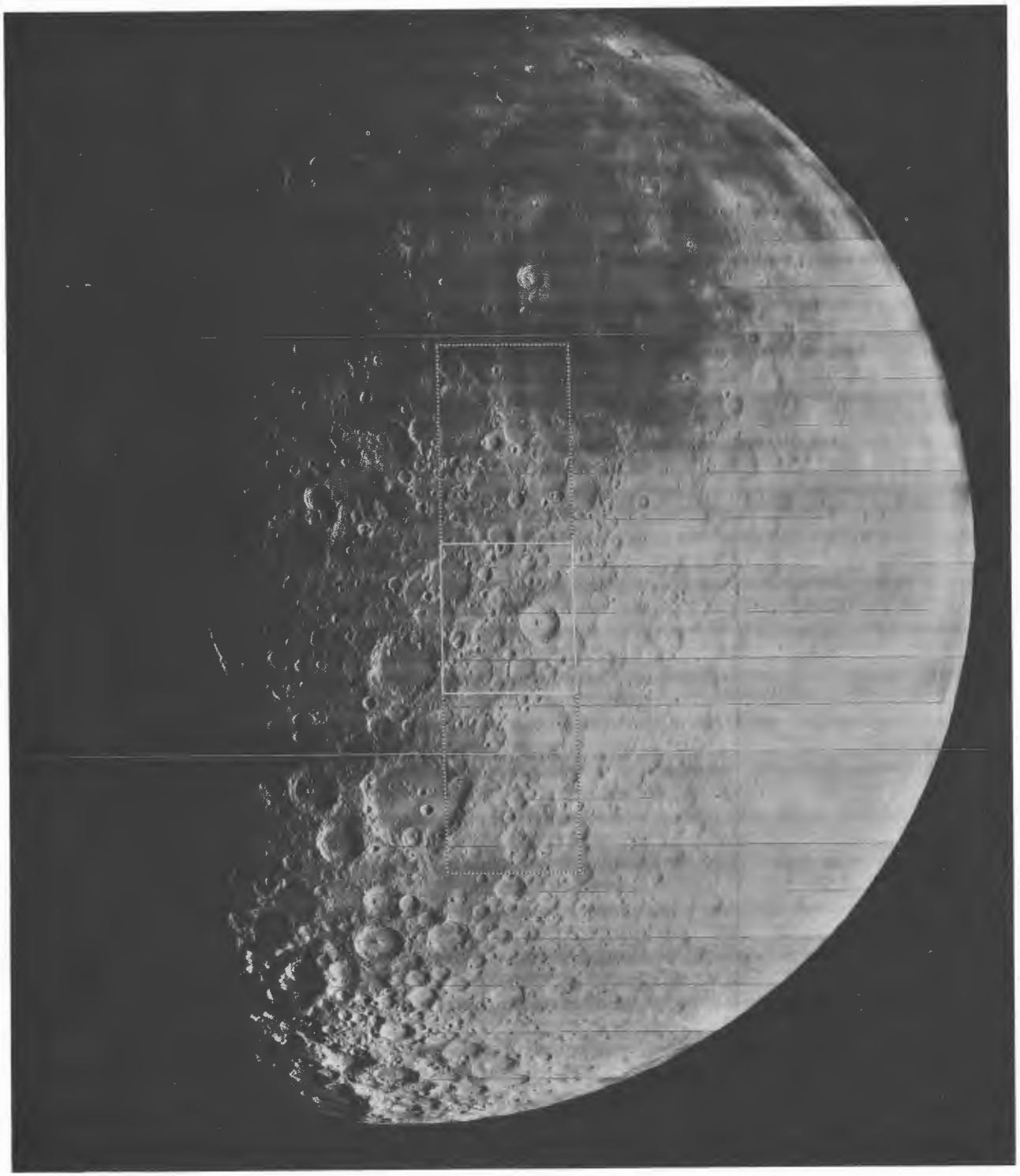

Centered at 14.1°W, 42.4°S.

Figure 4-38: Wide-Angle Frame 124, Site IV23A

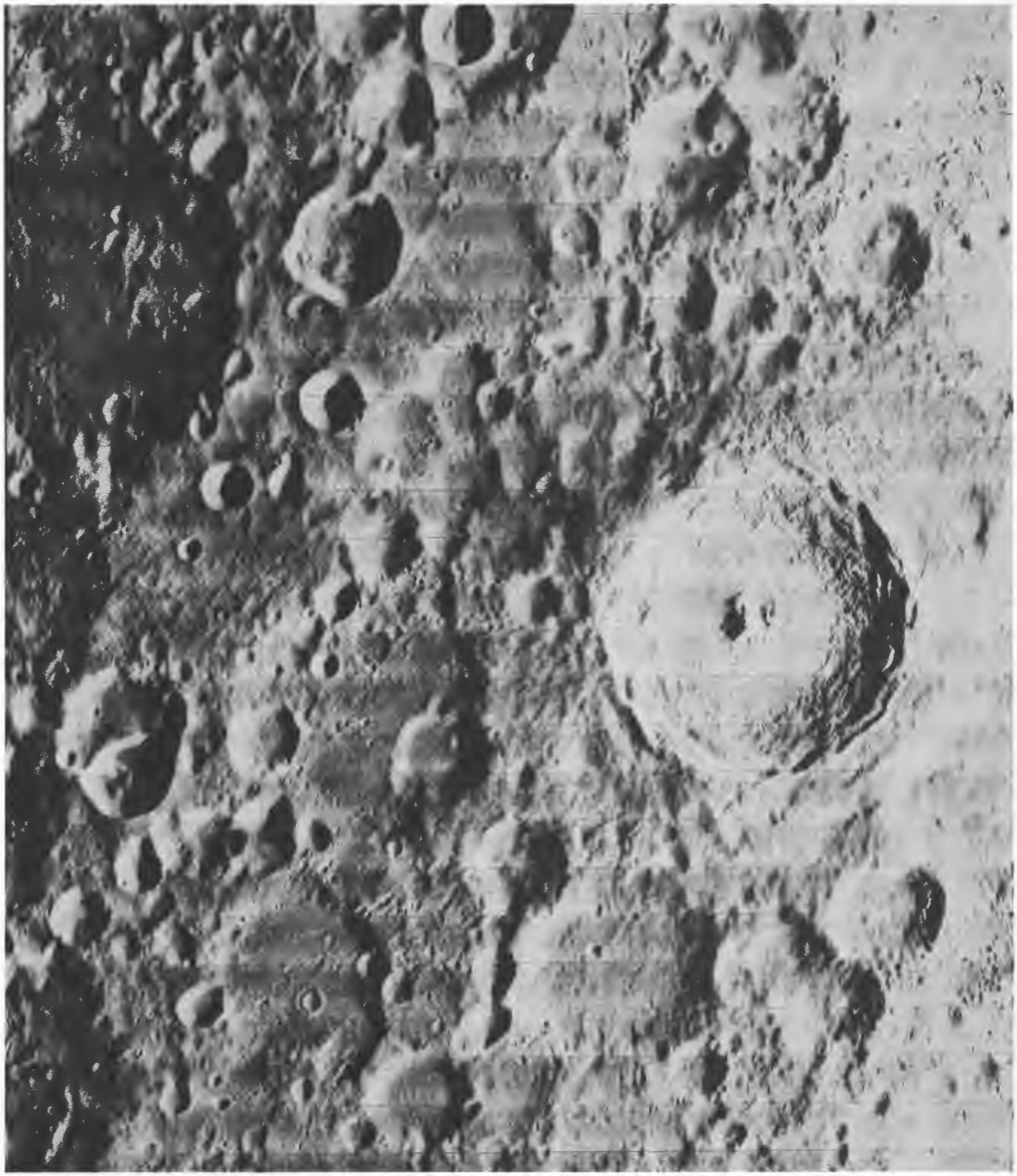

Crater Tycho.

Figure 4-39: Portion of Telephoto Frame 124, Site IV23A

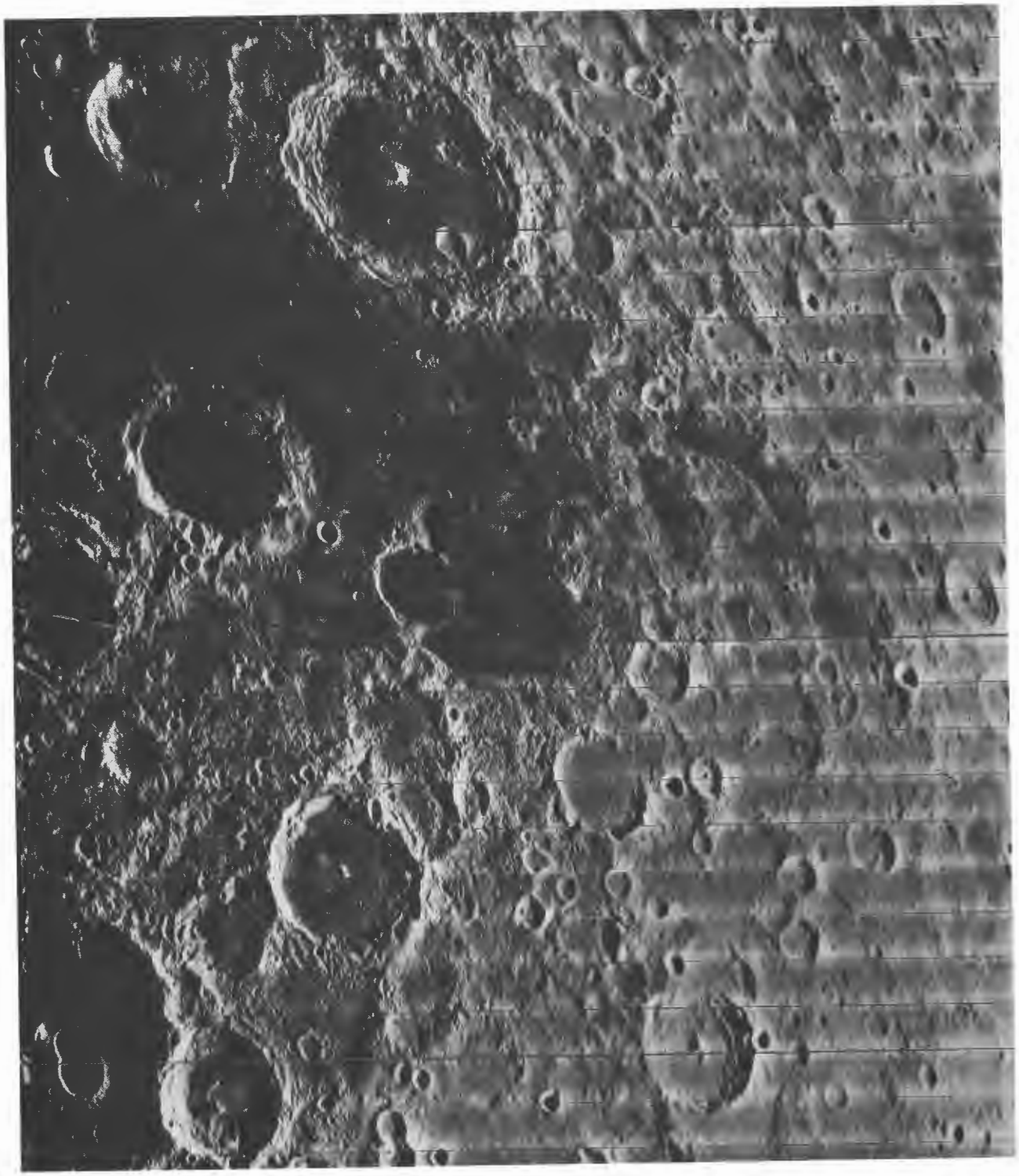

Recovery photo of Mare Smythii.

Figure 4-40: Portion of Telephoto Frame 165, Site IV29G

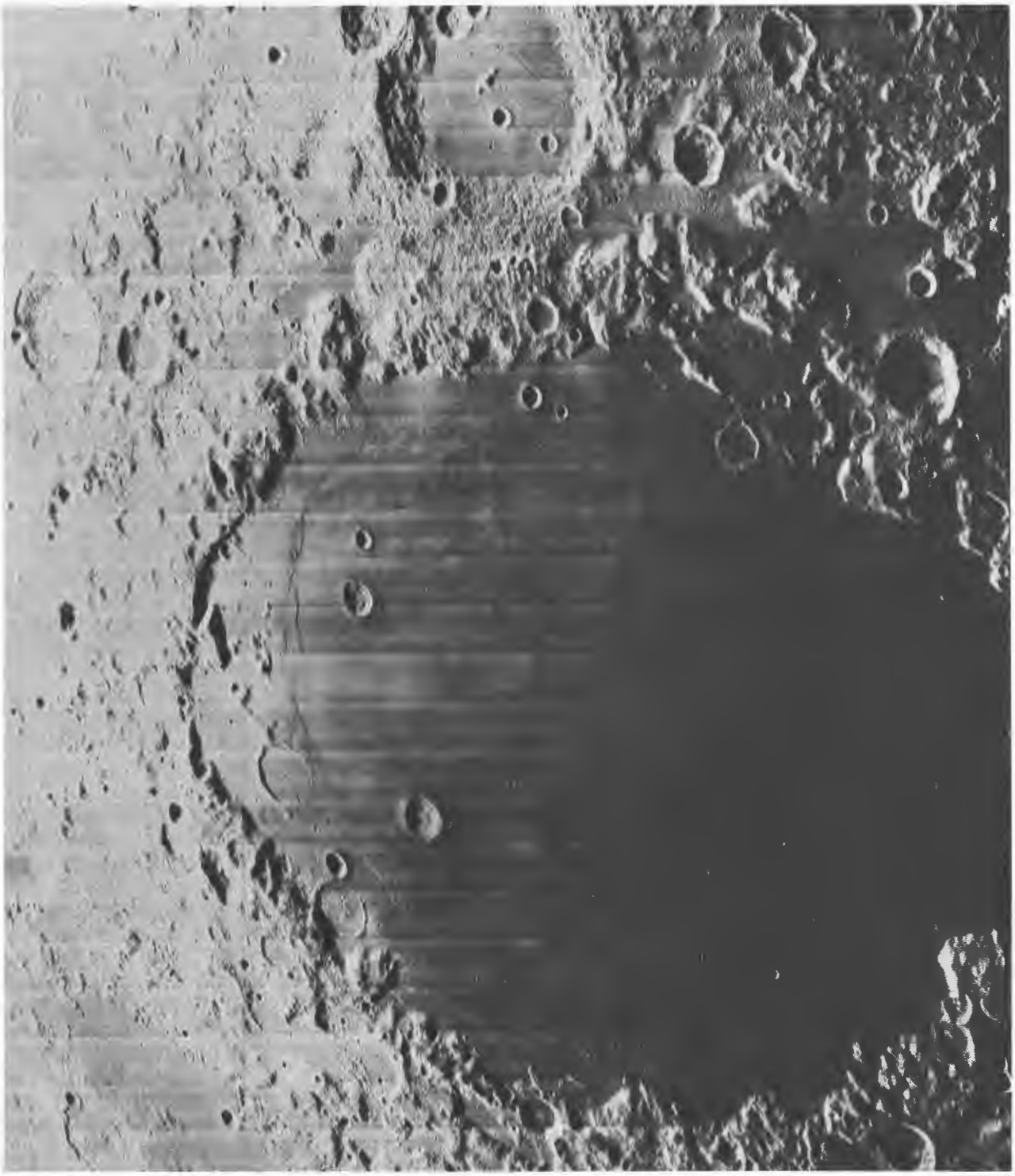

Recovery photo of Mare Crisium.

Figure 4-41: Portion of Telephoto Frame 191, Site IV33G

4.2 ENVIRONMENTAL DATA

Two types of telemetry instrumentation were installed on the Lunar Orbiter IV spacecraft to monitor the lunar environmental conditions. Two radiation dosimeters were mounted adjacent to the photo subsystem. Twenty individual micrometeoroid detectors were circumferentially mounted on the tank deck.

4.2.1 Radiation Data

Dosimeter 1, located near the film cassette, had a sensitivity of 0.25 rad per count, with a capacity of 0 to 255 counts. Dosimeter 2, located near the camera looper, had a sensitivity of 0.50 rad per count and a similar capacity of 0 to 255 counts; it was turned on after passing through the Van Allen belts. Due to the inherent shielding of the spacecraft, the photo subsystem structure, and the 2-grams-per-square-centimeter aluminum shielding provided by the film supply cassette, it was estimated that solar flares of magnitude 2 or less would have negligible effect on the undeveloped film. Flares of magnitude 3 or greater would produce considerable fog on the film.

The radiation dosimeter measurement system (RDMS) functioned normally throughout the mission and provided data on the Earth's trapped radiation belts as well as the radiation environment encountered in transit to the Moon and in orbits about the Moon. Radiation data obtained during the photographic mission are shown in Figure 4-41.

Data from Dosimeter 1 indicated the film cassette was exposed to a total of 5.5 rads during the transit through the outer Van Allen belt. Calculations indicate that this dosage resulted from low-energy electron bremsstrahlung. Increasing activity of solar cycle 20, as well as the occurrence of a large magnetic disturbance during the launch period, apparently resulted in electron enhancement of the outer belt.

On May 21 (Day 141), increasing solar activity culminated in a Class 3+ optical flare at 20°N 32°E at 19:45 GMT. There was no increase in radiation dosage detected from this event. Flare activity continued and a series of major

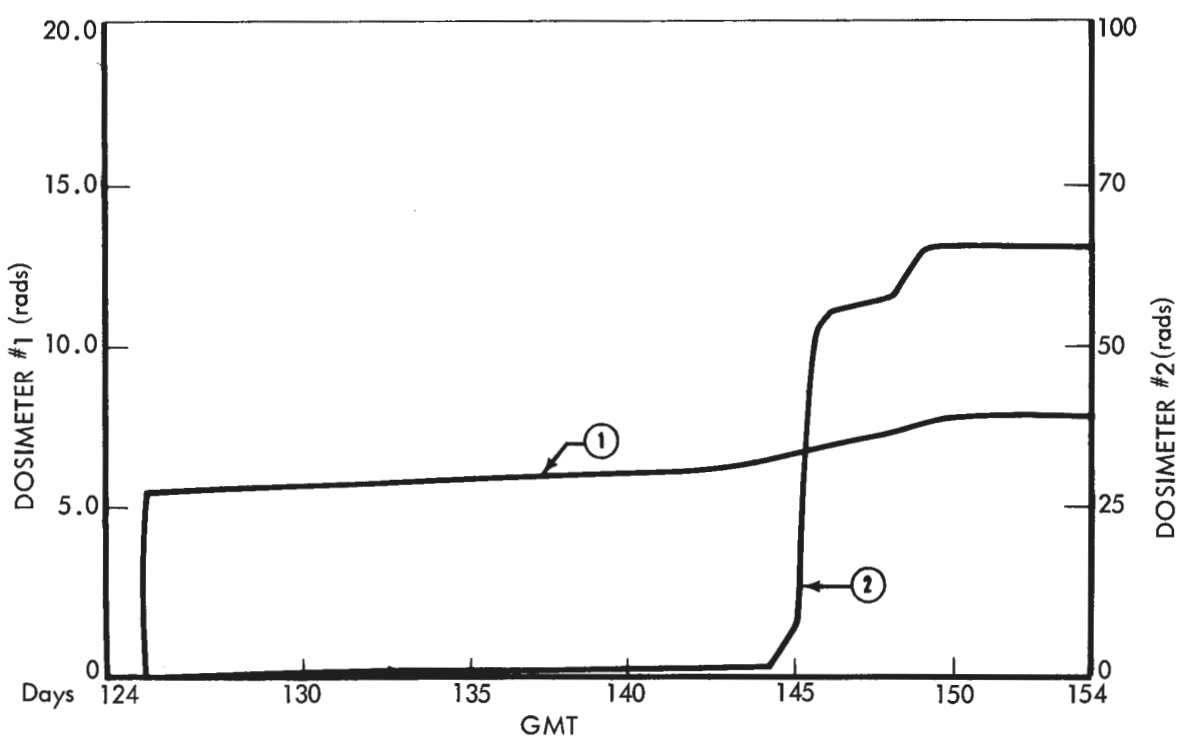

Figure 4-42: Radiation Dosage History

flares were detected at 18:09 GMT on May 23 (Day 143). There was no indication of any high-energy protons reaching the Lunar Orbiter spacecraft; however, a large low-energy plasma cloud produced a dosage change (at the camera looper) from 1.5 to 55.5 rads over a 41-hour period. The maximum change rate during this increase was nearly 5.7 rads per hour. Two days later, a normal solar cosmic-ray event was detected by both detectors. This increased the total dosage at the camera looper to 65.5 rads and 7.75 rads at the film cassette. During the remaining periods the normal increase attributed to background of galactic cosmic ray dose and dosimeter noise was recorded.

Postmission evaluation of film densities showed no visible degradation from the radiation exposure levels encountered.

4.2.2 Micrometeoroid Data

Two micrometeoroid hits were recorded during the photo mission of Lunar Orbiter IV. Discrete channel state changes were recorded at:

Detector 17	01:57:1.2 GMT, May 12
Detector 5	Between 22:24:16.8 GMT, May 18, and 0:04:53.2 GMT, May 19

There was no detectable effect on spacecraft performance at these impacts. The actual time of impact on Detector 5 is not known because the state change occurred during a period of loss of data associated with Earth occultation and reacquisition of the spacecraft and good telemetry data.

Figure 4-43 shows the position of the spacecraft in orbit and the relative Sun-Moon-Earth orientation at the time of impact. The figure

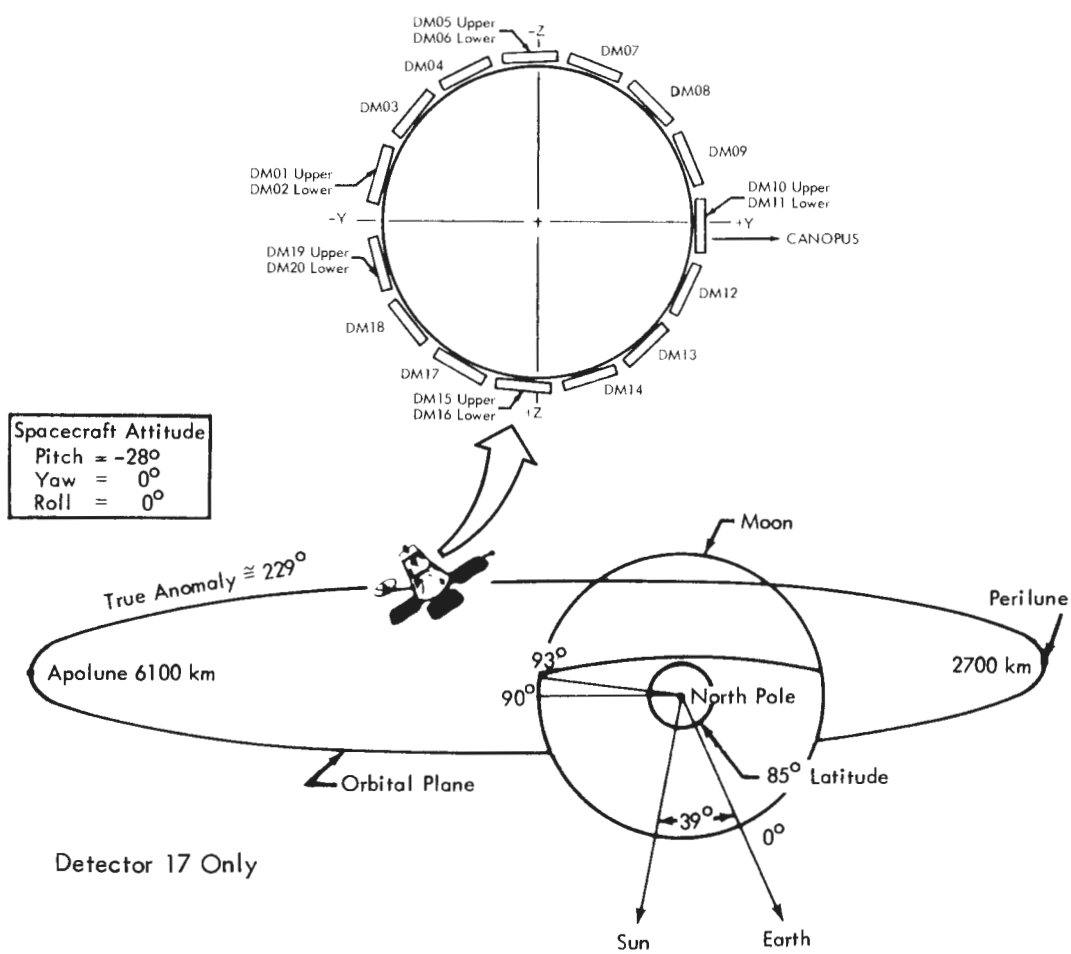

Figure 4-43: Micrometeoroid Impacts

also shows the relative position of the detectors on the spacecraft.

4.3 TRACKING DATA

Lunar Orbiter IV continued to provide lunar tracking data to augment the data obtained on the first three missions. The orbit parameters of the 85-degree inclination with relatively high apolune and perilune altitude provided new data for defining the lunar model coefficient and, in particular, data on the Moon's oblateness. At the end of the photo mission June 1, over 783 station hours of doppler tracking data had been recorded. Over 79 hours of ranging data and 15 station time correlation checks were also obtained. All of this data has been furnished to NASA and will be further evaluated to refine the mathematical model of the Moon. The following discussions are pertinent to the quality of the tracking data obtained and the performance accuracy of the tracking system.

4.3.1 DSIF Tracking Data System

Lunar Orbiter IV was one of three spacecraft orbiting the Moon and operating on the same frequency. To reliably track and communicate with Lunar Orbiter IV, and avoid commanding the other spacecraft, an offset track synchronization frequency was employed based on the best lock frequency of the transponder. In general, the offset value was 330 Hz. During initial implementation of this procedure, the tracking stations locked onto the sidebands instead of the main carrier. Minor refinements were made in the operational tuning sequences to eliminate the problem. Better than 98% of the data received was classified as good.

Ranging data was taken during the cislunar trajectory and the initial lunar orbits prior to taking the first photos. There was no ranging data obtained during photo taking and readout in accordance with an operational decision.

The ODPL prediction program performed without difficulty and maintained a high degree of accuracy. The station acquisition function was somewhat simplified by the lack of Earth occultation periods.

Tracking Data Validation – The tracking data validation function was accomplished by backfeeding the tracking data to the Goldstone computer facility for processing by the Tracking Data Monitoring Program (TDM). This program compared the received data against a set of predictions and computed the residuals. It also calculated the standard deviation of the last five data points and provided an estimate of data noise. Program outputs were transmitted to the SFOF by teletype and printed in tabular form. The program outputs were also plotted on the Milgo 30 X 30 plotter through the IBM 7044 plot routine. During the cislunar phase, the TDM generated its own predicted quantities by using an internal trajectory subprogram.

The internal trajectory subprogram of the TDM does not compute predictions for the lunar orbit phase. In this phase, the JPL predictions are used and the residuals increased, which reflects inaccuracies of the lunar model in the prediction program. No deviations in the rf carrier were observed during Mission IV. Noise estimates of the TDM remained fairly accurate, indicating the overall good quality of the data. An increase in the noise was observed when the spacecraft was tracked close to the Sun's disk. Spacecraft velocity changes were also monitored through the tracking data and showed good agreement with the other data.

Overall performance of the data validation system was very smooth and trouble-free. Tracking data quality reports were made consistently throughout the active mission.

4.3.2 Deep Space Network

Tracking data were recorded at the Deep Space Stations and the Space Flight Operations Facility to satisfy requirements for the selenographic data. The Deep Space Station recording was a five-level teletype paper tape. During the mission, the tracking data were transmitted to the SFOF via normal teletype messages. At the Space Flight Operations Facility, teletype data were received by communications terminal equipment and passed to the raw-data table on the 1301 disk by the IBM 7044 I/O processor. These data were processed by the TTYX program to separate the telemetry data and tracking

data in the messages received, and stored on the tracking raw-data file on disk. The tracking data processor (TDP) program generated the master tracking data table on the 1301 disk by smoothing and sorting the data from the tracking raw-data file by Deep Space Station identification. The output of this program was also recorded on magnetic tape and identified as the tracking data deliverable to NASA. An orbit data generator routine extracted selected master data file tracking data, smoothed it, sorted it according to time, and inserted it in the orbit determination program input file. Upon command from the FPAC area, orbit parameters were computed or predicted – based upon selected data from the orbit determination program input file and the orbit determination program – and inserted into the data display for subsequent display by the user.

The raw tracking data paper tapes recorded at each Deep Space Station and the output of the tracking data processor at the Space Flight Operations Facility, recorded on magnetic tape, were collected and delivered to NASA for follow-up on selenodetic analysis purposes.

4.4 PERFORMANCE TELEMETRY

Spacecraft performance telemetry data was obtained by three different methods. Prior to spacecraft separation, the data was transmitted via assigned subcarriers of the VHF Agena telemetry link. This data was recorded at AFETR and, after real-time demodulation, transferred to DSS-71 (Cape Kennedy) for retransmission to the SFOF computers. In addition, the AFETR stations recorded the S-band signal directly from the spacecraft. After separation, the performance data was received directly from the spacecraft by the Deep Space Stations and reformatted for transmission to the SFOF. In all cases, the data was available for the subsystem analysts to continuously monitor the operational status of all spacecraft subsystems and environmental conditions.

Mission support by the DSN began 6 hours prior to liftoff on May 4, 1967, on a 24-hour-coverage basis, and terminated with the conclusion of photo readout on June 1, 1967. Table 4-4 summarizes the data recorded by the DSN during the mission.

Table 4-4: DSN Telemetry Summary

Deep Space Station	Total Passes	Telemeter Frames Transmitted	Telemeter Frames Recorded	Percent Recovered
Goldstone	16	21,432	21,052	98.3
Woomera	16	17,329	16,253	93.8
Madrid	16	21,423	20,421	95.3
	Total	60,184	57,726	95.8

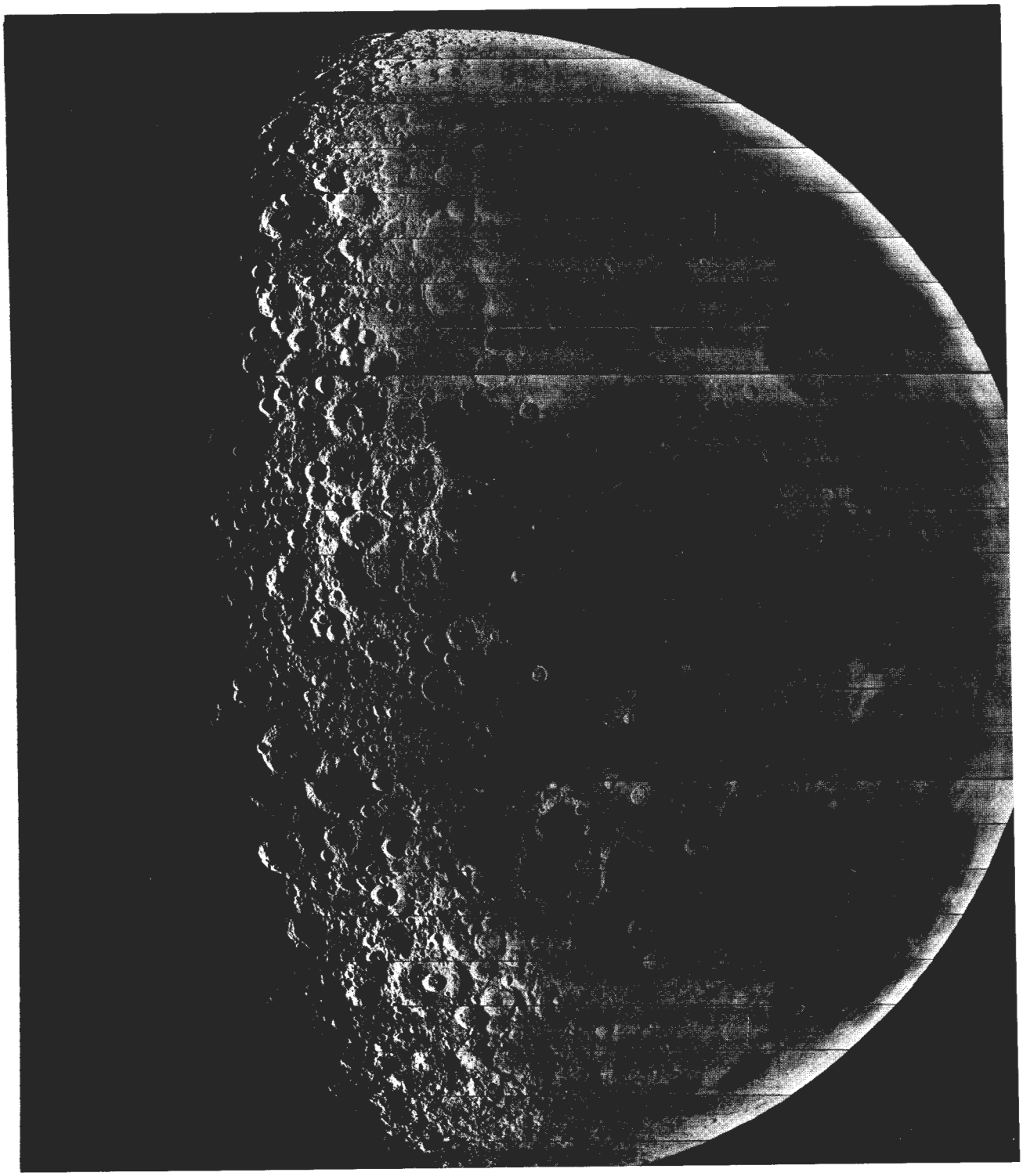

Wide-Angle Frame 183, Site IV32D
Centered at 74.4°W, 42.5°N;
includes Repsold, Pythagoras, northwest limb, and farside areas.

5.0 Mission Evaluation

Lunar Orbiter IV provided photographs containing an enormous amount of data and scientific information about the nearside of the Moon which will stand for many years as the primary source of data on lunar surface features for scientific analysis and planning later explorations of the Moon.

Significant accomplishments of the mission include, but are not limited to:

- Provided the first photographic mapping mission of a celestial body, other than Earth, from an orbiting spacecraft.

- Provided photographic coverage (over 99%) of the nearside of the Moon at resolutions at least 10 times better than Earth-based observations.

- Provided the first detailed near-vertical photographs and visibility of the polar regions and limb areas.

- Provided the first vertical photos of the spectacular geologic formations of the Orientale basin at the western limb.

- Successfully altered the cislunar trajectory, by the midcourse maneuver, to produce extensive changes in the lunar orbit parameters necessitated by the redefinition of the mission objectives.

- Provided data from which to determine the lunar mathematical model coefficients for an 85-degree orbit inclination with particular emphasis on oblateness characteristics.

- Provided photo data by which the photo sites for Lunar Orbiter V mission were relocated to increase the scientific data obtainable.

Mission IV was a completely different type of mission than Orbiters I, II, and III in that it was devoted entirely to providing data that will increase the scientific knowledge required to understand the Moon as an entity. The planned photo mission was completed despite some operational difficulties with the spacecraft subsystem. Mission operational procedures were revised to accomplish this. Attitude control flexibility and accuracy were again demonstrated by orienting the long axis of the telephoto coverage approximately parallel to the direction of flight instead of nearly perpendicular as on previous missions. Although spacecraft subsystem anomalies were encountered, the subsystem and mission planning analysts developed alternate commands and procedures that permitted the mission to continue and achieve all the desired objectives.

NATIONAL AERONAUTICS AND SPACE ADMINISTRATION
WASHINGTON, D. C. 20546

OFFICIAL BUSINESS

FIRST CLASS MAIL

POSTAGE AND FEES PAID
NATIONAL AERONAUTICS AND
SPACE ADMINISTRATION

POSTMASTER: If Undeliverable (Section 158 Postal Manual) Do Not Return

"The aeronautical and space activities of the United States shall be conducted so as to contribute . . . to the expansion of human knowledge of phenomena in the atmosphere and space. The Administration shall provide for the widest practicable and appropriate dissemination of information concerning its activities and the results thereof."

—NATIONAL AERONAUTICS AND SPACE ACT OF 1958

NASA SCIENTIFIC AND TECHNICAL PUBLICATIONS

TECHNICAL REPORTS: Scientific and technical information considered important, complete, and a lasting contribution to existing knowledge.

TECHNICAL NOTES: Information less broad in scope but nevertheless of importance as a contribution to existing knowledge.

TECHNICAL MEMORANDUMS: Information receiving limited distribution because of preliminary data, security classification, or other reasons.

CONTRACTOR REPORTS: Scientific and technical information generated under a NASA contract or grant and considered an important contribution to existing knowledge.

TECHNICAL TRANSLATIONS: Information published in a foreign language considered to merit NASA distribution in English.

SPECIAL PUBLICATIONS: Information derived from or of value to NASA activities. Publications include conference proceedings, monographs, data compilations, handbooks, sourcebooks, and special bibliographies.

TECHNOLOGY UTILIZATION PUBLICATIONS: Information on technology used by NASA that may be of particular interest in commercial and other non-aerospace applications. Publications include Tech Briefs, Technology Utilization Reports and Notes, and Technology Surveys.

Details on the availability of these publications may be obtained from:

SCIENTIFIC AND TECHNICAL INFORMATION DIVISION

NATIONAL AERONAUTICS AND SPACE ADMINISTRATION

Washington, D.C. 20546